USGS
science for a changing world

Prepared in cooperation with Kyungpook University, Republic of Korea

Characterization of the Partial Oxidation Products of Crude Oil Contaminating Groundwater at the U.S. Geological Survey Bemidji Research Site in Minnesota by Elemental Analysis, Radiocarbon Dating, Nuclear Magnetic Resonance Spectroscopy, and Fourier Transform Ion Cyclotron Resonance Mass Spectrometry

Open-File Report 2022–1042

U.S. Department of the Interior
U.S. Geological Survey

Characterization of the Partial Oxidation Products of Crude Oil Contaminating Groundwater at the U.S. Geological Survey Bemidji Research Site in Minnesota by Elemental Analysis, Radiocarbon Dating, Nuclear Magnetic Resonance Spectroscopy, and Fourier Transform Ion Cyclotron Resonance Mass Spectrometry

By Kevin A. Thorn, Ananna Islam, and Sunghwan Kim

Prepared in cooperation with Kyungpook University, Republic of Korea

Open-File Report 2022–1042

U.S. Department of the Interior
U.S. Geological Survey

U.S. Geological Survey, Reston, Virginia: 2022

For more information on the USGS—the Federal source for science about the Earth, its natural and living resources, natural hazards, and the environment—visit https://www.usgs.gov or call 1–888–ASK–USGS.

For an overview of USGS information products, including maps, imagery, and publications, visit https://store.usgs.gov/.

Suggested citation:
Thorn, K.A., Islam, A., and Kim, S., 2022, Characterization of the partial oxidation products of crude oil contaminating groundwater at the U.S. Geological Survey Bemidji research site in Minnesota by elemental analysis, radiocarbon dating, nuclear magnetic resonance spectroscopy, and Fourier transform ion cyclotron resonance mass spectrometry: U.S. Geological Survey Open-File Report 2022–1042, 91 p., https://doi.org/10.3133/ofr20221042.

ISSN 2331-1258 (online)

Acknowledgments

We thank Manhoi Hur and Arif Ahmed, Kyungpook University for their assistance in the Fourier transform ion cyclotron resonance mass spectrometry analyses. We also thank Barbara Bekins, U.S. Geological Survey, and David Podgorski, University of New Orleans, for their contributions.

Contents

Figures

Tables

Conversion Factors

International System of Units to U.S. customary units

Multiply	By	To obtain
	Length	
millimeter (mm)	0.03937	inch (in.)
meter (m)	3.281	foot (ft)
meter (m)	1.094	yard (yd)
	Volume	
barrel (bbl; petroleum, 1 barrel=42 gal)	0.1590	cubic meter (m^3)
liter (L)	33.81402	ounce, fluid (fl. oz)
liter (L)	0.2642	gallon (gal)
milliliter (mL)	0.03381402	ounce, fluid (fl. oz)
	Mass	
gram (g)	0.03527	ounce, avoirdupois (oz)
milligram (mg)	0.00003527	ounce, avoirdupois (oz)
	Energy	
joule (J)	0.0000002	kilowatt hour (kWh)

Temperature in degrees Celsius (°C) may be converted to degrees Fahrenheit (°F) as follows:

$$°F = (1.8 \times °C) + 32.$$

Datum

Vertical coordinate information is referenced to the National Geodetic Vertical Datum of 1929 [NGVD29]. Altitude, as used in this report, refers to distance above the vertical datum.

Abbreviations

ACOUSTIC	alternating compound one eighties used to suppress transients in the coil
DBE	double bond equivalent
DEPT	distortionless enhancement by polarization transfer
DOC	dissolved organic carbon
ESI	electrospray ionization
f_a	fraction aromatic, or aromacity
FTICR-MS	Fourier transform ion cyclotron resonance mass spectrometry
HPIA	hydrophilic acid
HPOA	hydrophobic acid
HPON	hydrophobic neutral
Hz	hertz
IGD	inverse gated decoupled
INEPT	insensitive nuclei enhanced by polarization transfer
MHz	megahertz
NMR	nuclear magnetic resonance
NOM	natural organic matter
NVOA	nonvolatile organic acid
ppm	parts per million (in NMR, resonant frequency in Hz/spectrometer frequency)
PTC	phase transfer catalysis
SARA	saturate, aromatic, resin, asphaltene
VPO	vapor pressure osmometry
ybp	years before the present

Chemical Symbols

$\delta^{13}C$	carbon-13 to carbon-12 ratio
^{1}H	hydrogen-1
^{13}C	carbon-13
^{14}C	carbon-14
^{15}N	nitrogen-15
dmso-d6	deuterated dimethyl sulfoxide
N	nitrogen
O	oxygen
S	sulfur

Other

~	approximately
°	degree
>	greater than
<	less than
(-)	negative-mode

Characterization of the Partial Oxidation Products of Crude Oil Contaminating Groundwater at the U.S. Geological Survey Bemidji Research Site in Minnesota by Elemental Analysis, Radiocarbon Dating, Nuclear Magnetic Resonance Spectroscopy, and Fourier Transform Ion Cyclotron Resonance Mass Spectrometry

By Kevin A. Thorn,[1] Ananna Islam,[2] and Sunghwan Kim[2]

Abstract

In oil spill research, a topic of increasing attention during the last decade has been the environmental impact of the partial oxidation products that result from transformation of the petroleum in freshwater, marine, and terrestrial ecosystems. This report describes the isolation and characterization of the partial oxidation products from crude oil contaminating groundwater at the long-term U.S. Geological Survey Bemidji research site in Minnesota. As the result of a pipeline burst in August 1979, a body of light aliphatic crude oil is present from the land surface to 2 meters below the water table in a shallow sand and gravel aquifer in a remote area outside Bemidji, Minnesota, United States. Biodegradation has resulted in the formation of a plume of dissolved organic carbon (DOC) downgradient from the oil body. Groundwater has also been contaminated in an area known as the spray zone, from vertical infiltration of DOC resulting from biodegradation of oil in the soil column, and possibly from photooxidation of oil at the soil surface. The majority of DOC in the contaminated groundwater is in the form of nonvolatile organic acids (NVOAs) which represent the partial oxidation products of the crude oil constituents. The NVOAs have been classified into three fractions according to their isolation on XAD resins: hydrophobic neutrals (HPON), hydrophobic acids (HPOA), and hydrophilic acids (HPIA). These fractions of NVOAs were isolated from wells downgradient from the oil body (sampling well numbers 533, 532, 530, 515), in the spray zone (603), and from an uncontaminated well upgradient of the oil body (310) between the years 1986 and 1989, and again from wells 530 and 603 in 1998. The samples have been characterized by elemental analysis, radiocarbon dating, carbon-13 nuclear magnetic resonance spectroscopy (^{13}C NMR), and negative-mode (-) electrospray ionization Fourier transform ion cyclotron resonance mass spectrometry (ESI FTICR-MS), with a particular focus on fractions from wells 310, 530, and 603.

All the characterization data indicate that the NVOAs from contaminated wells are distinguishable from the background DOC. Carbon-14 (^{14}C) ages of NVOAs from contaminated wells ranged from 3,615 to 18,985 years before the present, whereas the background DOC from the aquifer was post-bomb (post 1950). By elemental analysis, NVOAs from contaminated wells had higher sulfur but lower nitrogen contents than the background. By electrospray ionization Fourier transform ion cyclotron resonance mass spectrometry, number average molecular weights determined from assigned molecular formulas ranged from 416 to 486 daltons for the HPOA and HPIA fractions from both background and contaminant wells. NVOAs from contaminated wells had significantly greater numbers of assigned molecular formulas containing sulfur, with elevated concentrations of the $S_1O_{4\text{-}10}$ species in particular. Compared to the background, HPOA and HPIA fractions from contaminant wells had a broader range of double bond equivalents (DBEs) within O_n compound classes (n is number of atoms). Additionally, within O_n compound classes, contaminant well HPOA fractions had a greater abundance of lower n (less than eight) than the background. Contaminant well double bond equivalents versus carbon number ($C^{\#}$) plots of oxygen compound classes suggest oil-derived aliphatic compounds in the range from C_{12} to C_{22} in HPOA and HPIA fractions and oil-derived compounds containing aromatic or saturated rings in the approximate range from C_{20} to C_{30} are present in HPOA fractions.

[1]U.S. Geological Survey.

[2]Kyungpook University, Republic of Korea.

The data suggest the NVOAs originate from biodegradation of several classes of C_{12} and greater crude oil constituents: sulfur-containing constituents, including possibly the resins and asphaltenes; constituents containing aromatic rings substituted with methyl groups, including alkylaromatic and naphthenoaromatic compounds, and C_{12} to C_{22} alkyl constituents. The overall similarities of the carbon-13 nuclear magnetic resonance spectra for the well 603 and 530 samples from the two sampling dates suggest that a steady state in the composition of the partial oxidation products in each of the two wells had been reached between 1986–1989 and 1998.

Introduction

As the result of a pipeline burst in August 1979, a body of light aliphatic crude oil is present from the land surface to 2 meters (m) below the water table in a shallow sand and gravel aquifer in a remote area outside Bemidji, Minnesota (fig. 1). Biodegradation has resulted in the formation of a plume of dissolved organic carbon (DOC) downgradient from the oil body. Groundwater in an area called "the spray zone" has been contaminated from vertical infiltration of DOC resulting from biodegradation of oil in the soil column and possibly from photooxidation of oil at the soil surface. This report summarizes and expands on previously reported data characterizing the background DOC and oil-derived DOC from groundwater samples collected in the years 1986–1989 and in 1998 at the Bemidji site (Thorn and Aiken, 1998; Islam and others, 2016). The analytical techniques include elemental analysis, radiocarbon dating, nuclear magnetic resonance (NMR) spectroscopy, and Fourier transform ion cyclotron resonance mass spectrometry (FTICR-MS). The oil-derived DOC is composed primarily of the partial oxidation products of the crude oil in the form of nonvolatile organic acids (NVOAs). The term "partial oxidation products" is intended to include polar metabolites resulting from biodegradation of the crude oil, photochemical oxidation products of the oil, and autoxidation products that may result from introduction of the crude oil into oxic groundwater (for example, autoxidation of sulfides to sulfoxides [Waldo and others, 1991] and abiotic oxidation of steroids to steroid ketones [Charrié-Duhaut and others, 2000]). In this report, as in our previous (Thorn and Aiken, 1998), polar metabolites refer to petroleum constituents that have undergone microbial oxidation but not complete mineralization. They do not refer to expired microbial biomass or detritus. As discussed in the "Site Description" section, biodegradation is the predominant pathway leading to the partial oxidation products at the site. The objectives of the study were to determine (1) to what extent the oil-derived DOC can be distinguished from the naturally occurring background DOC in the aquifer and (2) to what degree of resolution the partial oxidation products of the oil can be traced to their parent constituents in the petroleum. Bemidji is one of the first, if not the first, study sites where the partial oxidation products resulting from biodegradation of crude oil were isolated and characterized as such (Aiken and others, 1987; Thorn, 1987).

Despite decades of research into oil spills, fundamental questions remain, especially in regard to groundwater contamination. Biodegradation pathways, both aerobic and anaerobic, have been determined for only a fraction of the up to 100,000 constituents comprising crude oil. The percentage of crude oil constituents that can be completely mineralized to carbon dioxide (CO_2) or methane (CH_4) microbially in groundwater is unknown, and, at present, there is no evidence to suggest that complete mineralization of all constituents can be expected. From this uncertainty then, the possibility of the development of a refractory pool of polar metabolites from the crude oil may be considered, where factors that contribute to the refractoriness of the naturally occurring background DOC itself pertain to the polar metabolites. These factors include the presence of structural features such as branched alkyl chains or xenophores that impede enzymatic degradation, whether the concentration and metabolic energy yield from individual constituents can sustain microbial populations, the diversity of the microbial populations themselves, and the availability of terminal electron acceptors (Williams, 2000). Furthermore, as the oil body becomes depleted in the most readily biodegradable constituents over time, the composition of the oil-derived DOC downgradient from the oil body may change from partial oxidation products of relatively biodegradable constituents to partial oxidation products of more refractory constituents (for example, resins, asphaltenes, and other high molecular weight constituents). Long-term research at Bemidji has the potential to answer these questions.

Aerobic and Anaerobic Biodegradation

Order of Biodegradation

Most of the older literature on biodegradation of petroleum hydrocarbons has focused on aerobic oxidation (Bossert and Bartha, 1984; Connan, 1984; Peters and Moldowan, 1993), but substantial progress has been made in the determination of anaerobic pathways since the mid 1990s (Gieg and Suflita, 2005; Prince and Walters, 2016). The general sequence of increasing resistance to biodegradation under aerobic conditions follows n-paraffins, isoprenoids, steranes, hopanes/diasteranes, aromatic steroids, and porphyrins (Peters and Moldowan, 1993). Among aromatic constituents, alkylbenzenes, dialkylbenzenes, and trialkylbenzenes are susceptible to microbial attack, but diaromatic and triaromatic fractions containing complex mixtures of alkylated naphthalenes, anthracenes and phenanthrenes are less susceptible. In general, the parent polynuclear aromatic hydrocarbons (PAHs) are degraded before their singly and doubly methylated analogues (Prince and Walters, 2016).

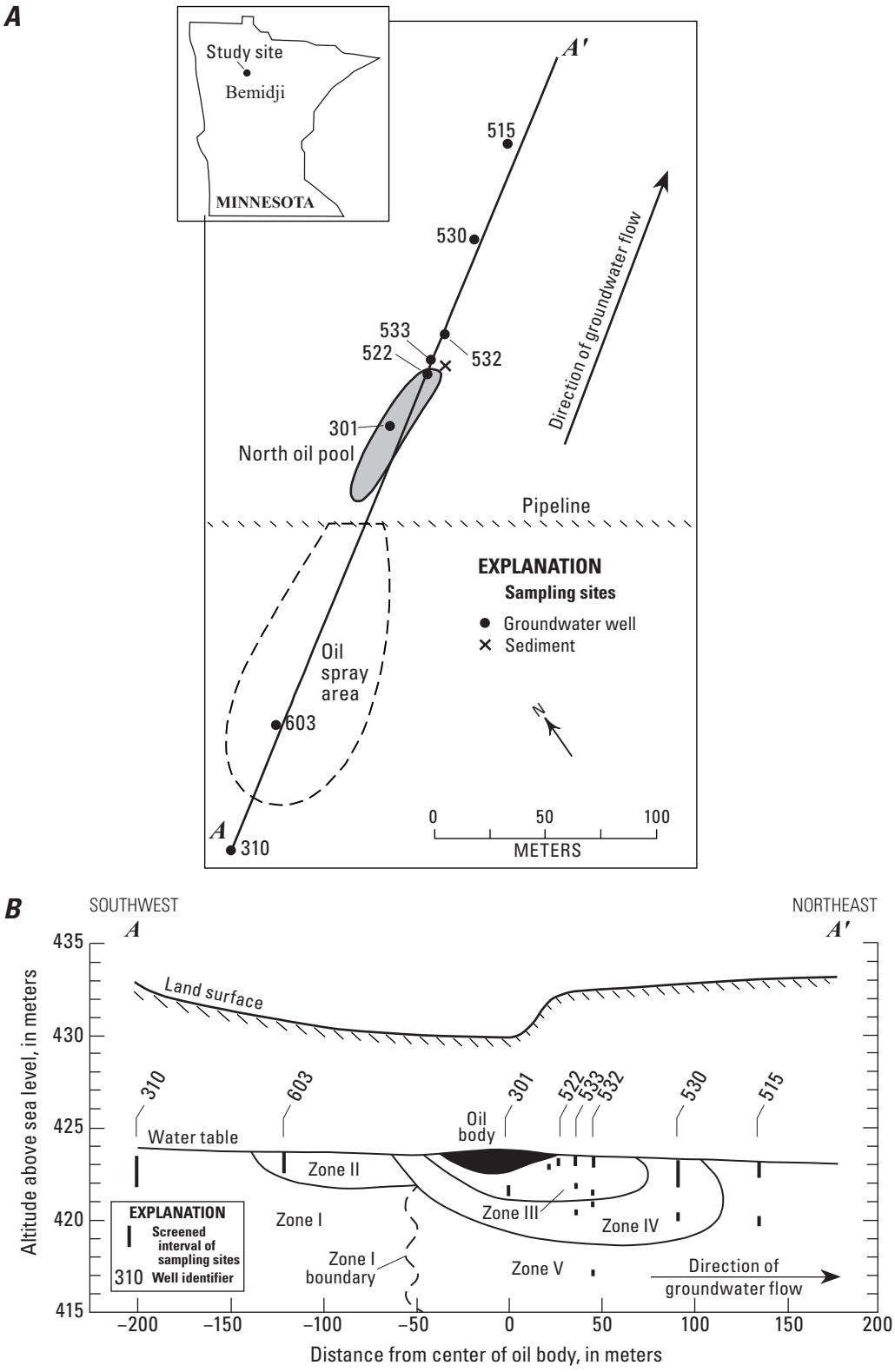

Figure 1. Details of the U.S. Geological Survey Bemidji study site in Minnesota. *A*, Map from Thorn and Aiken (1998) showing the location of wells (numbered) along the A–A′ transect in this study relative to the oil body and the spray zone created from the pipeline break. Index map shows the location of the study site in Minnesota. *B*, Cross section of the oil body showing well locations, the screened interval of sampling sites, and the location of the water table (from Baedecker and others, 1993). Zones I–V are defined by differing concentrations of dissolved organic carbon and dissolved oxygen.

As for aromatic sulfur constituents, benzothiophene and dibenzothiophene (DBT) are readily degraded aerobically (Fedorak, 1990). Kropp and others (1997) suggested the order of susceptibility to biodegradation of methyl-substituted dibenzothiophenes is 3,4-dimethyl-DBT, followed by 2,8-dimethyl-DBT, followed by 4,6-dimethyl-DBT. Highly condensed aromatic and cycloparaffinic systems with four or more condensed rings, resins, and asphaltenes have generally been thought to be most resistant to biodegradation. Asphaltenes in particular have been considered among the most microbially refractory constituents of crude oil, but their transformation by bacteria and fungi has been documented in an increasing number of laboratory studies (Hernández-López and others, 2015; Shahebrahimi and others, 2018; and references in those sources). Still, information on the biodegradation of asphaltenes under field conditions is limited. Anaerobic biodegradation pathways have been determined for several classes of petroleum hydrocarbons, including alkylbenzenes, polynuclear aromatic hydrocarbons, benzothiophenes, alkanes, and cycloalkanes, under a variety of terminal electron-accepting processes (TEAPS; Gieg and Suflita, 2005; Prince and Walters, 2016). The relative susceptibility to biodegradation differs for some classes of hydrocarbons under anaerobic compared to aerobic conditions. For example, mono-alicyclic compounds (unsubstituted, methyl-substituted, and ethyl-substituted cyclopentenes, cyclopentanes, and cyclohexanes) were degraded more rapidly under sulfate reducing and methanogenic conditions than would be expected under aerobic conditions (Townsend and others, 2004; Prince and Walters, 2016). At the Bemidji site, under methanogenesis, n-alkanes in the C_{18} to C_{25} range (18 to 25 carbons) were depleted before n-alkanes in the C_{10} to C_{15} range, opposite from aerobic degradation. Likewise, among n-alkylcyclohexanes, higher molecular weight homologues C_{18} and C_{19} were degraded before lower molecular weight homologues C_{13} and C_{14} (Hostettler and Kvenvolden, 2002; Bekins and others, 2005).

In early work at Bemidji, the detection of aromatic acids such as o-toluic, phenylacetic, 2,6-dimethylbenzoic, and p-methylphenylacetic was taken as evidence that anaerobic degradation of hydrocarbons was a significant process in zone III (fig. 1; Cozzarelli and others, 1990, 1994). For some petroleum constituents, differing aerobic and anaerobic biodegradation mechanisms may lead to the same metabolite, which is a consideration when examining effects of redox conditions on the composition of the oil-derived DOC.

Transformation Pathways

The aerobic oxidation pathways of numerous straight-chain, branched-chain, cyclic-alkane, and aromatic hydrocarbons have been determined. Some of these pathways are illustrated in figure 2, including schemes for n-tridecane (Singer and Finnerty, 1984), cyclohexane (Perry, 1984), cycohexanecarboxylic acid (Perry, 1984), and naphthalene (Cerniglia, 1984). Among the oxygen-containing functional groups formed are primary and secondary alcohols, phenolic hydroxyls, esters, lactones, ketones, aldehydes, quinones, carboxylic acids, and α-keto carboxylic acids. These same functional groups are likely formed during the aerobic oxidation of higher molecular weight constituents of petroleum. Cyclohexanecarboxylic acid proceeds through an aromatization step prior to ring-opening.

Anaerobic biodegradation pathways have been determined for several classes of petroleum hydrocarbons, including alkylbenzenes, polynuclear aromatic hydrocarbons, benzothiophenes, alkanes, and cycloalkanes (Gieg and Suflita, 2005; Prince and Walters, 2016). Of the pathways elucidated to date, the most common activation step is addition to fumarate yielding a substituted succinate (Biegert and others, 1996), followed to a lesser extent, especially in the case of polycyclic aromatics, by carboxylation via incorporation of CO_2 from bicarbonate (fig 3; Zhang and Young, 1997). Examples of the former include toluene, n-dodecane, and methylcyclopentane, and of the latter, naphthalene and phenanthrene. Thus, molecular formulas of the initial fumarate and bicarbonate adducts represent an increase in carbon number over those of their parent substrates. A limited number of substrates are oxidized to alcohols with the oxygen from water such as ethylbenzene and propylbenzene by means of *Azoarcus* bacteria (Rabus and Widdel, 1995; Ball and others, 1996; Prince and Walters, 2016).

Site Description

The site has been described in several reports (Eganhouse and others, 1993; Thorn and Aiken, 1998; Essaid and others, 2011; Ng and others, 2014; Bekins, 2019; U.S. Geological Survey, 2021). The major features are reiterated here. On August 20, 1979, a pipeline break resulted in the spill of approximately 1.7 x 10^6 liters (L; 10, 700 barrels) of a light aliphatic crude oil onto glacial outwash deposits. The oil sprayed over an area of about 6,500 square meters (m^2) (referred to as the "spray zone") and collected in a wetland and topographic depressions where the crude oil infiltrated through the unsaturated zone to the water table resulting in three subsurface oil bodies termed the north, middle, and south pools. An estimated 1.1 x 10^6 L (6,800 barrels) of the oil were removed through pumping of surface pools and trenches and 0.2 x 10^6 L (1,300 barrels) were removed through burning and excavation of soil, leaving approximately 0.4 x 10^6 L (2,600 barrels) in the subsurface after cleanup efforts were completed. The average linear velocity of groundwater flow has been estimated at 22 meters per year (m/year) (Essaid and others, 2011). From 1999 to 2004, a second remediation effort removed approximately 1.14 x 10^5 L of oil (about 27 percent of remaining oil) from the north, middle, and south pools using a pump and skim operation (Delin and Herkelrath, 2014). The oil body referred to in this report and illustrated in figure 1 is the north oil pool.

One of the most notable features documented at the site has been the development over time of a plume of DOC downgradient from the north oil body in the direction of

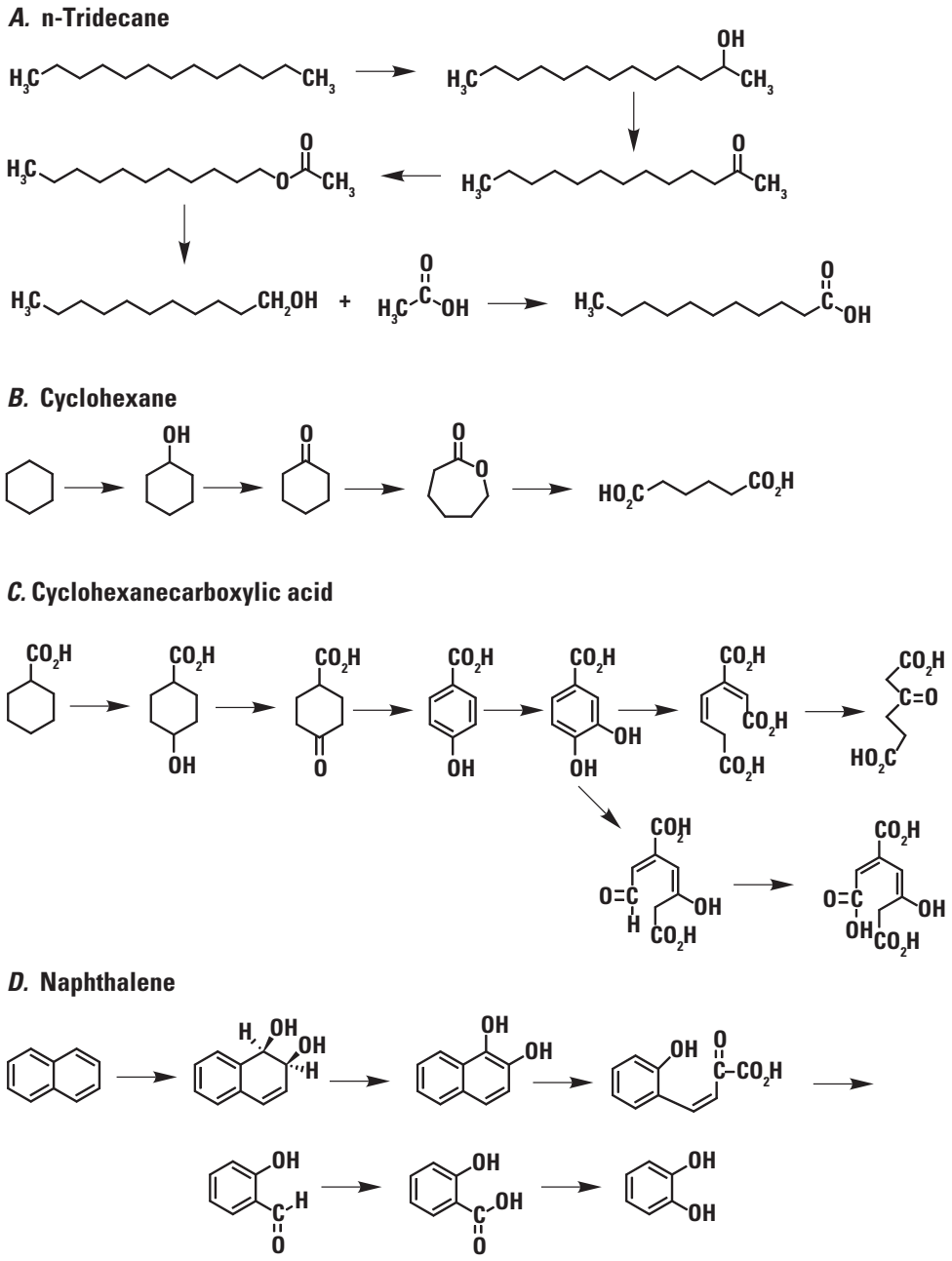

Figure 2. Illustrations of aerobic biodegradation pathways (modified from Thorn and Aiken, 1998). *A*, Subterminal oxidation of n-tridecane according to Singer and Finnerty (1984). *B*, Catabolism of cyclohexane according to Perry (1984). *C*, Biodegradation of cyclohexanecarboxylic acid via aromatization according to Perry (1984). *D*, Bacterial oxidation of naphthalene according to Cerniglia (1984). (C, carbon; H, hydrogen; O, oxygen)

groundwater flow as a result of aerobic followed by anaerobic biodegradation. The succession of terminal electron-accepting processes proceeded through molecular oxygen (O_2) reduction, manganese reduction, iron reduction, and then methanogenesis (Ng and others, 2014). The resulting dissolved methane plume has subsequently undergone attenuation through iron-mediated anaerobic methane oxidation (Amos and others, 2012). The predominant microbial physiologic types in the anaerobic zones have been identified as iron reducers, heterotrophic fermenters, and methanogens (Bekins and others, 1999). Nitrate and sulfate concentrations are low in the aquifer and do not play a significant role as terminal electron acceptors at the site. Hydrogen sulfide concentrations were typically less than (<) 0.05 milligrams per liter (mg/L). As of 2013, the nonvolatile fraction of the DOC plume (NVDOC) continued to expand laterally, reaching approximately 250 m from the center of

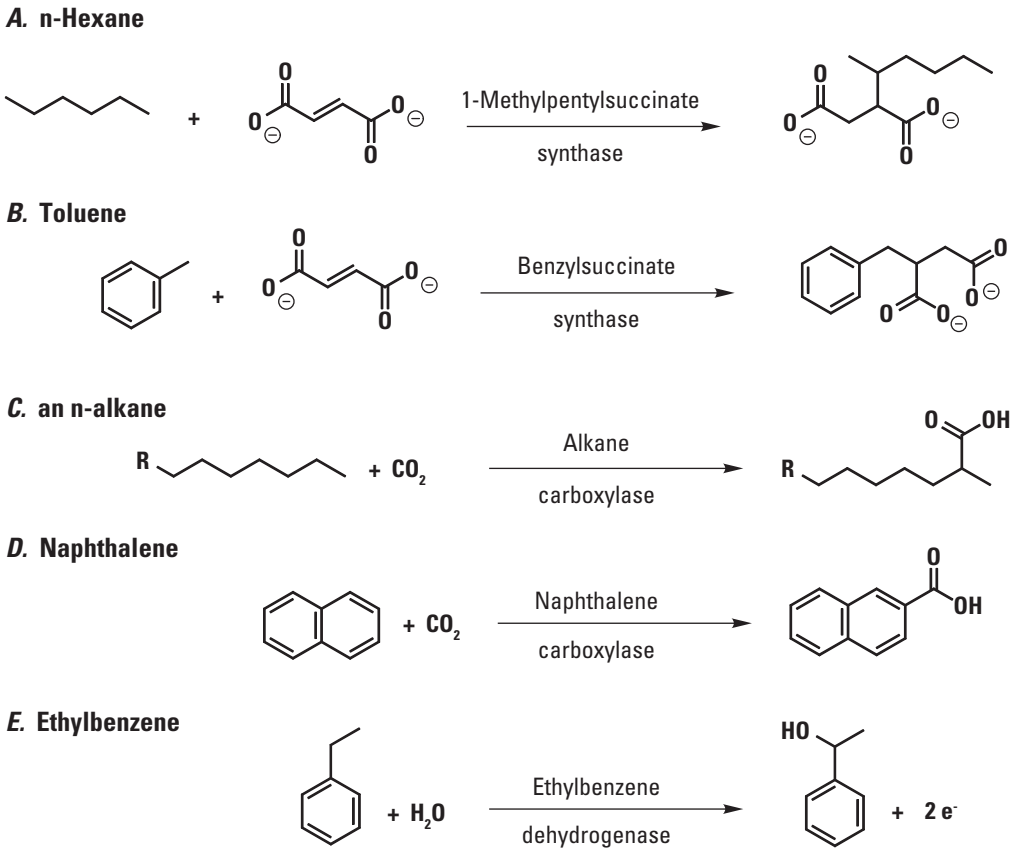

Figure 3. Illustrations of initial steps of anaerobic biodegradation pathways (Gieg and Suflita, 2005; Prince and Walters, 2016). *A*, Fumarate addition to n-hexane (modified from Biegert and others, 1996). *B*, Fumarate addition to toluene (modified from Biegert and others, 1996). *C*, Incorporation of bicarbonate into an n-alkane (modified from Zhang and Young, 1997). *D*, Incorporation of bicarbonate into naphthalene (modified from Zhang and Young, 1997). *E*, incorporation of oxygen abstracted from water into ethylbenzene (modified from Rabus and Widdel, 1995; Ball and others, 1996). (C, carbon; e-, electron; H, hydrogen; O, oxygen; R, attached group)

the oil body, while also increasing in concentration (Bekins and others, 2016). The NVDOC now represents the greatest source of reducing capacity in the downgradient region of the contaminant plume (Amos and others, 2012). A conceptual cross section of the site illustrating the microbial processes is presented in figure 4 (Ng and others, 2014).

As of 1990, biodegradation had resulted in the development of distinct zones in the aquifer where the groundwater chemistry was controlled by different processes (zones I–V, fig. 1). The five zones were delineated based on distributions of pH, molecular oxygen (O_2), total dissolved inorganic and organic carbon (TDIC and TDOC), methane (CH_4), sulfate (SO_4^{2-}), hydrogen sulfide (H_2S), nitrate (NO_3^-), ammonium (NH_4^+), ferrous iron (Fe^{2+}), manganese (Mn^{2+}) and carbon-13 to carbon-12 ratio ($\delta^{13}C$) values (fig. 1; Baedecker and others, 1993). The descriptions of the zones in figure 1 are relevant to the NVOA samples isolated during 1986–1989 and in 1998 for this study, but the boundaries of the zones have evolved since 1998, as shown in figure 4, which shows the boundaries as of 2016. Zone I in figure 1, upgradient of the oil body, represents oxygenated, uncontaminated groundwater with a naturally occurring DOC of approximately 3 milligrams of carbon per liter of groundwater (mg C/L). The DOC in zone II (the spray zone) rises to approximately (~) 16 mg C/L, either from vertical infiltration of DOC resulting from biodegradation of crude oil in the overlying unsaturated zone or from vertical infiltration of crude oil followed by degradation in the saturated zone. Infiltration of DOC from photooxidation of oil at the soil surface is also a possibility, and research is currently underway to establish if this is a relevant process at the site. Zone III represents the anoxic groundwater in contact with the oil body. It extends about 75 m downgradient and a few meters upgradient from the oil body, with a thickness of about 3 m (fig. 1). The DOC in zone III is in excess of 45 mg C/L. The primary processes coupled with the oxidation of hydrocarbons in the anoxic zone are reduction of iron and manganese minerals and methanogenesis. Zone IV consists of groundwater surrounding the anoxic zone and represents a transition area between highly contaminated groundwater in the anoxic zone and slightly contaminated groundwater at the downgradient edge of the plume that had near background concentrations of dissolved aqueous species. Groundwater in zone IV had low

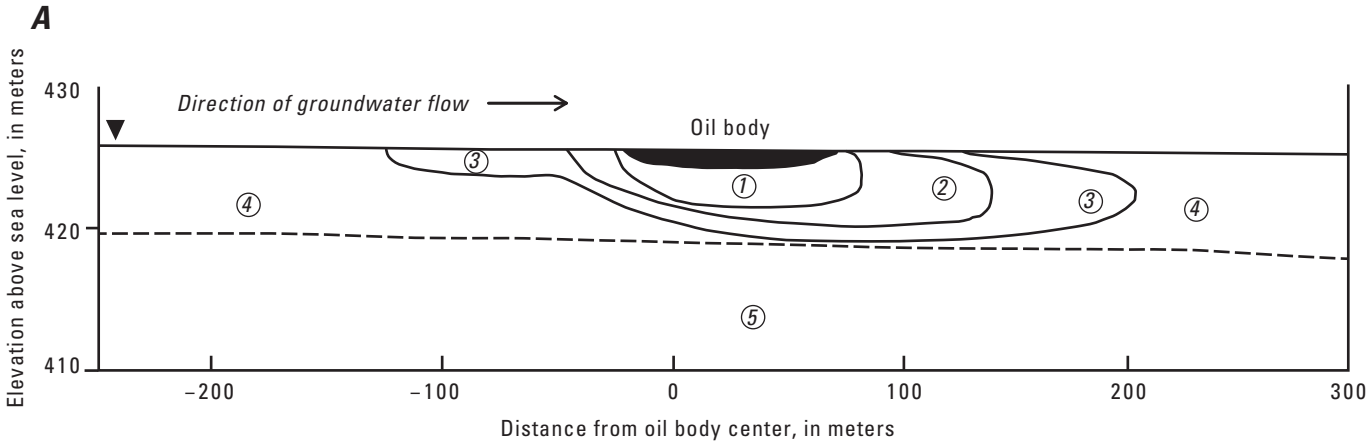

Zone	Redox	DO (µg/L)	Benzene (µg/L)	Dissolved Fe (mg/L)	Dissolved As (µg/L)
1	Anoxic; methanogenic	Low (<100)	High (>1,000)	High (>25)	High (>50)
2	Anoxic; Fe-reducing	Low (<100)	Moderate (15–1,000)	Moderate (1–25)	Moderate (10–50)
3	Suboxic; "transition"	Moderate (100–1,000)	Low (5–15)	Low (0.5–1.0)	Low (1–10)
4	Oxic	High (>1,000)	Negligible (<5)	Negligible (<0.5)	Negligible (<0.5)
5	Suboxic	Moderate (100–1,000)	Negligible (<5)	Low (0.5–1.0)	Low (1–10)

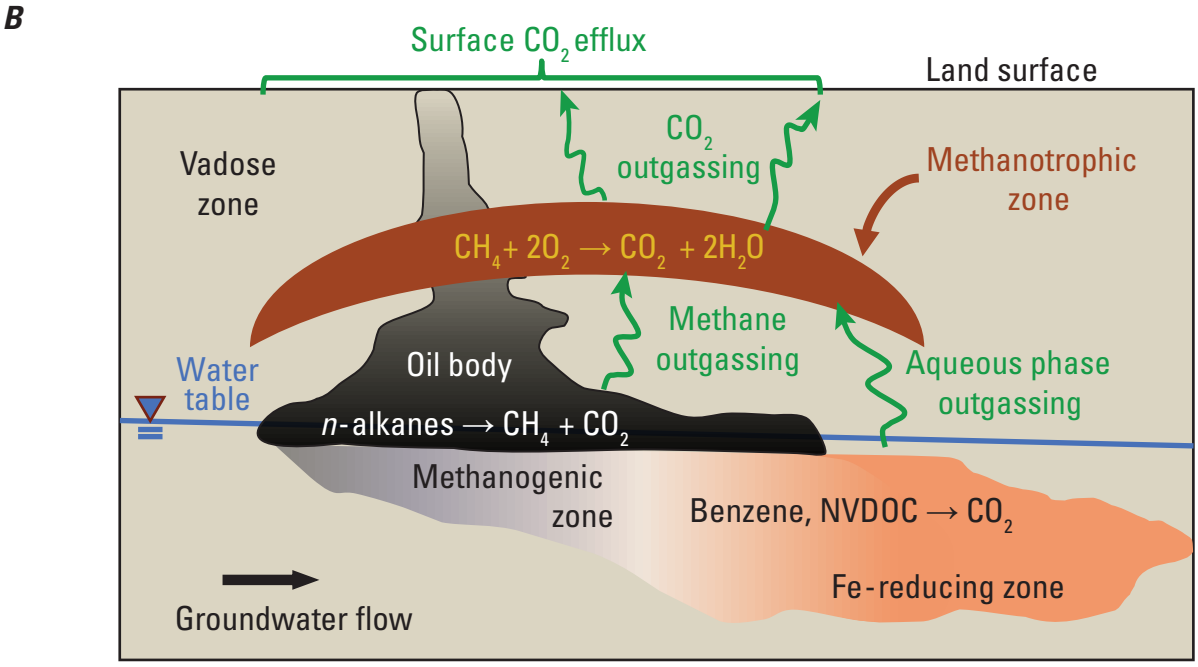

Figure 4. Conceptual cross sections illustrating the microbial processes at the Bemidji Research Site. *A*, Model for general redox zones in proximity to the north oil body as of 2016 (from Cozzarelli and others, 2016). *B*, Site conceptualization model (modified from Sihota and others, 2011; Ng and others, 2014). The site conceptual model of microbial activity shows the methanotrophic zone and iron-reducing zones. (>, greater than; <, less than; As, arsenic; CH_4, methane; CO_2, carbon dioxide; DO, dissolved oxygen; Fe, iron; H_2O, water; µg/L, micrograms per liter; mg/L, milligrams per liter; NVDOC, nonvolatile dissolved organic carbon; O_2, oxygen)

concentrations of O_2 (< 0.03 millimolar) and DOC concentrations reaching 21 mg C/L. Farther downgradient from the plume, Zone V represents oxygenated groundwater where the DOC declines to near-background levels.

More recent work at the site has addressed the potential toxicities of the oil-derived DOC within 100 m of the north pool and the ability of optical spectroscopy to monitor the development and migration of the contaminant plume. Total extracts of nonvolatile compounds from wells located within 100 m of the north oil pool exhibited increased activity of toxicologically relevant transcriptional pathways and human nuclear receptors in human liver cells (McGuire and others, 2018; Bekins and others, 2020). Excitation emission matrix spectrum (EEMS) analyses indicated a shift in fluorescent dissolved organic matter (DOM) from short to long wavelength along the contaminant plume transect downgradient from the oil body (Podgorski and others, 2018a). Solid-phase extracts of DOC isolated in 2016 have been the subject of further NMR and FTICR-MS analyses (Podgorski and others, 2021). DOC isolated by liquid-liquid extraction (methylene chloride) from water samples collected in 2016 were analyzed by two-dimensional gas chromatography time-of-flight mass spectrometry (GCxGC TOF MS) and Orbitrap electrospray ionization mass spectrometry (ESI-MS; O'Reilly and others, 2019; Mohler and others, 2020).

Methods

Sample Isolation

Preparative isolations of DOC fractions were performed in June 1986, May 1987, May 1989, and August 1998. Wells 530, 532, and 533 were sampled in 1986, wells 310, 603, 532, 530, 522, and 515 in 1987, and wells 530 and 310 in 1989. Wells 530 and 603 were sampled again on August 3, 1998. The isolation procedure was described in Thorn and Aiken (1998). In brief, water samples were passed through Balston filters, acidified to a pH of 2 with hydrochloric acid (HCl), and pumped through a two-column array of XAD-8 and XAD-4 resins according to the procedure described in Aiken and others (1992). Hydrophobic acids (HPOA) and the hydrophobic neutral fraction (HPON) of organic acids adsorb to the XAD-8 resin, whereas hydrophilic acids (HPIA) adsorb to the XAD-4 resin. Hydrophobic acids were eluted from XAD-8 and hydrophilic acids from XAD-4 with 0.1 Normal sodium hydroxide. The XAD-8 was re-acidified, and the hydrophobic neutrals were subsequently eluted with 50 percent acetonitrile. The acetonitrile was removed from the eluates under a rotary evaporator, and the remaining aqueous solutions were freeze dried. Some volatile hydrocarbons co-eluted with the hydrophobic neutral fractions from the contaminated wells but were removed during concentration on the rotary evaporator. The HPOA, HPON, and HPIA fractions are collectively referred to as nonvolatile organic acids (NVOAs) in this report.

The DOC and dissolved oxygen (DO) concentrations of the wells are listed in table 1. For well 532, 1986 values are unavailable, so 1987 values are reported. Transformed crude oil constituents in well 603 (Zone II, spray zone) result from aerobic biodegradation, with the possibility of photochemical oxidation from residual crude oil at the soil surface. Transformed crude oil constituents in wells 533 (Zone III), 532 (Zone III), and 530 (Zone IV), downgradient from the oil body, result primarily from anaerobic biodegradation, although aerobic biodegradation can occur on the fringes of the contaminant plume in contact with aerobic water. Transformed crude oil constituents in well 515 (Zone V) likely result from a combination of anaerobic and aerobic biodegradation. The proportions of anaerobic versus aerobic biodegradation from the oil body itself have been estimated at 15–17 percent and 83–85 percent, respectively (Essaid and others, 2003; Amos and others, 2012). If photodegradation occurred at the soil surface of the spray zone and photo-oxidized constituents percolated into the Zone II groundwater, it is possible these constituents were transported

Table 1. Dissolved organic carbon (DOC) and dissolved oxygen (DO) concentrations of sampled wells at the Bemidji research site in Minnesota.

[m, meters; mg C/L, milligrams of carbon per liter of groundwater; mg/L, milligrams per liter; ND, not determined]

Sample	Distance[1] (m)	Zone	DOC (mg C/L)	DO (mg/L)	Sample	Zone	DOC (mg C/L)	DO (mg/L)
1987 310	−200	I	2.9	9.1				
1987 603	−100	II	15.0	7.6	1998 603	II	ND	8.8
1986 533	39	III	ND	ND				
[2]1987 532	45.7	III	31.5	0.0				
1986 530	91.3	IV	21.0	[3]0.3	1998 530	IV	24.0	0.3
1987 515	137	V	8.1	0.8				

[1]Distance from the center of oil body (north oil pool) in meters. Positive and negative distances correspond to wells downgradient and upgradient of the oil pool, respectively.

[2]1986 values are unavailable.

[3]Value is from 1987.

downgradient into the location of well 530 by 1986, assuming a groundwater velocity of 22 m/year. At this velocity, aerobically biodegraded constituents from the spray zone could also have reached well 530 by 1986.

For the 1998 sampling, the HPOA, HPON, and HPIA fractions comprised 77, 12, and 10 percent of the well 530 NVOAs, and 79, 12, and 7 percent of the well 603 NVOAs, respectively. The solvent eluate of the XAD-4 resin was a minor fraction of the well 603 NVOAs at 2 percent.

Elemental Analyses, Vapor Pressure Osmometry, and Carbon-14 Dating

Elemental analyses and vapor pressure osmometry (VPO) measurements were performed by Huffman Hazen Laboratories in Golden, Colorado. Carbon-14 ages and $\delta^{13}C$ values were determined at the University of Arizona Accelerator Mass Spectrometry laboratory in Tucson, Arizona for the 1986–1989 samples and at the National Ocean Sciences Accelerator Mass Spectrometry facility of Woods Hole Oceanographic Institute, Woods Hole, Massachusetts for the 1998 samples.

Crude Oil Chromatography (Saturate, Aromatic, Resin, and Asphaltene Fractionation)

Crude oil was taken in 1987 from well 301 at the center of the oil body. It was found to be essentially identical in all major characteristics to a reference sample of the oil obtained from the pipeline company after the spill in 1979 (Eganhouse and others, 1993). Fractionation of the whole crude oil from well 301 was performed using column chromatography. The asphaltenes were precipitated with pentane. The pentane soluble fraction of the whole crude oil (maltene fraction) was chromatographed on silica gel (100–200 mesh) into saturate (heptane elution), aromatic (benzene elution), and resin (50 percent benzene:methanol elution) fractions. Number average molecular weights for the asphaltene and resin fractions were determined from four concentration points using VPO. The solvents for the VPO measurements of the asphaltene and resin fractions were benzene and chloroform, respectively.

Functional Group Derivatizations (Spin Labelling) for Nuclear Magnetic Resonance Analyses

Selective samples were derivatized with isotopically labeled reagents. The 1987 310 HPOA, 1986 530 HPOA, and 1989 530 HPON samples were dissolved in dimethylformamide and methylated with ^{13}C-labeled diazomethane generated from *N*-Methyl-^{13}C-*N*-nitroso-*p*-toluenesulfonamide, 99 atom percent ^{13}C (chemical is from Cambridge Isotope Laboratories). The 1987 603 HPON sample was methylated using a phase transfer catalysis (PTC) procedure, which employed tetrahydrofuran as the solvent, methyl iodide (99 atom percent ^{13}C; chemical is from Sigma-Aldrich), and tetra-n-butyl ammonium hydroxide (40 percent, chemical is from Sigma-Aldrich; Rose and Francisco, 1987). The 1989 530 HPON sample, 260 milligrams (mg), was refluxed for 3 hours in 50 milliliters (mL) of methanol with 50 microliters µL aniline, 99 atom percent ^{15}N (chemical is from ISOTEC International Inc.).

Nuclear Magnetic Resonance Spectroscopy

Liquid-state carbon-13 (^{13}C) and nitrogen-15 (^{15}N) NMR spectra were recorded on a Varian XL300 or Gemini 2300 NMR spectrometer at resonant frequencies of 75.4 and 30.4 megahertz, respectively. Carbon-13 spectra of the crude oil and saturate, aromatic, resin, and asphaltene (SARA) fractions were recorded in deuterated chloroform ($CDCl_3$), 99.9 atom percent ^{12}C, as previously described in Thorn and Aiken (1998). The ^{13}C analyses of the HPOA or HPIA fractions were recorded on sodium salts of the samples in deuterium oxide (D_2O) or on the H^+-saturated (hydrogen-saturated) samples dissolved in dimethyl-^{12}C, d_6 sulfoxide. For aqueous phase analysis, approximately 100–150 mg of the H^+-saturated sample was titrated to a pH of 6 with 0.1 Normal sodium hydroxide (NaOH), freeze dried, and redissolved in 1.5 mL D_2O and 0.5 mL water (H_2O; 10-millimeter NMR tube). Dioxane (67.4 parts per million; ppm) was used as an external reference standard. Samples recorded in deuterated dimethyl sulfoxide (dmso-d_6) were referenced on the solvent peak. Quantitative ^{13}C NMR spectra employed a 50,000 hertz (Hz) spectral window, 45-degree (°) pulse angle, 0.2 second acquisition time, 7.0 to 10.0 second pulse delay, and inverse gated decoupling.

An advantage of recording the H^+-saturated samples in dmso-d_6 is that a greater signal-to-noise ratio can be achieved per unit of spectrometer time compared to comparable concentrations of the sodium salts in D_2O, a consideration when multiple NMR experiments are performed on the same sample (Thorn and others, 1989). The greater signal-to-noise ratio is due in part to the fact that the lower dielectric constant of the sample in dmso-d_6 results in less sample heating from proton decoupling. It is noteworthy that, in aqueous solution, the ^{13}C NMR chemical shifts of carboxylic acid carbons change as a function of pH, moving downfield as the carboxylic acid group is converted from the H^+-saturated form at low pH to the H^+-dissociated form at high pH. For example, the carboxylic acid carbon of butyric acid in aqueous solution moves downfield from 178.4 ppm to 183.7 ppm as the pH is increased from 2 to 13 (Thorn and others, 1989). Phenolic carbons likewise move downfield as phenolic hydroxyls are converted to phenolate anions with increasing pH. Spectra of H^+-saturated natural organic matter (NOM) samples recorded in dmso-d_6 frequently exhibit a splitting of the carboxyl carbons into separate peaks at approximately 167–168 ppm and 172–174 ppm, the former corresponding to benzenecarboxylic acids and α,β-unsaturated carboxylic acids, and the latter to alkyl, benzylic, and ortho-hydroxybenzene carboxylic acids.

Acquisition parameters for the refocused insensitive nuclei enhancement by polarization transfer (INEPT) ^{15}N spectrum (proton decoupled; Morris and Freeman, 1979) included a 15,649.5 Hz spectral window, 0.5 second acquisition time, 90 ° pulse angle, and 2.0 second pulse delay for proton relaxation. The polarization transfer time and refocusing delay were set equal to 1/4 J, or 2.78 millisecond (assuming $^1J_{NH}$=90.0 Hz, where $^1J_{NH}$ is the one bond nitrogen to proton coupling constant), values optimal for signal enhancement of singly protonated nitrogens. Parameters for the alternating compound one-eighties used to suppress transients in the coil (ACOUSTIC; Patt, 1982) spectrum included a 15,649.5 Hz spectral window, 0.5 second acquisition time, 90 ° pulse angle, 2.0 second pulse delay, and tau pulse delay of 0.1 millisecond. Neat formamide (112.4 ppm) was used as an external reference standard. Nitrogen-15 NMR chemical shifts are reported in ppm downfield from ammonia, taken as 0.0 ppm.

Solid-state constant amplitude cross polarization/magic angle spinning (CP/MAS) ^{15}N NMR spectra were recorded on a Chemagnetics CMX-200 spectrometer at 20.3 megahertz using a 7.5-millimeter ceramic probe (zirconium pencil rotors). Acquisition parameters included a 26.0-kilohertz spectral window (1,315.3 ppm), 17.051 millisecond acquisition time, 0.2 second pulse delay, 2.0 millisecond contact time, and spinning rate of 5 kilohertz. Nitrogen-15 NMR chemical shifts were referenced to glycine, taken as 32.6 ppm, and are reported downfield from ammonia, taken as 0.0 ppm.

Mass Spectrometry and Spectral Interpretation

Analytical samples were prepared by diluting each of the resin eluate samples to 0.1 milligrams per milliliter in a high-pressure liquid chromatography (HPLC)-grade mixture of 50 percent toluene and 50 percent methanol. The prepared samples were directly injected with a syringe pump (equipment from Harvard, Holliston, MA) at a flow rate of 500 microliters per hour (µL/h) for negative-mode (-) electrospray ionization (ESI) analysis coupled with a 15 Tesla FTICR-MS (equipment from Korea Basic Science Institute, Ochang-eup, Korea). ESI sources were purchased from Bruker Daltonics in Billerica, MA. Nitrogen was used as the drying and nebulizing gas. Typically, a nebulizing temperature of 350 degrees Celsius (°C) was used with a flow rate of 2.0 L per minute. The drying gas temperature was 210 °C with a flow rate of 2.3 L per minute, and the spray voltage was maintained between 2,500 and 3,500 volts (V). The skimmer voltage was set to 15.0 V to minimize in-source fragmentation. Each sample was analyzed three times, and the data were found to be reproducible with an error of less than 5 percent. High resolution and mass accuracy were achieved by obtaining 4 Megabyte Word data points for each spectrum. A resolution (m/m_{50}) of 500,000 at 400 m/z was routinely obtained (m is mass and m/z is the mass to charge ratio).

Spectral interpretation was performed using the Statistical Tool for Organic Mixtures' Spectra software (STORMS 1.0) with an automated peak-picking algorithm for more reliable and faster results (Hur and others, 2009). Elemental formulae were calculated from the calibrated peak list and assigned based on m/z values, within an error range of 1 ppm. Normal conditions for petroleum data ($C_cH_hN_nO_oS_s$, c unlimited, h unlimited, $0 \le n \le 5$, $0 \le o \le 5$, $0 \le s \le 4$) were used for these calculations (≤, less than or equal to). Double-bond equivalent (DBE) values represent the sum of the number of rings and the number of carbon double bonds in a given molecular formula. DBE values can be calculated for the elemental formula $C_cH_hN_nO_oS_s$ using equation 1:

$$DBE = c - h/2 + n/2 + 1, \quad (1)$$

where:

c is number of carbons;
h is number of hydrogens; and
n is number of nitrogens.

Quantitation in Nuclear Magnetic Resonance and Fourier Transform Ion Cyclotron Resonance Mass Spectrometry

When appropriate pulse sequences and acquisition parameters are used, NMR has the potential to detect all ^{13}C and ^{15}N nuclei quantitatively in samples of multicomponent mixtures. In this study, inverse gated decoupled (IGD) liquid-state ^{13}C NMR spectra of the naturally abundant ^{13}C nuclei in the crude oil and NVOA fractions employed acquisition parameters for quantitative accuracy, in other words, peak areas accurately reflect the number of ^{13}C nuclei resonating. These acquisition parameters include inverse gated decoupling to eliminate nuclear Overhauser enhancement (NOE) effects and pulse delays 3–5 times the longest spin lattice relaxation times (T_1s) present in the samples to eliminate differential saturation effects. In (-) ESI FTICR-MS on the other hand, of the molecules which are ionized under negative electrospray ionization, the relative abundance of individual assigned molecular formulas is dependent on the relative ionization efficiency of the individual constituent, so accurate quantitation is not guaranteed.

Results

Elemental Analyses

The following SARA fractionation of the crude oil was reported by Eganhouse and others (1993): 58–61 percent saturates, 33–36 percent aromatics, 4–6 percent resins, and 1–2 percent asphaltenes. Elemental analyses of the whole crude oil and crude oil fractions are characteristic for an oil characterized as paraffinic/paraffinic-naphthenic (table 2). The oxygen (O), nitrogen (N), and sulfur (S) heteroatoms are concentrated in the aromatic, resin, and asphaltene fractions. Most significantly, the elemental sulfur contents of the aromatic, resin, and asphaltene fractions are 2.54, 2.86, and 3.09 percent, respectively.

Table 2. Elemental analyses, number average molecular weights, and carbon-13 nuclear magnetic resonance aromaticities (f_a) for nonvolatile organic acid fractions, crude oil, and crude oil fractions at the Bemidji research site in Minnesota.

[Carbon (C), hydrogen (H), oxygen (O), nitrogen (N), and sulfur (S) are reported on an ash and moisture-free basis. C/M, number of carbons per molecule by vapor pressure osmometry; f_a, carbon-13 nuclear magnetic resonance aromaticity; M_n, number average molecular weight determined by vapor pressure osmometry; N, nitrogen; O, oxygen; <, less than; —, not determined]

Sample name	C	H	O	N	S	Ash	C/H	O/C	C/N	M_n	C/M	f_a
Whole crude oil	86.41	12.83	0.47	0.38	0.64	<0.01	6.7	0.01	227.4	—	—	0.17
Saturate fraction	86.0	14.55	0.17	0.02	0.03	<0.05	5.9	<0.01	4300.0	—	—	0.04
Aromatic fraction	86.45	9.42	1.20	0.36	2.54	1.27	9.2	0.01	240.1	—	—	0.51
Resin fraction	80.02	9.59	5.12	1.37	2.86	0.28	8.3	0.06	58.4	586	39	0.33
Asphaltene fraction	86.45	7.22	2.58	1.39	3.09	<0.1	12.0	0.03	62.2	3598	259	0.63
1987 310 HPIA[1]	52.20	5.05	40.34	1.75	0.67	2.02	10.3	0.77	29.8	513	22	0.17
1987 310 HPOA[1]	55.95	5.88	37.08	0.71	0.39	5.06	9.5	0.66	78.8	536	25	0.18
1987 603 HPIA[1]	50.62	5.8	39.69	0.72	3.13	4.20	8.7	0.78	70.3	—	—	0.19
1987 603 HPOA[1]	62.5	6.4	27.8	0.4	2.71	3.8	9.8	0.44	156.3	—	—	0.24
1987 603 HPON	64.32	7.63	24.44	0.18	3.42	19.92	8.4	0.38	357.3	—	—	—
1998 603 HPIA	—	—	—	—	—	—	—	—	—	—	—	0.12
1998 603 HPOA	60.02	6.11	31.41	0.38	2.08	5.46	9.8	0.52	157.9	—	—	0.21
1998 603 HPON	65.7	6.5	24.3	0.9	3.0	1.9	10.1	0.37	73.0	—	—	—
1986 530 HPIA[1]	52.66	5.52	38.99	1.27	1.56	3.26	9.5	0.74	41.5	412	18	0.16
1986 530 HPOA[1]	62.18	6.75	29.09	0.32	1.66	2.32	9.2	0.47	194.3	362	19	0.19
1989 530 HPON	67.47	7.27	22.56	0.49	2.85	3.53	9.3	0.33	137.7	395	22	0.27
1998 530 HPIA	—	—	—	—	—	—	—	—	—	—	—	0.06
1998 530 HPOA[1]	60.85	6.38	30.42	0.43	1.91	4.44	9.5	0.50	141.5	—	—	0.12
1998 530 HPON[1]	62.86	7.46	22.71	0.38	6.28	0.6	8.4	0.36	165.4	—	—	0.20
1987 515 HPOA	62.53	6.4	28.57	0.38	1.93	3.57	9.8	0.46	164.6	417	—	0.22

[1]Sample is analyzed by Fourier transform ion cyclotron resonance mass spectrometry.

Comparing the background 1987 310 HPOA and HPIA fractions, characteristically of these two fractions from most natural waters, the HPOA has lower oxygen and nitrogen contents than the HPIA fraction. The HPIA is the more oxidized fraction.

All five HPOA fractions from contaminated wells 1986 530, 1998 530, 1987 603, 1998 603, and 1987 515 contain higher carbon and sulfur but lower oxygen and nitrogen contents than the background well 1987 310 HPOA fraction. The two HPIA fractions from contaminated wells 1986 530 and 1987 603 contain higher sulfur but lower oxygen and nitrogen contents than the background well 1987 310 HPIA fraction, although the differences in oxygen content are less pronounced than in the HPOA fractions.

Elemental analyses are not available for the 1987 310 HPON fraction, so comparison with the HPON fractions from contaminated wells is not possible. For the 1986–1989 530 and 1987 603 contaminant well fractions, carbon contents successively decrease, and oxygen contents increase from HPON to HPOA to HPIA, illustrating the trend in relative oxidation states among these three fractions. This trend also pertains to the 1998 530 and 1998 603 HPON and HPOA fractions. Thus, the HPON fraction contains the least oxidized and the HPIA fraction the most oxidized petroleum constituents.

All HPIA, HPOA, and HPON fractions from contaminated wells contain significant concentrations of sulfur (greater than or equal to 1.66 percent), which may be considered a signature for an origin in part from the sulfur-containing constituents of the crude oil. The concentrations of sulfur in the HPON fractions are especially noteworthy, all at about 3 percent and as high as 6.28 percent in the 1998 530 sample. In contrast, elemental sulfur contents for 1987 310 HPOA and HPIA are 0.39% and 0.67%, respectively.

Radiocarbon Dating

The ^{14}C ages, in years before present (ybp), with their corresponding values for fraction modern carbon, as well as $\delta^{13}C$ values of the NVOA isolates, are listed in table 3, and fraction modern carbon values are plotted in figure 5. The ^{14}C ages of the 1987 310 HPOA and HPIA samples are both post-bomb (post 1950; fraction modern carbon values of 1.2

Table 3. Carbon-14 and carbon-13 to carbon-12 ratio ($\delta^{13}C$) ages for nonvolatile organic acid fractions isolated from samples collected at the Bemidji research site in Minnesota.

[Post bomb indicates the sample is younger than 1950. m, meters; HPIA, hydrophilic acid; HPOA, hydrophobic acid; HPON, hydrophobic neutral; ybp, years before present; —, not determined]

Distance[1] (m)	Well	Fraction modern carbon	Radiocarbon age (ybp)	$\delta^{13}C$	Well	Fraction modern carbon	Radiocarbon age (ybp)	$\delta^{13}C$
−200	1987 310 HPOA	1.1519±0.0253	Post bomb	−27.0	—	—	—	—
−200	1987 310 HPIA	1.1147±0.0075	Post bomb	−26.4	—	—	—	—
−100	—	—	—	—	1998 603 HPON	0.1062±0.0018	18,013±140	−27.43
−100	—	—	—	—	1998 603 HPOA	0.1473±0.0019	15,385±100	−27.39
−100	—	—	—	—	1998 603 HPIA	0.4667±0.0018	6,105±30	−26.57
91.3	1989 530 HPON	0.2254±0.0028	11,980±105	−27.0	1998 530 HPON	0.0941±0.0019	18,985±160	
91.3	1986 530 HPOA	0.2342±0.0026	11,661±89	−27.7	1998 530 HPOA	0.1610±0.0018	14,671±90	−27.35
91.3	1986 530 HPIA	0.5568±0.0042	4,700±55	−25.9	1998 530 HPIA	0.4722±0.0020	6,028±35	−26.25
137	1987 515 HPOA	0.2645±0.0034	10,680±100	−27.4	—	—	—	—
137	1987 515 HPIA	0.6376±0.0054	3,615±67	−25.9	—	—	—	—

[1]Distance in meters from center of oil body (north oil pool). Positive and negative distances correspond to wells downgradient and upgradient of the oil pool, respectively.

and 1.1, respectively), indicating that these groundwater fulvic and hydrophilic acids are recently derived from the native vegetation overlying the aquifer. The ^{14}C ages of 11,980, 11,666, and 4,700 ybp for the 1989 530 HPON, 1986 530 HPOA, and 1986 530 HPIA samples, respectively and the ^{14}C ages of 10,680 and 3,615 ybp for the 1987 515 HPOA and HPIA samples, respectively confirm that these isolates contain partial oxidation products of the crude oil. The decrease in ^{14}C ages and the increase in fraction modern carbon values in the sequence of HPON followed by HPOA followed by HPIA within the 1986 530 water sample indicate a decreasing contribution of the crude oil to the NVOAs in that order. Wells 530 (DOC=21) and 515 (DOC=8.1) are located 91.3 m and 137 m downgradient from the oil body, respectively. The fraction modern carbon values of the farther-downgradient 1987 well 515 HPOA and HPIA samples are 0.2645 and 0.6376, respectively. They are higher than the corresponding 1986 well 530 HPOA and HPIA fraction modern carbon values of 0.2342 and 0.5568, respectively, which likely indicates some mineralization of the oil-derived DOC occurred in addition to dilution of the contaminant plume between the two wells.

The same pattern of decreasing ^{14}C ages from the HPON to HPOA to HPIA isolates is reproduced in the 1998 530 and 1998 603 samples, but the decreases from HPON to HPOA are greater. In the case of the 1998 samples, the ^{14}C ages of the individual fractions from each of the two wells are notably close to one another. For example, the ^{14}C ages of 1998 530 HPIA and 1998 603 HPIA are 6,105 and 6,028 ybp, respectively. Moreover, each of the fractions in the 1998 samples have older ^{14}C ages than their corresponding 1986–1989 samples. At least in the case of the well 530 samples, a straightforward explanation for the older ^{14}C ages of the 1998 samples compared to 1986–1989 is that the contaminant plume had migrated further downgradient. Considering the overall similarity of the well 530 NMR spectra from the two separate dates, however, another factor may come into play, which relates to the incorporation of bicarbonate into certain classes of petroleum hydrocarbons during anaerobic biodegradation (for example, naphthalene and phenanthrene, fig. 3). At the point of initial transition from aerobic to anaerobic conditions in the development of the contaminant plume, the bicarbonate available for incorporation into petroleum hydrocarbons should be modern. As the release of CO_2 from biodegradation of petroleum constituents becomes an increasing source of bicarbonate to the groundwater, the bicarbonate pool available for incorporation into petroleum hydrocarbons under anaerobic conditions has an older ^{14}C age. Thus, partial oxidation products formed from pools of bicarbonate differing in overall ^{14}C ages could have the same chemical structures but different ^{14}C ages. In other words, partial oxidation products formed from the incorporation of modern bicarbonate would have younger ^{14}C ages than those formed from the incorporation of older bicarbonate. An analogous situation may occur with the addition of fumarate, which is modern in the bacteria whose growth is induced at the early stages of the biodegradation process.

Nuclear Magnetic Resonance Spectra

Crude Oil Nuclear Magnetic Resonance Spectra

Liquid-state hydrogen-1 (^{1}H), ^{13}C, and ^{15}N NMR spectra of the whole crude oil and SARA fractions have been described previously (Thorn and Aiken, 1998; Thorn and

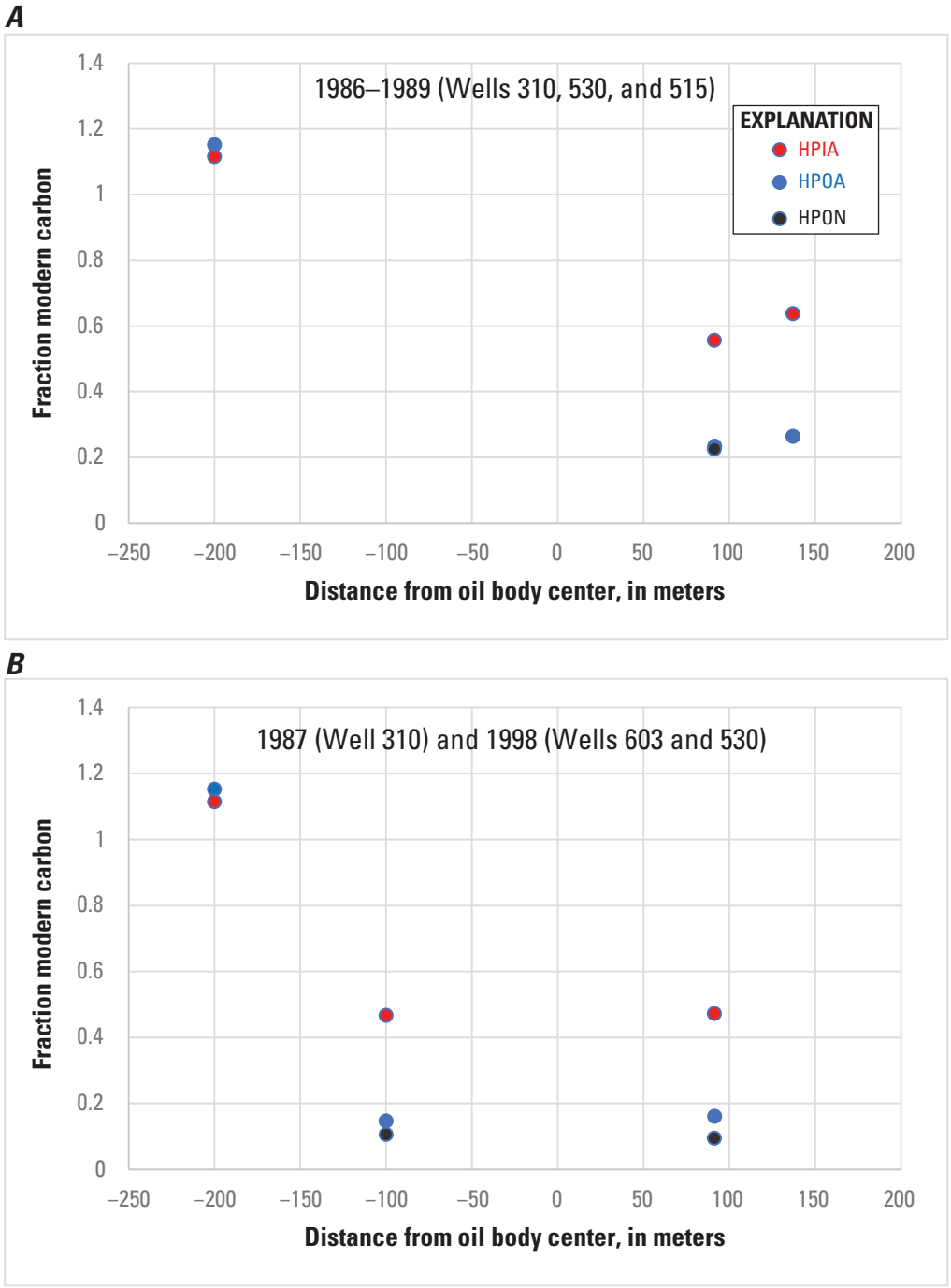

Figure 5. Fraction modern carbon for hydrophilic acid (HPIA), hydrophobic acid (HPOA), and hydrophobic neutral (HPON) fractions for samples from *A,* wells 310 (–200 m), 530 (91.3 m), and 515 (137 m) for samples from years 1986–1989 and *B,* well 310 (–200 m) from 1987 and wells 603 (–100 m) and 530 (91.3 m) for samples from 1998. (m, meters)

Cox, 2015). The quantitative IGD ^{13}C spectra are reproduced in figures 6–8. Percent aliphatic (0–60 ppm) and aromatic (160–90 ppm) carbons are listed in table 4. The fraction aromatic carbon, or aromaticity, (f_a), calculated as the peak area from 110–160 ppm divided by the total peak area of the quantitative spectrum, is 0.17 for the whole crude oil. The ^{13}C NMR f_a values for the SARA fractions are 0.04, 0.51, 0.33, and 0.63, respectively. Heteroatom functional groups detected in the resin and asphaltene fractions via spin labelling include carboxylic acids, alkyl and phenolic hydroxyls, ketones,

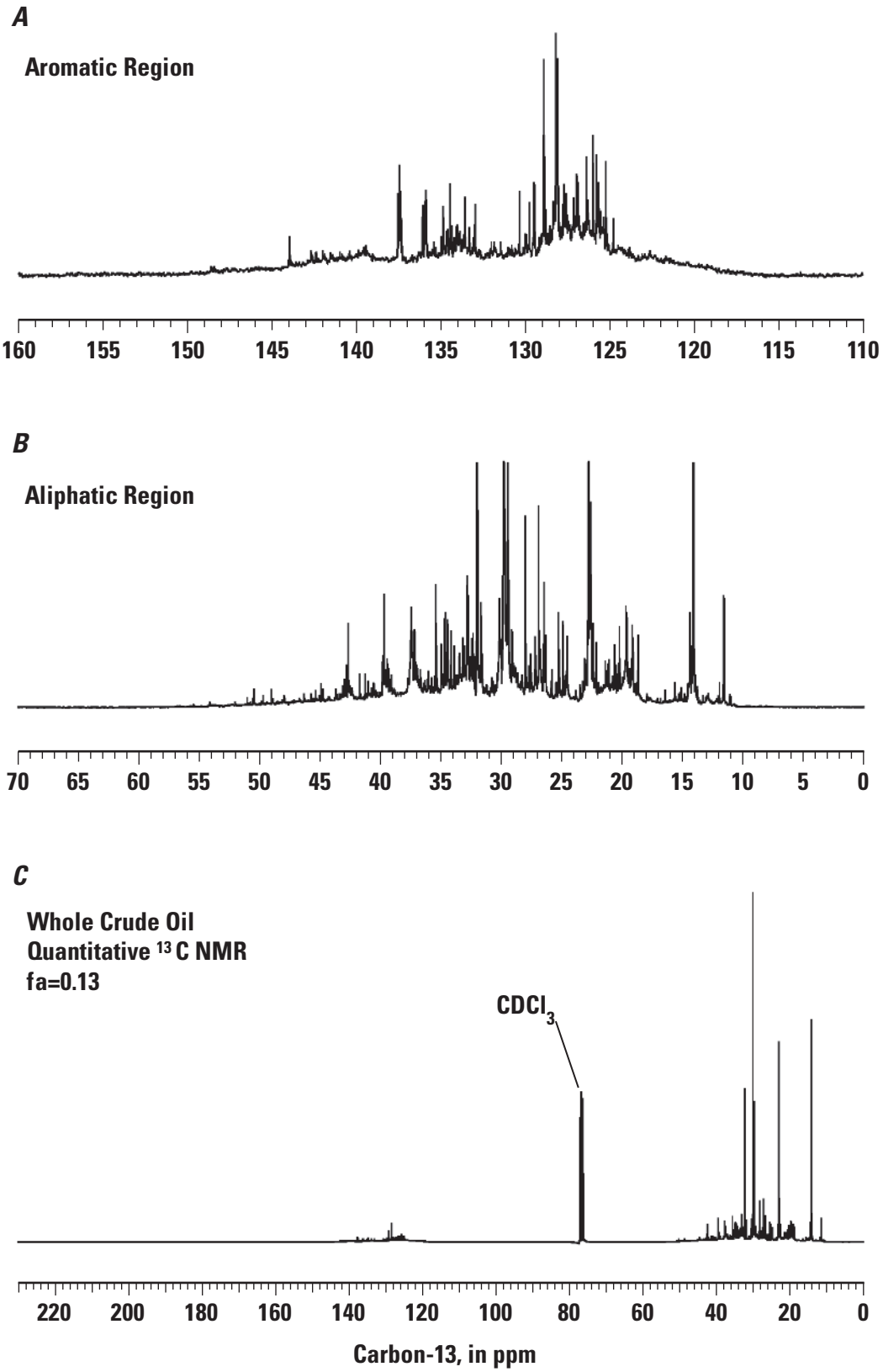

Figure 6. Liquid-state inverse gated decoupled carbon-13 nuclear magnetic resonance spectrum of Bemidji whole crude oil recorded in deuterated chloroform ($CDCl_3$) for *A*, the aromatic region, *B*, the aliphatic region, and *C*, whole crude oil. Figure is from Thorn and Aiken, 1998. Line broadening = 1.0 hertz. (^{13}C, carbon-13; f_a, carbon-13 aromaticity; ppm, parts per million)

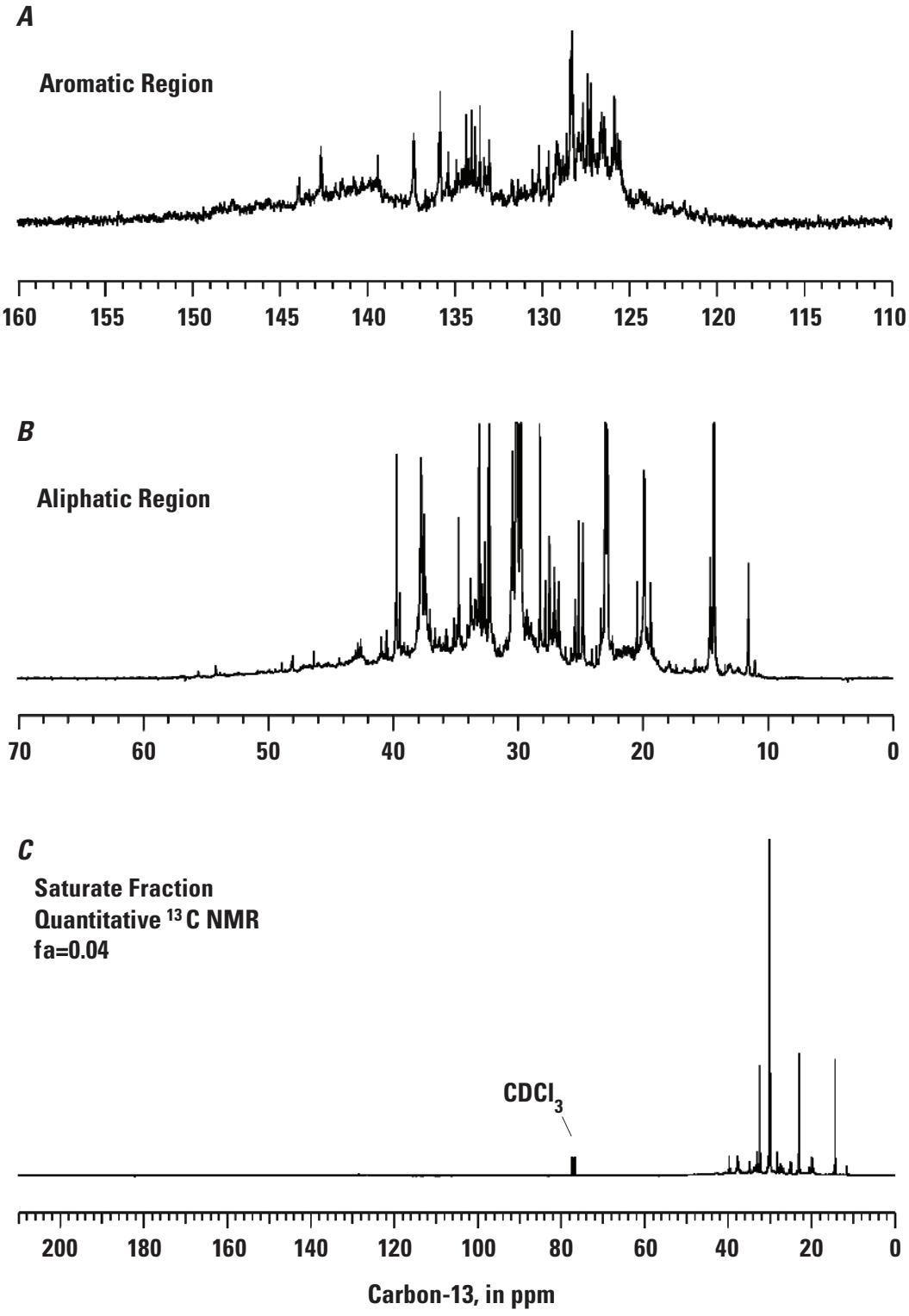

Figure 7. Liquid-state inverse gated decoupled carbon-13 nuclear magnetic resonance (NMR) spectrum of saturate fraction of Bemidji whole crude oil recorded in deuterated chloroform ($CDCl_3$) for *A*, the aromatic region, *B*, the aliphatic region, and *C*, the whole saturate fraction. Line broadening = 1.0 hertz. (^{13}C, carbon-13; f_a, carbon-13 aromaticity; ppm, parts per million)

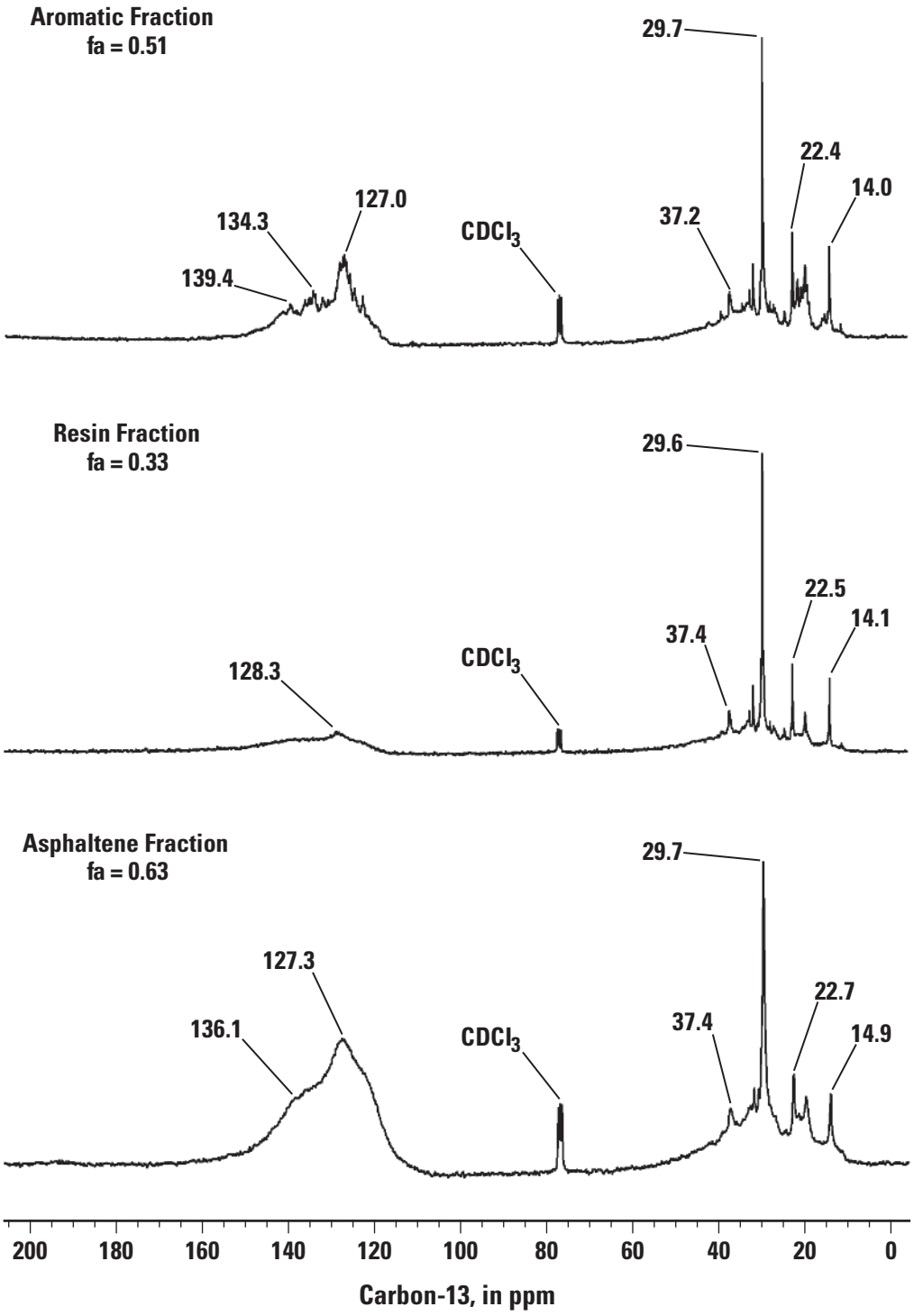

Figure 8. Liquid-state inverse gated decoupled carbon-13 nuclear magnetic resonance (NMR) spectra of aromatic (line broadening = 5.0 hertz), resin (line broadening = 5.0 hertz), and asphaltene (line broadening = 10.0 hertz) fractions of Bemidji crude oil recorded in deuterated chloroform ($CDCl_3$). Figure is from Thorn and Aiken (1998). (f_a, carbon-13 aromaticity; ppm, parts per million)

Table 4. Peak areas as percent of total carbon for quantitative carbon-13 (^{13}C) nuclear magnetic resonance spectra of crude oil, crude oil fractions, and nonvolatile organic acids, carbon-13 aromaticities (^{13}C f_a), percent sp^2 versus sp^3 hybridized carbons, and percent of carbons bonded to oxygen (O–C) for samples from the Bemidji research site in Minnesota.

[Crude oil, saturate, aromatic, resin, and asphaltene samples were recorded in deuterated chloroform ($CDCl_3$). Nonvolatile organic acid samples collected between 1986 and 1989 were recorded in deuterated dimethyl sulfoxide (dmso-d_6), and those collected in 1998 were recorded in deuterium oxide (D_2O). For samples recorded in $CDCl_3$ and dmso-d_6, ^{13}C f_a = 160-110/230-0, and for samples recorded in D_2O, ^{13}C f_a = 165-110/230-0. Percent sp2 hybridized carbons are calculated as the percent of total carbons from 230 to 90 parts per million (ppm). Percent sp3 hybridized carbons are calculated as the percent of total carbons from 90 to 0 ppm. The sp3 hybridized carbon calculation excludes anomeric carbons that can overlap with protonated aromatic carbons from 90–110 ppm. The percent of O–C combines peak areas from 230 to 180 ppm, 180 to 160 ppm, and 90 to 60 ppm. The percent of O–C calculation excludes anomeric carbons that can overlap with protonated aromatic carbons from 90–110 ppm and phenolic carbons that can overlap with other substituted aromatic carbons from 135–165 ppm. Asph, asphaltene; HPIA, hydrophilic acid; HPOA, hydrophobic acid; HPON, hydrophobic neutral; —, not determined]

Sample	230–180 ppm ketone, quinone	180–160 ppm carboxyl, ester, amide	160–110 ppm aromatic, olefinic	110–90 ppm acetal, hemiacetal, anomeric, protonated aromatic	160–90 ppm	90–60 ppm alcohol, ether, carbohydrate	60–0 ppm aliphatic	^{13}C f_a	sp2	sp3	O-C
Crude oil	—	—	—	—	17	—	83	0.17	17	83	—
Saturate	—	—	—	—	4	—	96	0.04	4	96	—
Aromatic	—	—	—	—	51	—	49	0.51	51	49	—
Resin	—	—	—	—	33	—	67	0.33	33	67	—
Asph	—	—	—	—	63	—	37	0.63	63	37	—
1987 310 HPON	6	11	13	5	18	16	49	0.13	35	65	33
1987 310 HPOA	5	15	18	7	24	18	38	0.18	44	56	38
1987 310 HPIA	4	17	17	9	27	20	32	0.17	48	52	41
1987 603 HPOA	4	12	24	5	29	11	44	0.24	45	55	27
1987 603 HPIA	4	15	19	7	26	17	38	0.19	45	55	36
1989 530 HPON	4	8	27	2	29	7	53	0.27	40	60	19
1986 530 HPOA	3	14	19	4	23	12	48	0.19	40	60	29
1986 530 HPIA	7	16	16	8	24	17	36	0.16	47	53	40
1998 530 HPON	4	6	20	0	20	9	61	0.20	30	70	19
1987 515 HPOA	4	13	22	5	27	11	44	0.22	45	55	28
1987 515 HPIA	4	17	18	9	27	19	33	0.18	48	52	40
Sample [1]	230–190	190–165	165–110	110–90	165–90	90–60	60–0	^{13}C f_a	sp2	sp3	O–C
1998 603 HPOA	5	12	21	1	21	8	55	0.21	37	63	25
1998 603 HPIA	5	17	12	5	17	17	45	0.12	38	62	39
1998 530 HPOA	4	13	12	0	12	7	63	0.12	30	70	24
1998 530 HPIA	4	18	6	5	11	17	50	0.06	33	67	39

[1]Different peak area intervals reflect slightly different demarcation of peaks and troughs in nuclear magnetic resonance spectra recorded in dmso-d_6 versus D_2O.

esters, quinones, acidic nitrogens such as amides and amines that are amenable to methylation, and thiols (Thorn and Cox, 2015). The major form of nitrogen in the asphaltene fraction appears to be carbazole (Thorn and Cox, 2015), evident from the peak at 113 ppm in the natural abundance CP/MAS ^{15}N NMR spectrum of figure 9.

1986–1989 Nonvolatile Organic Acids Nuclear Magnetic Resonance Spectra

The quantitative liquid-state ^{13}C NMR IGD spectra for the 1986–1989 well 310, 530, and 603 fractions recorded in dmso-d_6 and reported previously (Thorn and Aiken, 1998) are reproduced in figures 10 and 11. Peak areas, ^{13}C aromaticities, percentages of sp^2 versus sp^3 hybridized carbons, and percentages of carbons bonded to oxygens are reported in table 4.

General assignments for the ^{13}C NMR spectra are as follows:

- 0–60 ppm—Aliphatic carbons; sp^3 hybridized carbons bonded primarily to other carbons, but also to nitrogen, sulfur, and some oxygen (for example, α carbon to amino acids, 40–65 ppm; methoxyl carbon, 54–58 ppm).
- 60–90 ppm—Aliphatic carbons (sp^3 hybridized) bonded to oxygen, including alcohols, ethers, and carbohydrates.
- 90–110 ppm—Acetal, hemiacetal, anomeric carbons of carbohydrates, and protonated aromatic carbons.
- 110–160 ppm—Aromatic and olefinic carbons.
- 160–180 ppm—Carboxylic acid, ester, and amide carbons.
- 180–230 ppm—Ketone and quinone carbons.

More detailed chemical shift dispersions in the carbonyl and phenolic carbon regions are shown in figure 12.

Consistent with elemental analyses, the order of oxidation increases from HPON to HPOA to HPIA, as evident in the increase in proportion of O-alkyl carbons (60 to 90 ppm), for both the background well 310 and the contaminant well 530 and 603 wells. This relationship of increased oxidation from HPON to HPOA to HPIA is further illustrated when the percentage of carbons bonded to oxygens (O–C) is tabulated by adding the peak areas for ketone (180 to 230 ppm), carboxylic acid/amide (160 to 180 ppm), and O-alkyl (60 to 90 ppm) carbons (table 4). Among the three sets of samples where quantitative spectra were recorded for all three fractions (1987 310, 1986-1989 530, and 1998 530), the percent O–C increases from 19 to 29 to 40 in 1989 530 HPON, 1986 530 HPOA, and 1986 530 HPIA, respectively. Lower concentrations of O-alkyl carbons in turn distinguish the contaminant well 530 and 603 HPON, HPOA, and HPIA fractions from each of their corresponding well 310 fractions.

Characteristically for XAD-4 and XAD-8 isolates, the HPIA fractions contain greater proportions of carboxylic acid (160–180 ppm) and O-alkyl (60–90 ppm) carbons than their corresponding HPOA fractions. The O-alkyl carbons (60–90 ppm) are primarily methine, with minor contributions of methylene, as determined by distortionless enhancement by polarization transfer (DEPT) analyses (Thorn and Aiken, 1998). Of the carbohydrate material that isolates on XAD resins, there is preferential sorption to XAD-4 over XAD-8 (Thurman and others, 2020). For the O-alkyl peaks at 60–90 ppm in the ^{13}C NMR spectra to be considered as carbohydrate, anomeric carbons at ~106 ppm also need to be detected, which is the case for the 1987 310 HPIA and 1987 603 HPIA spectra (figs. 10–11). However, in the absence of independent carbohydrate analyses by wet chemical means, it is not possible to ascertain the exact contribution of carbohydrates to these spectra. Attribution of peaks to carbohydrates is further complicated by the overlap in ^{13}C NMR chemical shifts of anomeric carbons with protonated aromatic carbons in the approximate region from 90 to 110 ppm. In the case of the crude oil derived NVOAs, especially the HPOA and HPON fractions, there is a strong likelihood that O-alkyl carbons (60–90 ppm) may represent secondary alcohols resulting from oxidation of methylene carbons in the parent petroleum constituents. Examples of secondary alcohol formation include the oxidation of methylene carbons in cyclic hydrocarbon structures (cyclohexane oxidation; fig. 2), subterminal oxidation of methylene carbons in linear or branched alkyl hydrocarbon structures (tridecane oxidation; fig. 2), and the anaerobic oxidation of ethylbenzene (fig. 3). In general, spectra of the HPON fractions from the background and contaminant wells show no evidence of carbohydrates.

For background well 310, the ^{13}C aromaticity (f_a) of the HPON fraction (0.13) is less than the HPOA and HPIA fractions (0.18 and 0.17, respectively), which are approximately equal. In contrast, for 1986 well 530, the order of decreasing aromaticity is HPON followed by HPOA followed by HPIA. Likewise, 1987 603 HPOA has a higher aromaticity than its corresponding HPIA fraction. By visual inspection of the spectra, the 530 HPON fraction has a greater concentration of aromatic carbons than the 310 HPON fraction, suggesting a contribution from polar metabolites of aromatic constituents of the crude oil in the former.

Well 515 was the farthest downgradient from the oil body from which NVOAs were isolated between 1986–1989. The quantitative ^{13}C NMR spectra, not previously reported, also show a consistent relationship between the 1987 515 HPIA and HPOA fractions, with the HPOA having a lower concentration of carboxyl/amide and O-alkyl carbon but higher aromaticity and C-alkyl carbon content than the HPIA fraction (fig. 13). The 1987 515 HPOA fraction in turn is distinguishable from the background 1987 310 fraction. The 1987 515 HPOA, like the 1986 530 HPOA, contains a notably lower concentration of O-alkyl carbons than 1987 310 HPOA.

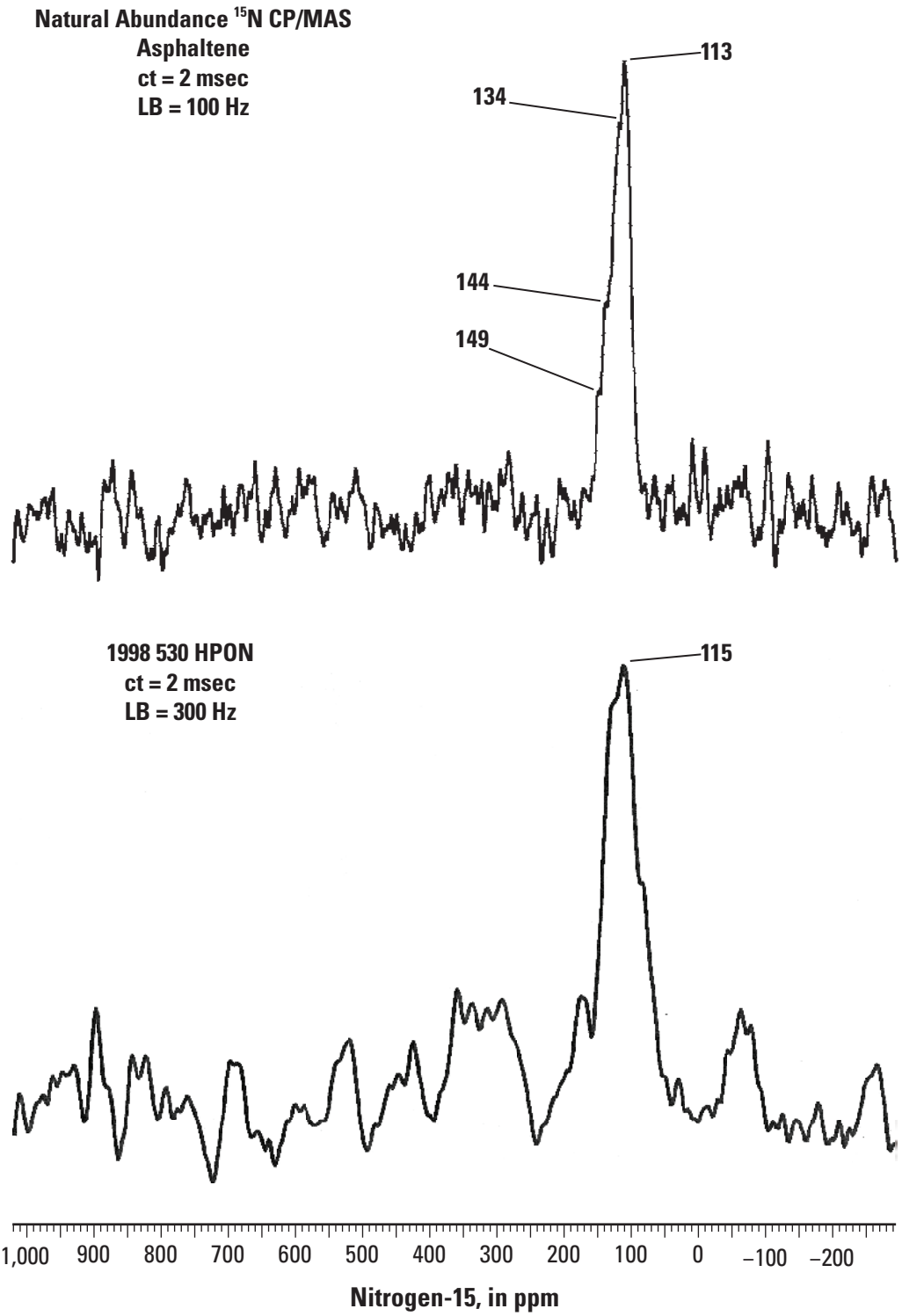

Figure 9. Solid-state cross polarization/magic angle spinning (CP/MAS) nitrogen-15 nuclear magnetic resonance (NMR) spectra of naturally abundant nitrogen in asphaltene fraction of crude oil (top) and 1998 well 530 hydrophobic neutral (HPON) fraction (bottom). (ct, contact time; Hz, hertz; LB, line broadening; msec, milliseconds; ^{15}N, nitrogen-15; ppm, parts per million)

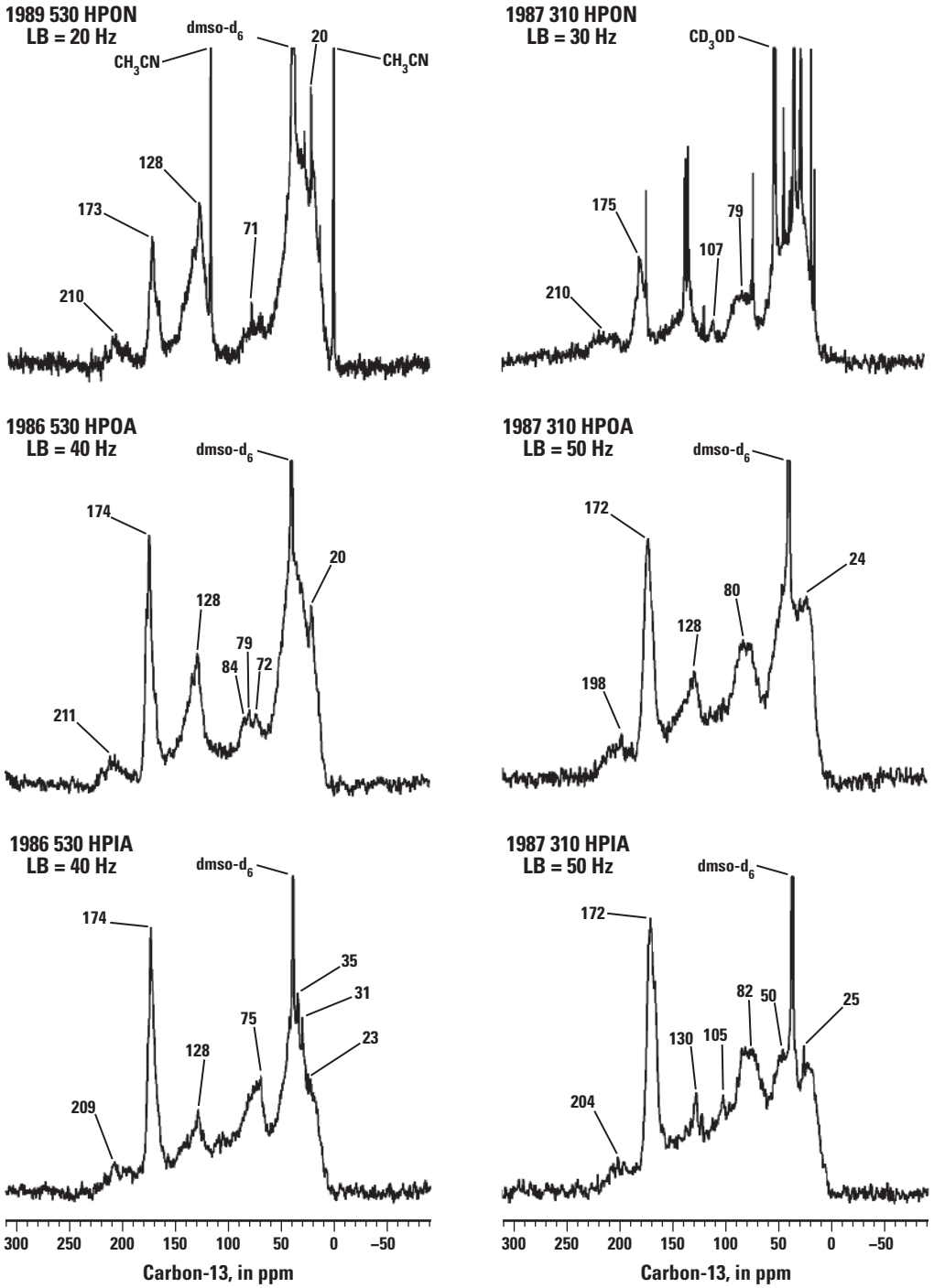

Figure 10. Liquid-state inverse gated decoupled carbon-13 nuclear magnetic resonance (NMR) spectra of 1986–1989 well 530 and 1987 well 310 hydrophobic neutral (HPON), hydrophobic acid (HPOA), and hydrophilic acid (HPIA) fractions. Figure is from Thorn and Aiken (1998). (CD_3OD, deuterated methanol; dmso-d_6, deuterated dimethyl sulfoxide; Hz, hertz; LB, line broadening; ppm, parts per million)

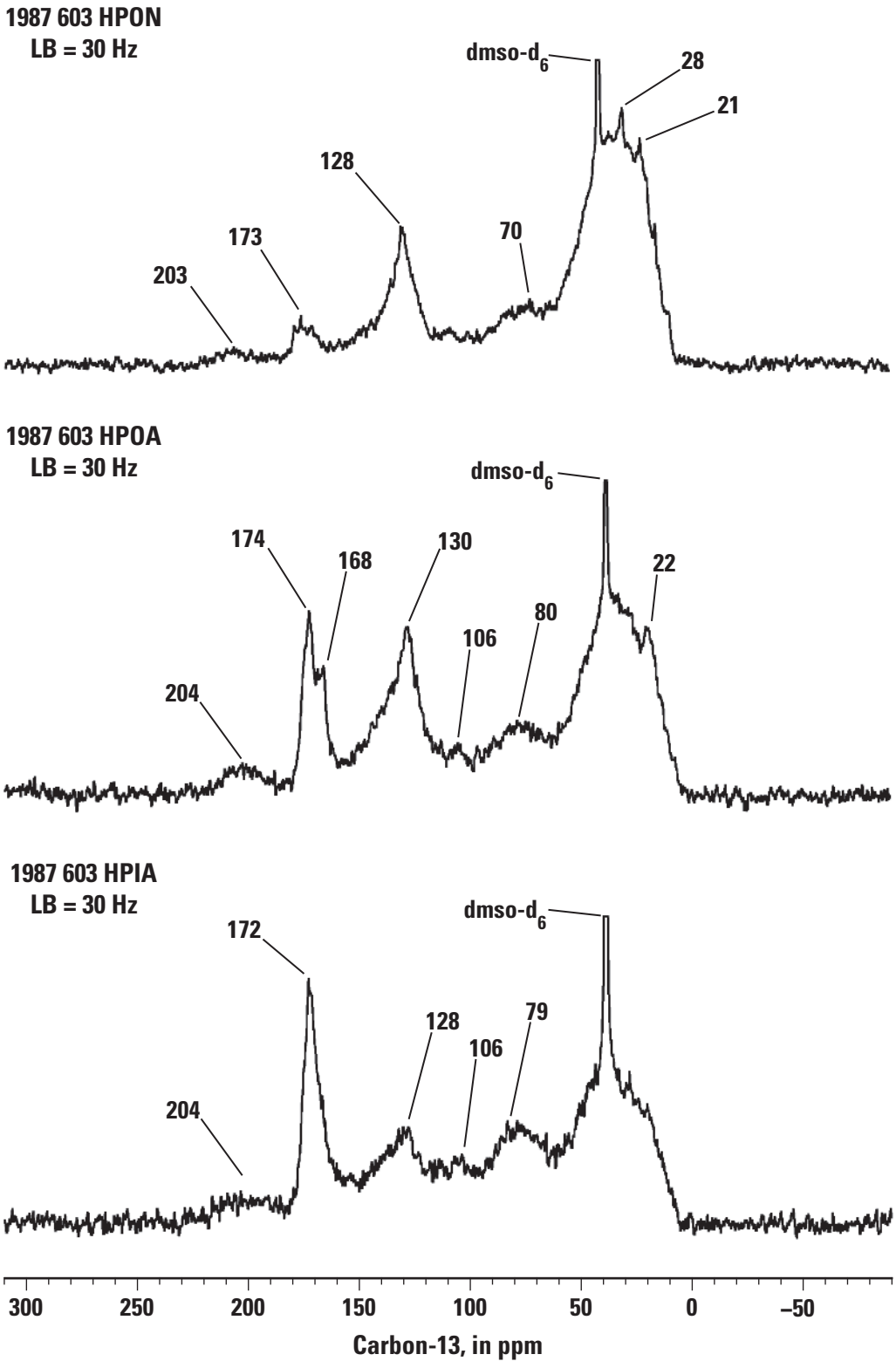

Figure 11. Liquid-state carbon-13 nuclear magnetic resonance (NMR) spectra of 1987 well 603 hydrophobic neutral (HPON), hydrophobic acid (HPOA), and hydrophilic acid (HPIA) fractions. NMR experiments were run as continuous decoupled for the HPON fraction and as inverse gated decoupled for the HPOA and HPIA fractions. Figure is from Thorn and Aiken (1998). (dmso-d_6, deuterated dimethyl sulfoxide; Hz, hertz; LB, line broadening; ppm, parts per million)

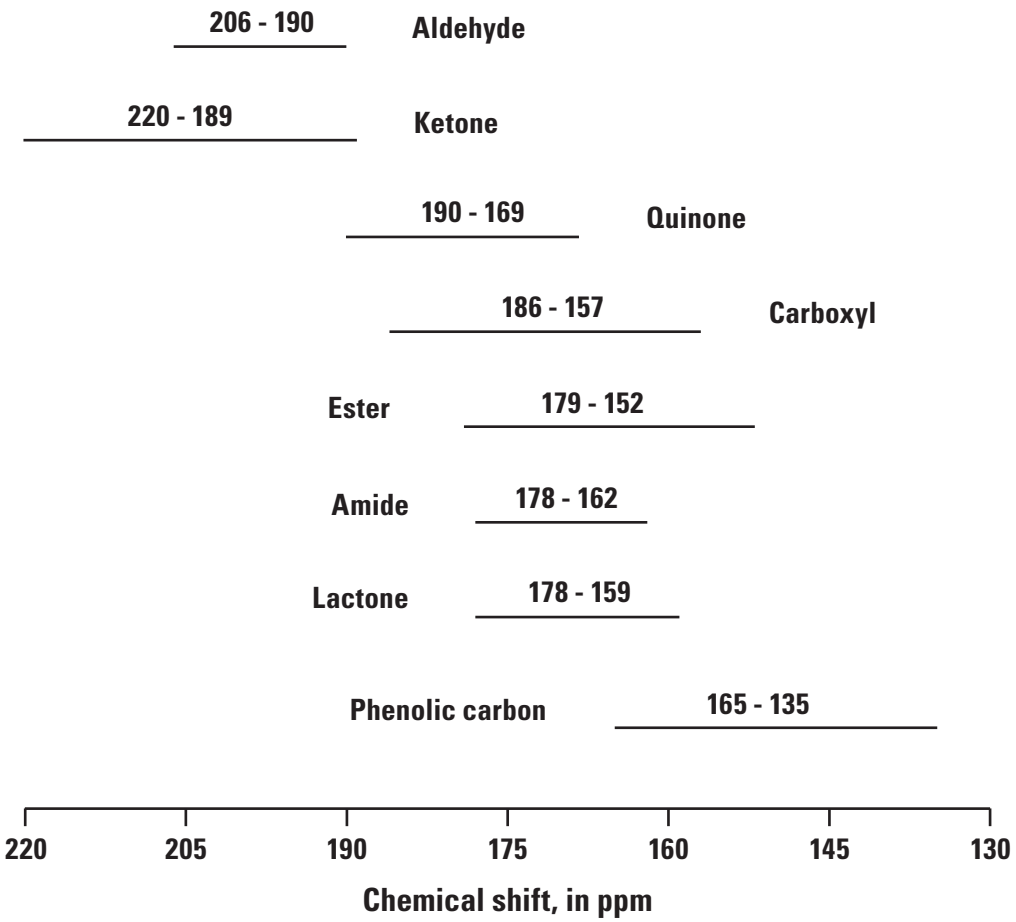

Figure 12. Carbon-13 nuclear magnetic resonance chemical shift ranges in parts per million (ppm) for carbonyl and phenolic carbons.

Percent sp^3 hybridized carbons, calculated as the peak area from 90 to 0 ppm divided by the total spectrum area, range from 52 to 70 percent for the 1986–1989 NVOA samples and for the 1998 samples described in the next section (table 4). These are minimum values, as anomeric carbons (90 to 110 ppm) are not included in the determination because of overlap with protonated aromatic carbons.

Liquid-state DEPT ^{13}C NMR and ^{1}H NMR spectra of the 1987 310 and 1986–1989 530 NVOA fractions were reported previously (Thorn and Aiken, 1998). The DEPT experiment generates subspectra containing all protonated carbons, methine carbons only, methylene carbons only, and methyl carbons only. Significant concentrations of sp^3 hybridized methine carbons bonded to other carbons (peak maxima at ~41 to 48 ppm) were detected in the HPON, HPOA, and HPIA fractions from both the background and contaminant wells, suggesting that branched or cyclic moieties are important in the alkyl structures of both the aliphatic and alkylaromatic molecules of the DOC. On the other hand, ^{1}H NMR spectra of the contaminant well 530 and 603 HPOA and HPIA fractions showed elevated intensities of peaks at 2.1 to 2.2 ppm compared to the background well 310 HPOA and HPIA samples. These peaks correspond to methyl groups bonded to aromatic carbons and are evidence that the 530 and 603 HPOA and HPIA fractions contain polar metabolites from methyl-substituted aromatic constituents of the oil, including constituents from the aromatic (for example, alkylaromatic, naphthenoaromatic, and benzothiophene), resin, and asphaltene fractions of the oil (Thorn and Aiken, 1998).

The nature of the carboxyl groups in the ^{13}C NMR spectra can be inferred from a consideration of the chemical shifts of model carboxylic acid compounds listed in table 5. The ^{13}C NMR spectrum of 1987 603 HPOA in figure 11 most clearly illustrates the splitting of the carboxyl peak into maxima at 174 ppm and 168 ppm, where the carboxylic acids are partially resolved into alkyl-, benzylic- and ortho-hydroxybenzene carboxylic acids on one hand (174 ppm) and benzene- and α,β-unsaturated carboxylic acids (168 ppm) on the other (table 5; Thorn and others, 1989). The carboxylic acid peak maxima in all the NVOA fractions recorded in dmso-d_6 occur at 172–175 ppm, which is in the range of alkyl-, benzylic-, and ortho-hydroxybenzene carboxylic acids (figs. 10, 11, and 13).

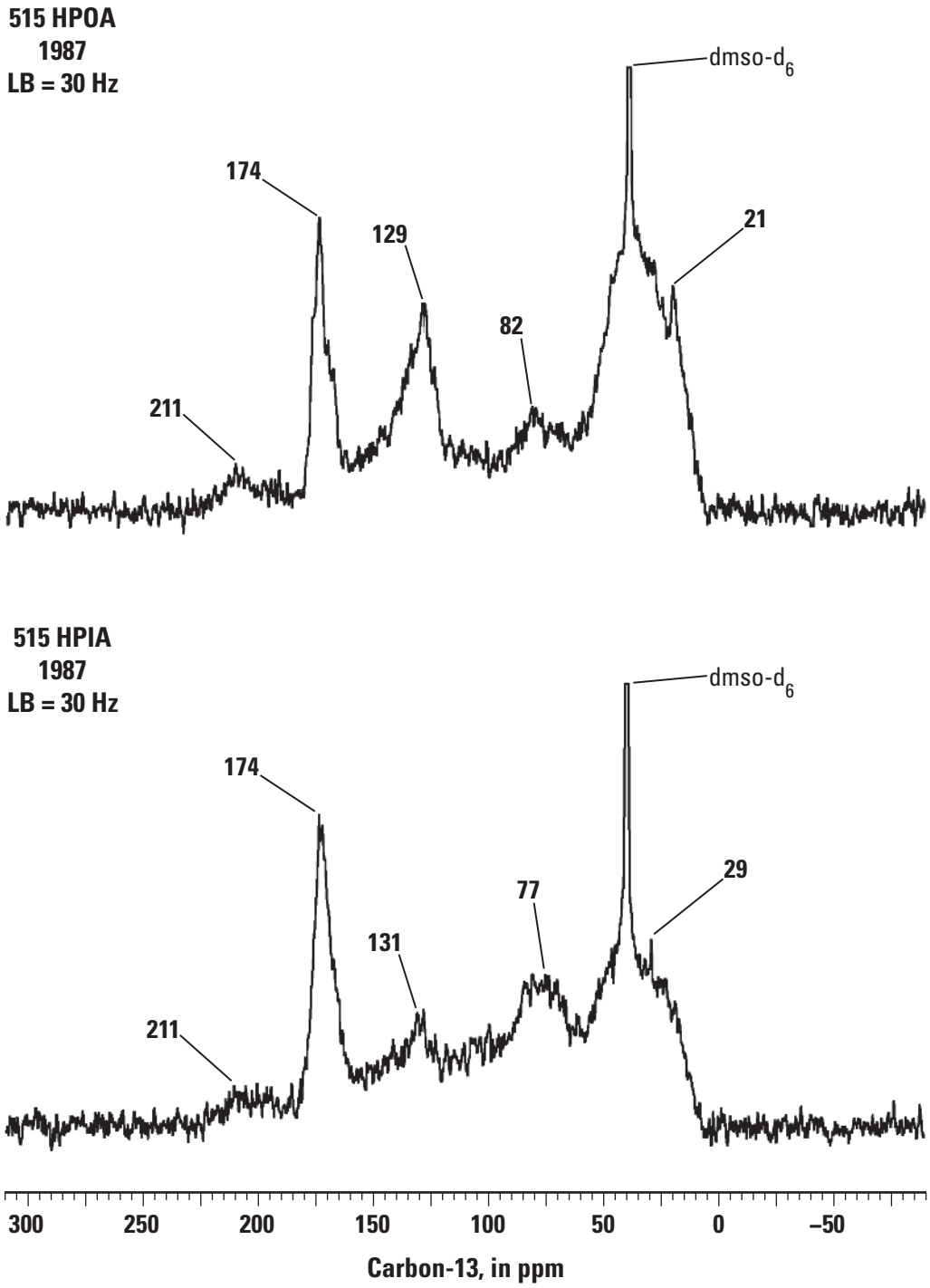

Figure 13. Liquid-state inverse gated decoupled carbon-13 nuclear magnetic resonance (NMR) spectra of 1987 well 515 hydrophobic acid (HPOA) and hydrophilic acid (HPIA) fractions. (dmso-d_6, deuterated dimethyl sulfoxide; Hz, hertz; LB, line broadening; ppm, parts per million)

In general, the ^{13}C NMR chemical shifts of dialkyl ketones (~205 to 224 ppm) are downfield of alkylaryl and alkyl- α,β-unsaturated ketones (~195 to 207 ppm), which in turn are downfield of diaryl ketones (~176 to 197 ppm; table 5; Breitmaier and Voelter, 1987). The chemical shift range of the ketone peaks in the NVOA spectra encompasses all these structural configurations of ketones. Ketones derived from 5- and 6- membered alicyclic rings such as the androstanone and cholestanone classes of keto steroids, bicycloalkanones such as 2- and 7-norbornanone, and alkanones with bulky substituents such as 2,4-dimethyl-, 2,2,4-trimethyl-, and 2,2,4,4-tetramethyl-3-pentanone, have the furthest

Table 5. Carbon-13 nuclear magnetic resonance chemical shifts of carboxylic acids and ketones in deuterated dimethyl sulfoxide (dmso-d_6).

[Chemical shift in dmso-d_6 data are from Thorn (1989). ppm, parts per million]

Carboxylic acid	Chemical shift in dmso-d_6 (ppm)	Ketone	Chemical shift in dmso-d_6 (ppm)
2-furanoic	159.6	Cycloheptanone	[1]215.0
3-furoic	164.0	4-heptanone	209.6
Benzoic	167.4	Methyl ethyl ketone	208.0
Crotonic	167.5	Levulinic acid	207.3
4-hydroxybenzoic	167. 7	Butyl levulinate	205.5
3,4-dihydroxybenzoic	167.7	Phenyl-2-propanone	205.4
Gallic	168.0	2,2',4,4'-tetrahydroxy-benzophenone	199.3
Phthalic	169.0	3-penten-2-one	197.3
Galacturonic	170.8	Acetophenone	197.2
2.5-dihydroxybenzoic	172.0	2,4,4'-trihydroxy-benzophenone	197.2
2.4-dihydroxybenzoic	172.1	Benzophenone	195.6
Salicylic	172.2	Chalcone	189.2
2,6-dihydroxybenzoic	172.4	Quercetin	176.0
Phenylacetic	172.6		
2,3-dihydroxybenzoic	172.7		
1-hydroxy-2-naphthoic	173.4		
Trans-3-hexenoic	173.4		
Levulinic	174.1		
Heptanoic	174.5		
Cyclohexane	[1]182.1		
Cyclopentane	[1]183.8		

[1]Data are from Breitmaier and Voelter (1987), where the solvent is unspecified.

downfield chemical shifts at approximately 215 to 224 ppm (fig. 14; Breitmaier and Voelter, 1987). The chemical shifts of the ketone peaks in the well 310 NVOA fractions include this downfield region from approximately 215 to 230 ppm, which is evidence for the occurrence of ketones of such cyclic structures in the background DOC (fig. 10). Although alkanones with bulky substituents cannot be ruled out, cyclic ketones are the more likely, given the abundance of precursor natural product compounds containing unsaturated ring structures. The NVOA fractions from contaminant wells also show evidence for cyclic ketones, as the chemical shifts of the ketone peaks also extend downfield to ~ 230 ppm (figs. 10–11, 13, 15–20). An origin of the cyclic ketones in the contaminant well fractions from oxidation of 5- and 6-membered rings of constituents in crude oil such as hopanes and steranes, among others, cannot be inferred from the NMR spectra alone, but in conjunction with the ^{14}C ages of the samples, this inference becomes a possibility, especially with the HPON fractions.

Figure 15 shows quantitative liquid-state ^{13}C NMR spectra IGD recorded in D_2O of the HPOA fractions collected along the transect from well 310 to well 515 in 1986 and 1987. The discrete peaks at approximately 160 ppm in the 533, 532, 530, and 515 fractions correspond to bicarbonate. The spectra of the well 310, 603, and 530 fractions reproduce the features observed for the spectra of these same samples recorded in dmso-d_6 (figs. 10, 11, and 13). Spectra of the fractions from the contaminated wells in the spray zone (603) and downgradient from the oil body (533 to 515) are again differentiated from the background well (310) by (1) their lower concentrations of O-alkyl carbons (60 to 90 ppm), (2) the lack of well-resolved anomeric carbon peaks at 106 ppm attributable to carbohydrates, and (3) the relatively lower concentration of carboxylic acid carbons (165 to 190 ppm). The O-alkyl peaks (60–90 ppm) in the contaminant well spectra cannot be assigned as carbohydrate carbons, as there is no concomitant detection of anomeric carbons (106 ppm). Reiterating from the previous discussion then, the O-alkyl carbons (60 to 90 ppm) in the contaminant well spectra may plausibly have a

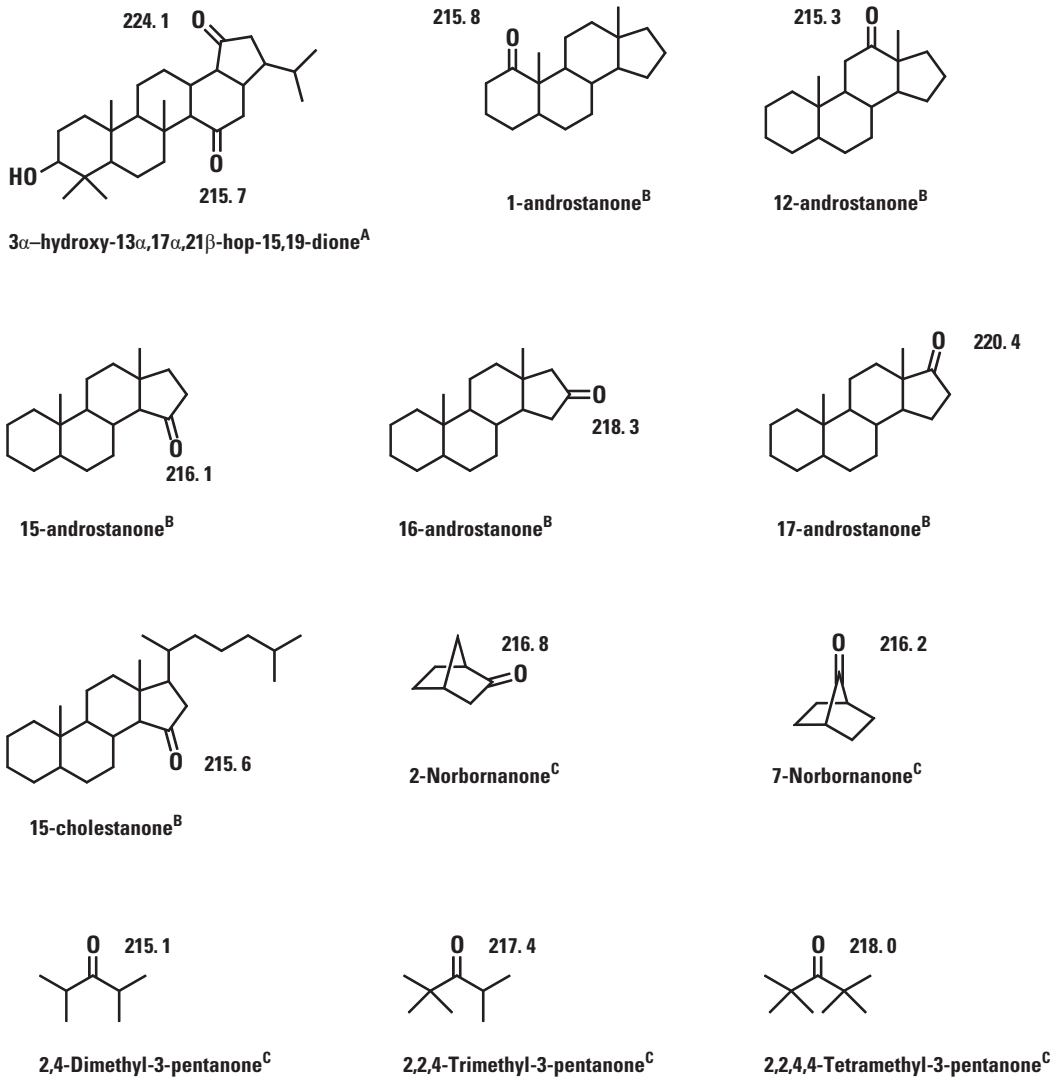

Figure 14. Carbon-13 nuclear magnetic resonance (NMR) chemical shifts of keto steroids, cyclic ketones, and sterically hindered ketones in parts per million (ppm). [A]—Ruiz and others (2006), [B]—Eggert and Djerassi (1973), and [C]—Breitmaier and Voelter (1987). (α, alpha; β, beta; O, oxygen, H, hydrogen)

contribution from alcohols that result from oxidation of alkyl constituents of the petroleum (figs. 2-3). Previously reported ^{1}H and ^{13}C NMR spectra indicated that the aromatic carbons in the 310 HPOA fraction are more substituted or condensed than in the 530 HPOA and 603 HPOA fractions (Thorn and Aiken, 1998). This difference manifests itself slightly differently in the spectra of figure 15 recorded in D_2O, in that the aromatic carbon peaks (110–165 ppm) appear narrower and of greater signal intensity in the contaminant well fractions compared to the 310 HPOA fraction. The aromatic carbon peaks in the contaminant well samples uniformly exhibit a splitting at approximately 128 and 136 ppm, the former primarily aromatic carbons bonded to protons, and the latter primarily substituted aromatic carbons. Without interference from the dmso-d_6 peak, the C-alkyl region (0–60 ppm) of the 310 HPOA fraction shows two distinct peak maxima at 24 ppm (predominantly methyl carbon) and 44 ppm (predominantly methine carbon). This feature is absent in the C-alkyl region of the contaminated well fractions, which instead exhibit a shoulder at approximately 20 ppm to the peak maxima at 38–39 ppm. These signatures of the HPOA fractions from the contaminated wells (fig. 15) suggest that the ^{13}C NMR spectra of this fraction can be used as a tracer for oil contamination in the groundwater, albeit a more labor and time-intensive technique compared to other approaches such as ^{14}C dating and optical spectroscopy. The ^{13}C NMR spectra suggest general similarities in the composition of the DOC from the contaminated wells in the spray zone and along the transect downgradient from the oil body as of 1986–1987. Although the HPOA fraction is only one component of the total DOC, it is the major fraction. Noteworthy is the resemblance of the 533 and 515 HPOA spectra, in view of the decrease in DOC from 32 or

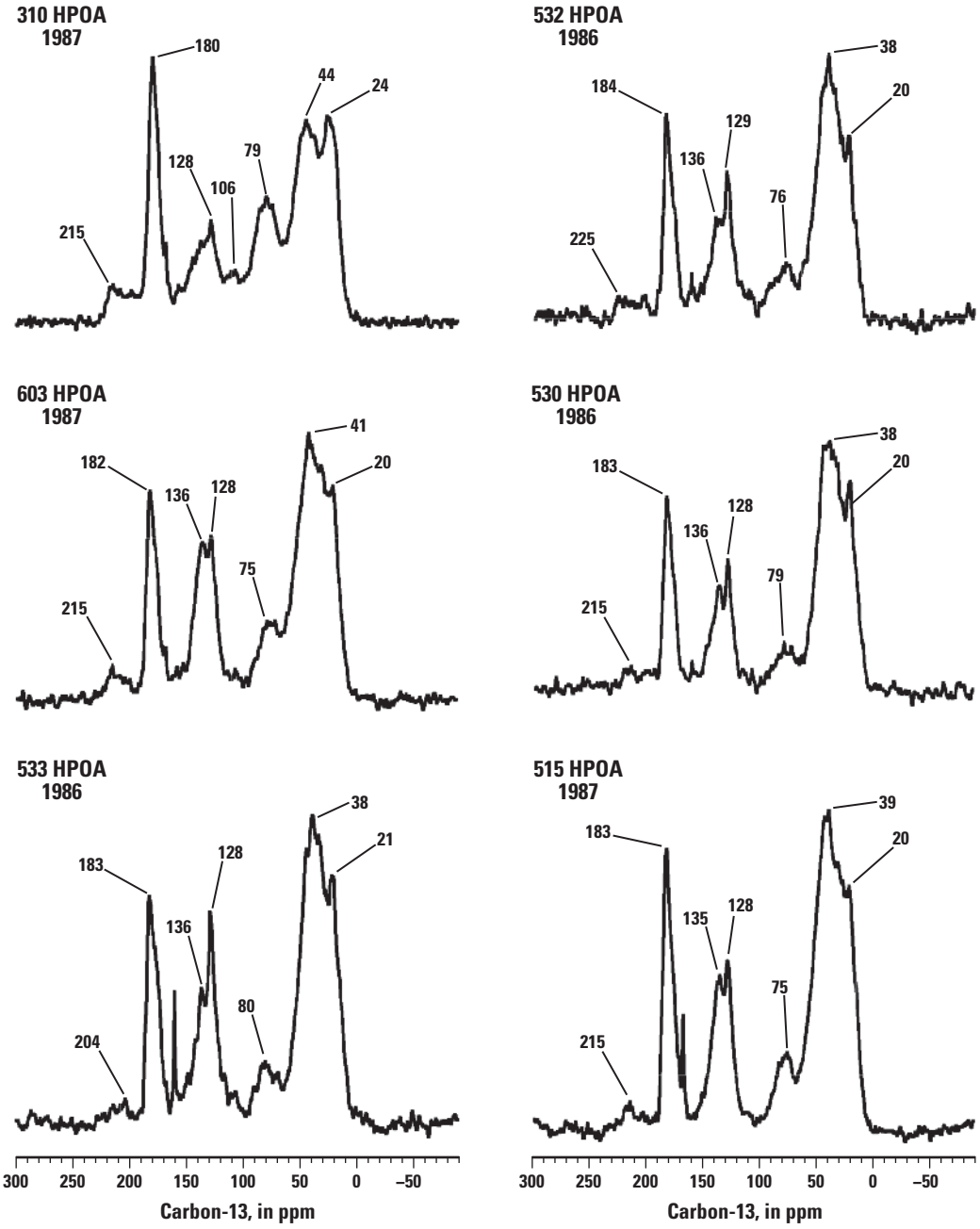

Figure 15. Liquid-state inverse gated decoupled carbon-13 nuclear magnetic resonance (NMR) spectra recorded in deuterium oxide (D_2O) of hydrophobic acid (HPOA) fractions along the A–A′ transect from well 310 to well 515. Line broadening for each spectrum = 100 hertz. Well distances are -200 meters (well 310), -100 m (well 603), 39 m (well 533), 45.7 m (well 532), 91.3 m (well 530), and 137 m (well 515). (ppm, parts per million)

greater to 8.1 between the two wells, and the resemblance of the 515 and 603 HPOA spectra, considering the downgradient and spray zone locations. The FTICR-MS analyses do reveal differences between the well 603 and 530 HPOA fractions at the molecular formula level that cannot be inferred from the ^{13}C NMR spectra, as shown in the "Fourier Transform Ion Cyclotron Resonance Mass Spectrometry Analyses" section.

1998 Nonvolatile Organic Acids Nuclear Magnetic Resonance Spectra

Liquid-state ^{13}C NMR spectra were recorded on the HPON, HPOA, and HPIA fractions isolated from well 530 in 1998 (fig. 16), enabling a direct comparison with the 1986–1989 samples (figs. 10–11, 13, 15–19). Apart from the varying signal-to-noise ratios attained, the spectra from the two

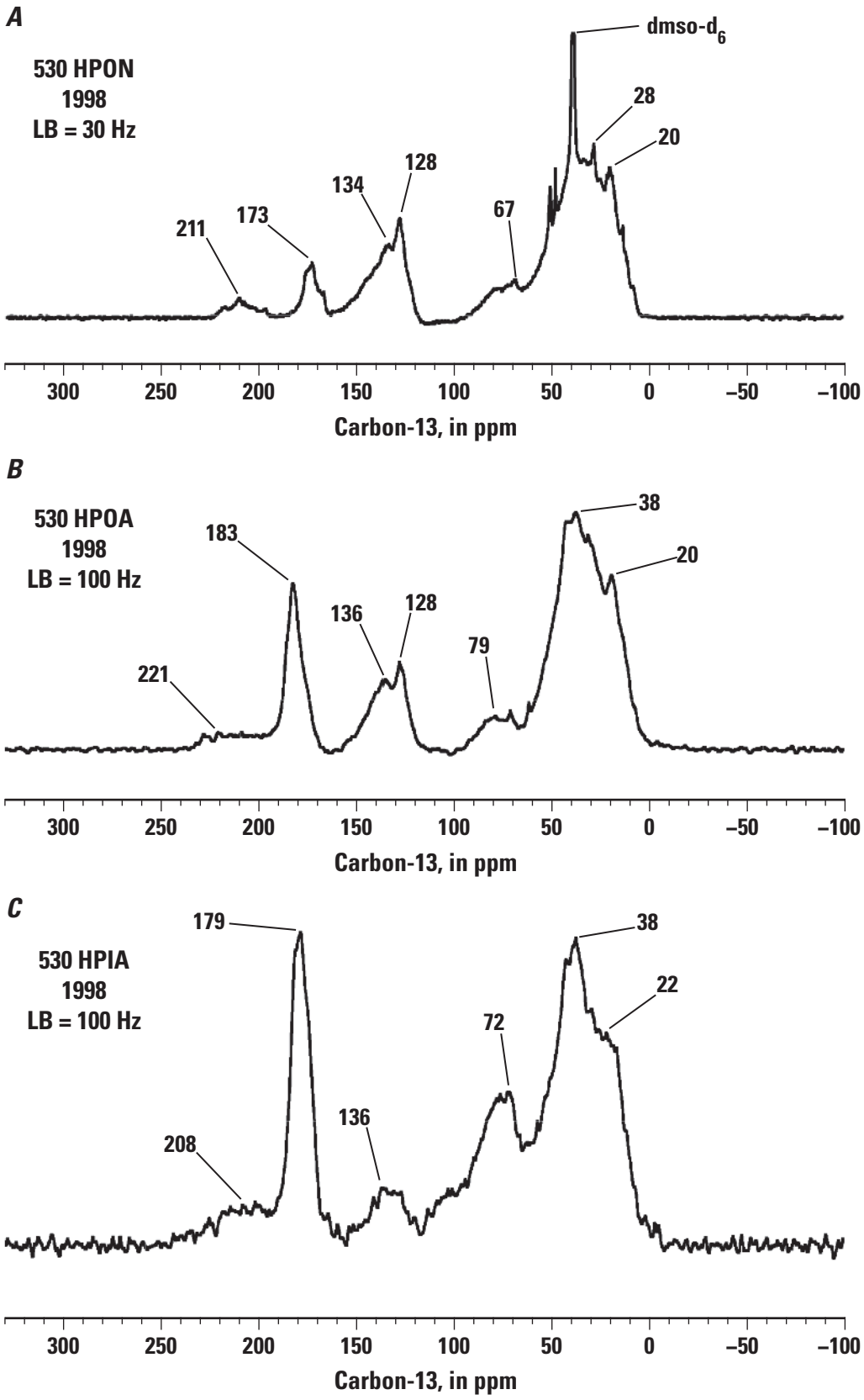

Figure 16. Liquid-state inverse gated decoupled carbon-13 nuclear magnetic resonance (NMR) spectra of *A,* 1998 well 530 hydrophobic neutral (HPON); *B*, hydrophobic acid (HPOA); and *C,* hydrophilic acid (HPIA) fractions. HPOA and HPIA recorded in deuterium oxide (D_2O). (dmso-d_6, deuterated dimethyl sulfoxide; Hz, hertz; LB, line broadening; ppm, parts per million)

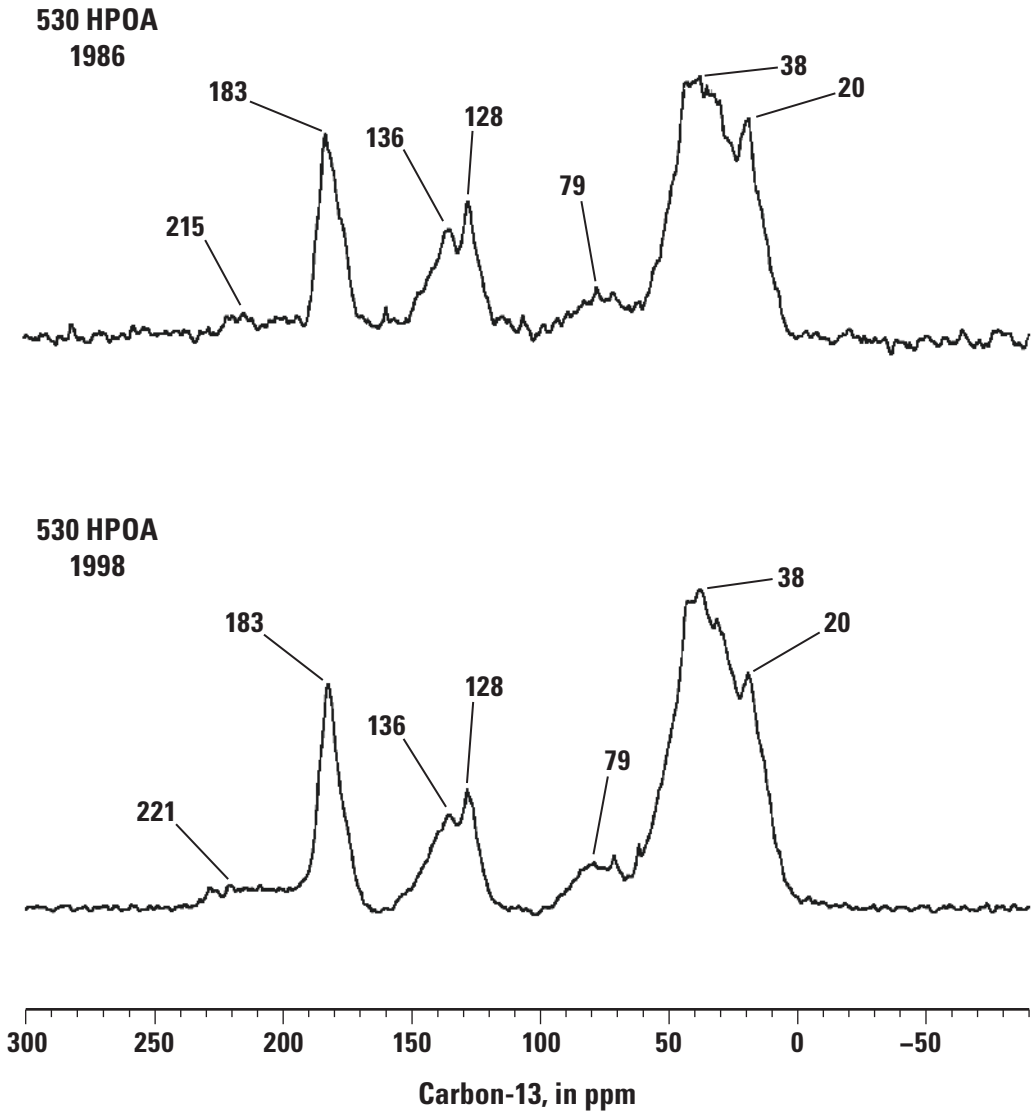

Figure 17. Liquid-state inverse gated decoupled carbon-13 nuclear magnetic resonance (NMR) spectra of 1986 and 1998 well 530 hydrophobic acid (HPOA) fractions recorded in deuterium oxide (D_2O). Line broadening = 100 hertz. (ppm, parts per million)

sampling dates are remarkably similar for each of the three sets of fractions, and they show the same structural relationships among the fractions reported for the 1986–1989 samples with respect to concentrations of carboxylic acid, aromatic, and O-alkyl carbons. For example, the spectra of the 1986 and 1998 530 HPOA fractions share the same peak maxima at 20, 38, 79, 128, 136, and 183 ppm (fig. 17). Peak intensities of the 1986 and 1998 530 HPIA spectra match closely (fig. 18). Spectra of the 1989 and 1998 530 HPON fractions share peak maxima at 128, 134, 173, and 210–211 ppm, the latter in the region of dialkyl ketones (fig. 19).

Liquid-state ^{13}C NMR spectra were also recorded on the HPOA and HPIA fractions from well 603 in 1998 (fig. 20). Spectra of the 1987 and 1998 603 HPOA fractions again bear a close resemblance to one another. Compared to the 1998 603 HPOA fraction, the 1998 603 HPIA fraction characteristically shows a greater concentration of carboxylic acid (180–160 ppm) and O-alkyl (90–60 ppm) but a lesser concentration of aromatic carbons. The 1987 603 HPIA spectrum was recorded in dmso-d_6. It, too, reproduces the features of the 1998 603 HPIA spectrum recorded in D_2O.

The similarities between the 1986–1989 and 1998 well 530 NVOA spectra and between the 1987 and 1998 well 603 NVOA spectra suggest that a generally steady state in the composition of the partial degradation products contaminating the groundwater at these wells had been reached between 1986 and 1998. This result is not a predictable one in that the contaminant DOC was introduced into the groundwater at the two well locations via different pathways, and that partial oxidation products in well 530 (downgradient from oil body)

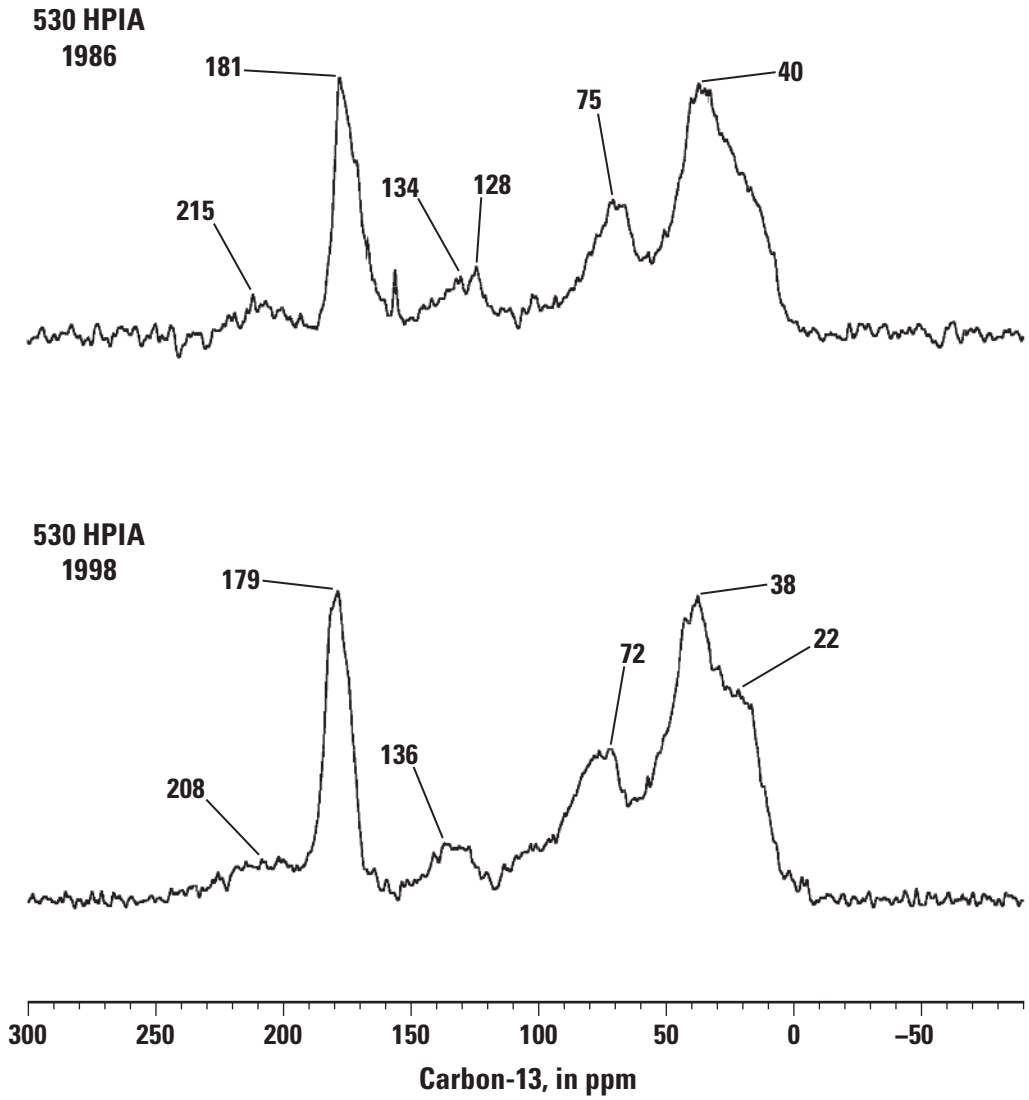

Figure 18. Liquid-state inverse gated decoupled carbon-13 nuclear magnetic resonance (NMR) spectra of 1986 and 1998 well 530 hydrophilic acid (HPIA) fractions recorded in deuterium oxide (D_2O). Line broadening = 100 hertz. (ppm, parts per million)

formed primarily from anaerobic biodegradation, but in well 603 (spray zone), they formed from aerobic biodegradation and possibly photooxidation.

The solid-state CP/MAS ^{15}N NMR spectrum of the naturally abundant nitrogen in the 1998 530 HPON sample is shown in figure 9. The peak maximum occurs at 115 ppm in the carbazole region, similar to the asphaltene. Considering the low value of 0.0941 for the fraction modern carbon of the 1998 530 HPON sample (table 3) and the similarity of its nitrogen spectrum to that of the asphaltene, it would be attractive to speculate that this fraction originates in part from the asphaltene. However, an improvement in the signal-to-noise ratio for the HPON fraction and an analysis of the nitrogen functionality in the aromatic and resin fractions of the oil would be necessary to further establish this connection. Nitrogen-15 NMR spectra of naturally abundant nitrogen in NOM isolates from uncontaminated waters typically show amide (including peptide), aminoquinone, heterocyclic (excluding pyridine-like), and amine (terminal amines of peptides and amino sugars) nitrogens (Thorn and Cox, 2009). These nitrogens are presumed to be present in the well 310 HPOA and HPIA fractions.

Functional Group Analyses by Spin Labelling

The overlap of ^{13}C NMR chemical shift ranges for carbonyl and phenolic carbons are illustrated in figure 11. Carboxylic acid carbons, for example, occur from about 157 to 186 ppm and overlap with quinone, ester, amide, and lactone carbons. Phenolic carbons, including catechol and hydroquinone carbons that have the potential to oxidize to quinones,

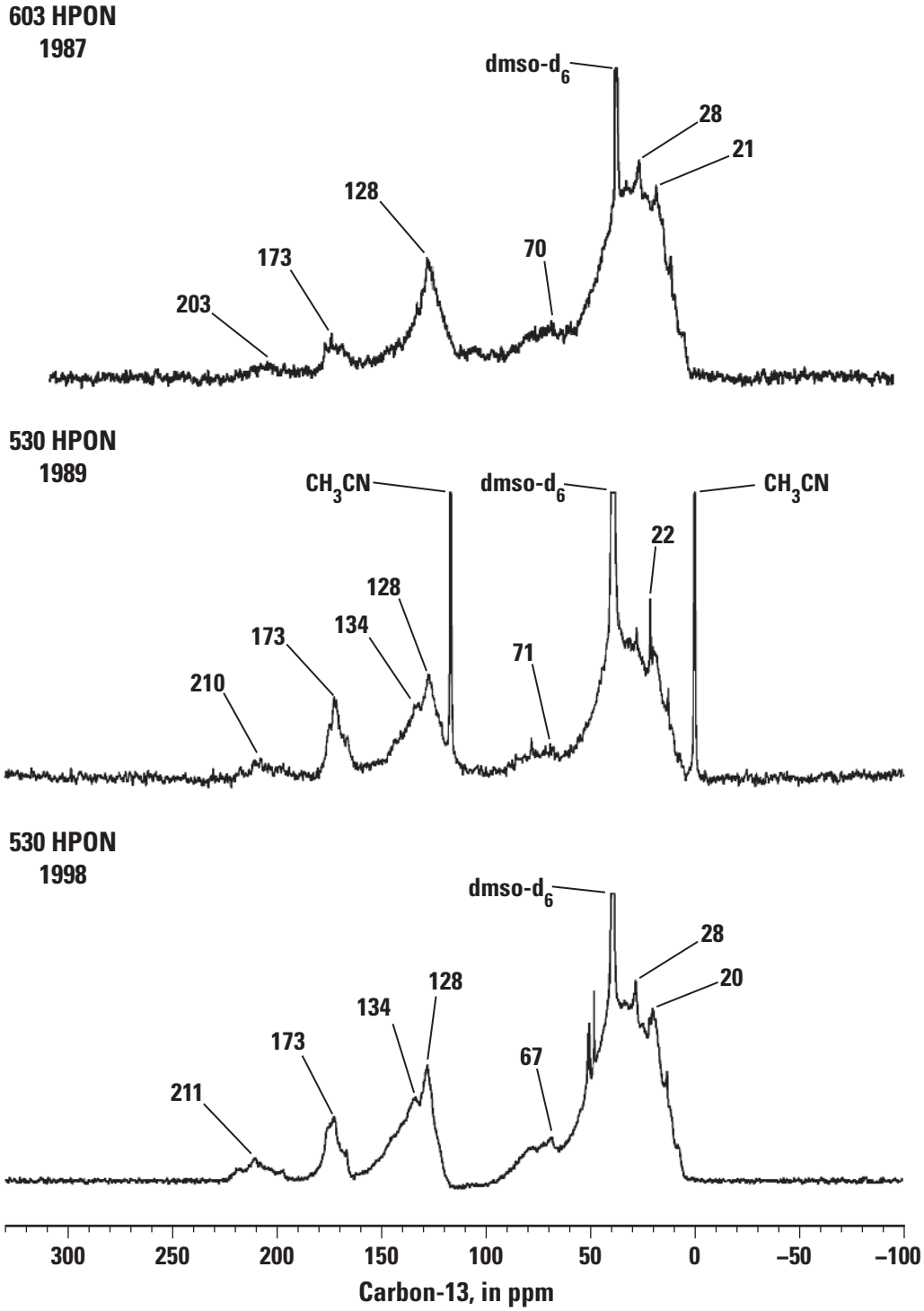

Figure 19. Liquid-state carbon-13 nuclear magnetic resonance (NMR) spectra of wells 1987 603 (continuous decoupled) and 1989 and 1998 530 (inverse gated decoupled) hydrophobic neutral (HPON) fractions. Line broadening = 30 hertz. (dmso-d_6, deuterated dimethyl sulfoxide; ppm, parts per million)

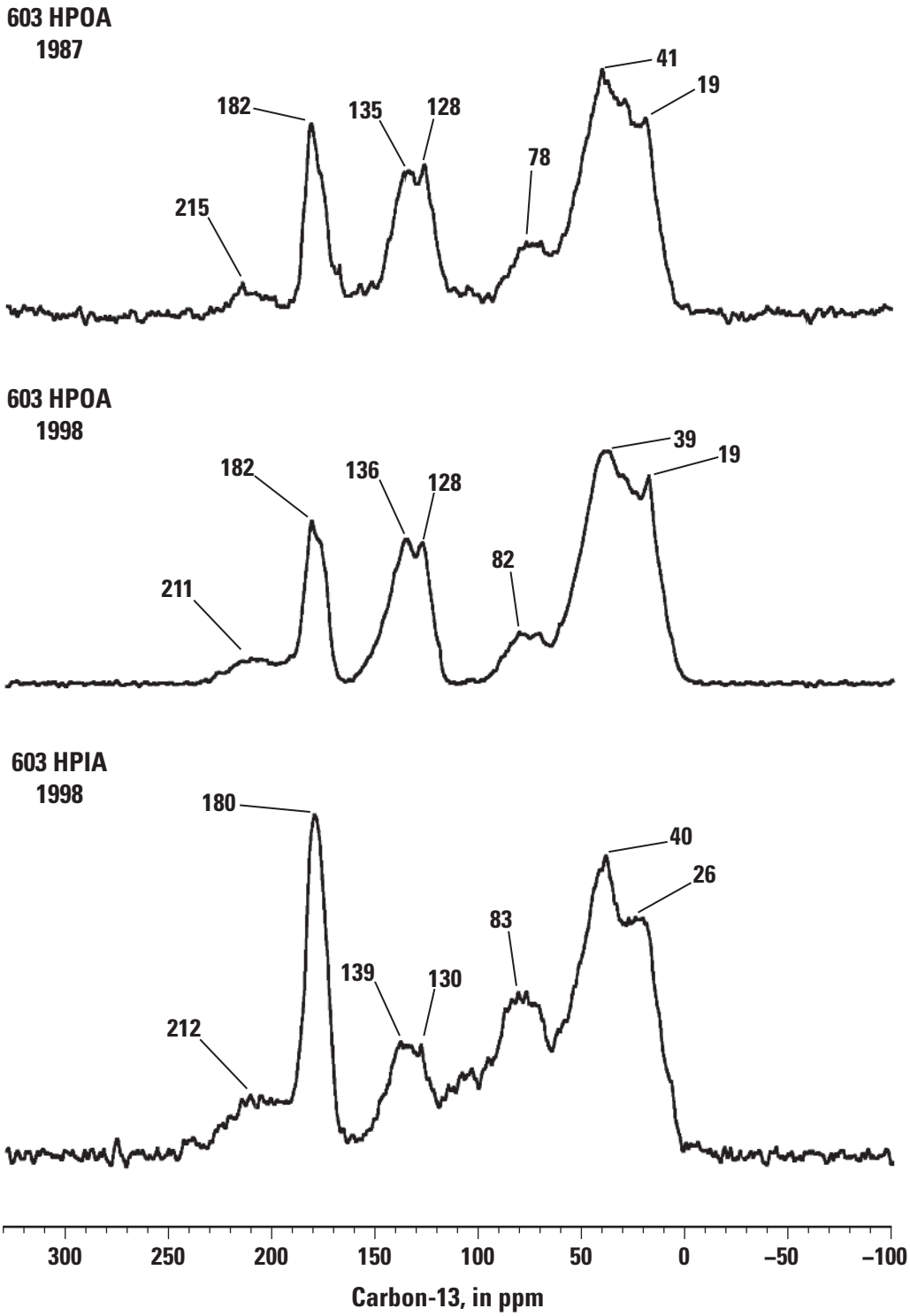

Figure 20. Liquid-state inverse gated decoupled carbon-13 nuclear magnetic resonance (NMR) spectra of 1987 and 1998 well 603 hydrophobic acid (HPOA) and 1998 603 hydrophilic acid (HPIA) fractions recorded in deuterium oxide (D_2O.) Line broadening = 100 hertz. (ppm, parts per million)

occur from about 135 to 165 ppm and overlap with other substituted aromatic carbons (~123 to 160 ppm) as well as carbonyl carbons. From potentiometric titrations, and considering that protonation and deprotonation of carboxylic acid groups with adjustment of pH accounts in large part for the sorption and desorption of the HPOA and HPIA fractions to and from XAD resins, the major peaks from approximately 160 to 180 ppm in the naturally abundant ^{13}C NMR spectra of the NVOA fractions can be assumed to be predominated by carboxylic acids. Carboxylic acid and strongly acidic phenolic hydroxyl groups can be directly detected via their methyl ester and methyl ether derivatives upon derivatization with ^{13}C-labeled diazomethane, which, without a catalyst, is selective for these hydroxyl groups (fig. 21; Thorn and others, 1987). Carboxylic acids, phenolic hydroxyls, and alcohol hydroxyls, including carbohydrate hydroxyls, are all methylated in the PTC procedure, which employs methyl iodide and tetra-n-butyl ammonium hydroxide (fig. 21; Rose and Francisco, 1987).

Carbon-13 NMR spectra of the 1987 310 HPOA, 1986 530 HPOA, and 1989 530 HPON fractions methylated with ^{13}C-labelled diazomethane and without catalyst are shown in figures 22, 23, and 24, respectively. The on-scale spectra all show peaks at 52 ppm, corresponding to the methyl esters of carboxylic acids, and peaks at 56 ppm, corresponding to methyl ethers of phenolic hydroxyls (Thorn and others, 1987). Vertical expansion reveals low intensity peaks from 60 to 65 ppm, corresponding to methyl ethers of phenolic hydroxyls adjacent to two substituents, where an aromatic ring juncture counts as a substituent (see the methyl ether at 63 ppm of diazomethylated 1-hydroxy-2-naphthoic acid in fig. 21). Peaks at 66 and 67 ppm in the 1986 530 HPOA and 67 ppm in the 1987 310 HPOA spectra may also represent methyl ethers of phenolic hydroxyls adjacent to two substituents, but chemical shifts this far downfield have not been reported. The relatively low intensities of the methyl ether peaks compared to the methyl ester peaks are consistent with the low carbon aromaticities of these three samples. Spectra of more highly aromatic soil and aquatic NOM samples methylated with diazomethane have shown greater proportions of methyl ethers to methyl esters (Thorn and others, 1987, 2010; Thorn, 1989).

The ^{13}C NMR spectrum of the 1987 603 HPON fraction methylated using the PTC procedure also shows methyl esters of carboxylic acids at 52 ppm and methyl ethers at 56 ppm and 59 ppm (fig. 25). The peaks at 56 ppm and 59 ppm may now include methyl ethers of both phenolic hydroxyls and alkyl hydroxyls. Resonances up field of approximately 34 ppm correspond to the naturally abundant ^{13}C nuclei in the

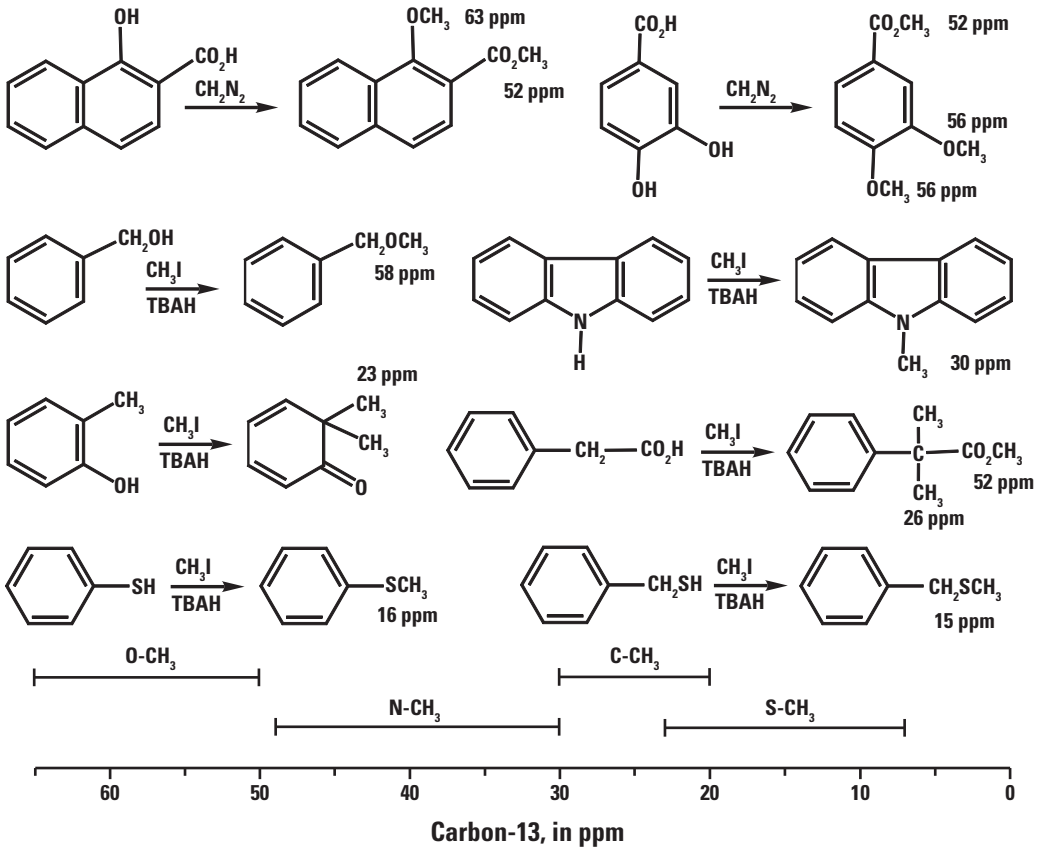

Figure 21. Methylation reactions and carbon-13 nuclear magnetic resonance (NMR) chemical shift ranges for O-, N-, C-, and S-methyl groups in parts per million (ppm). (C, carbon; H, hydrogen; I, iodine; N, nitrogen; TBAH, tetra-n-butyl ammonium hydroxide; O, oxygen; S, sulfur)

sample, except for the peak at 24 ppm, which corresponds to C-methyl groups from the methylation of activated carbons. The N-methyl peak at 45 ppm in the vertical expansion results from methylation of nitrogen.

Reactions of aniline with carbonyl groups are illustrated in figure 26. Liquid-state ^{15}N NMR spectra of the 1989 530 HPON fraction reacted with ^{15}N-labelled aniline are shown in figure 27. The two major peaks in the ACOUSTIC spectrum are the unreacted aniline at 57 ppm and the imines at 324 ppm, the latter resulting from 1,2-nucleophilic addition of aniline to quinone groups (Schiff base formation). Peaks at 79 and 95 ppm in the INEPT spectrum correspond to anilinohydroquinone and anilinoquinone adducts, respectively, from 1,4-nucleophilic addition of aniline to quinones (Thorn and Cox, 2015). The peak at 136 ppm corresponds to heterocyclic nitrogens (indole and quinolone, for example) resulting from intramolecular condensation reactions of aniline with carbonyl groups. Quinone groups occur naturally in aquatic NOM (Thorn and others, 1992) and are present in the resin and asphaltene fractions of the crude oil (Thorn and Cox,

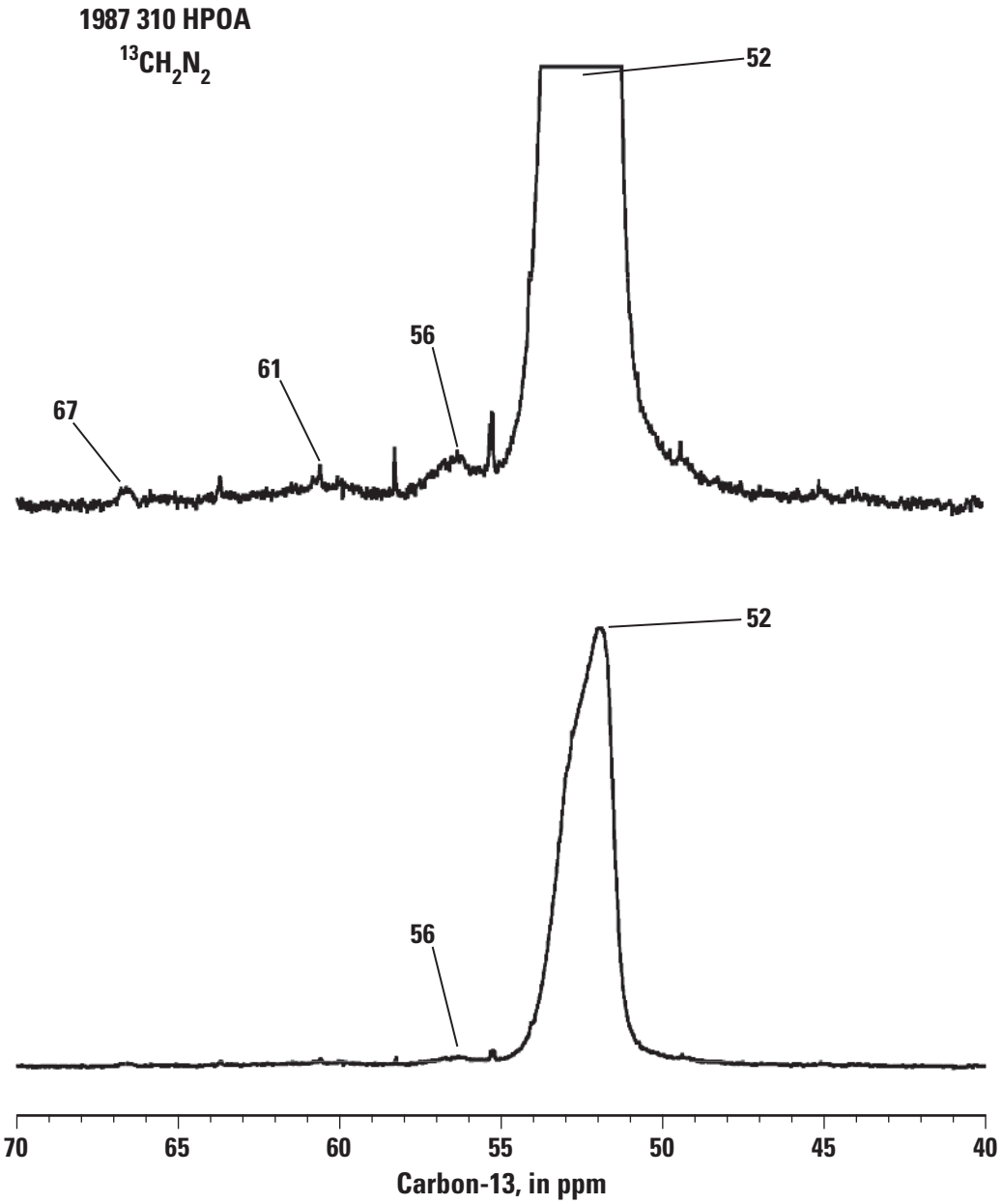

Figure 22. Liquid-state continuous decoupled carbon-13 nuclear magnetic resonance (NMR) spectrum of diazomethylated 1987 well 310 hydrophobic acid (HPOA) fraction. Line broadening = 1.0 hertz. The top spectrum is the vertical expansion, and the bottom spectrum is on scale. ($^{13}CH_2N_2$, diazomethane; ppm, parts per million)

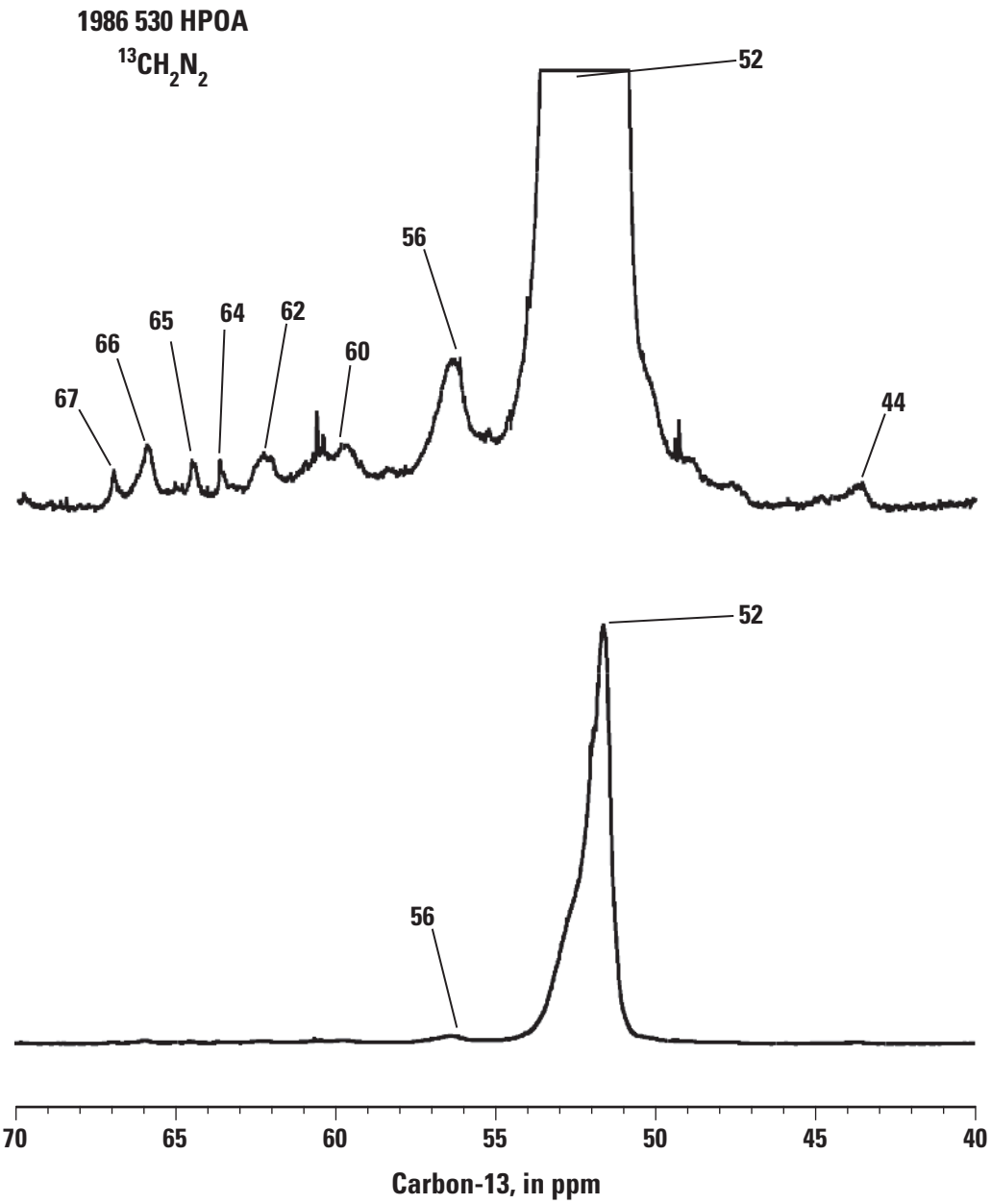

Figure 23. Liquid-state continuous decoupled carbon-13 nuclear magnetic resonance (NMR) spectrum of diazomethylated 1986 well 530 hydrophobic acid (HPOA) fraction. Line broadening = 1.0 hertz. The top spectrum is the vertical expansion, and the bottom spectrum is on scale. ($^{13}CH_2N_2$, diazomethane; ppm, parts per million)

2015). They may also arise from microbial and photochemical oxidation of crude oil constituents. Thus, the source of quinones in the NVOA fractions in contaminated wells may be a combination of the background DOC, the crude oil itself, and the oxidation products of the crude oil constituents. Whatever the origin, the quinone functionality imparts the ability of the NVOAs to mediate redox reactions.

Ester groups have not been analyzed in the NVOAs of this study, but previous work has shown that they are typically present naturally in both soil and aquatic NOM samples and can be detected by ^{15}N NMR as the hydroxamic acid derivatives from reaction with hydroxylamine (Thorn and others, 1992). As illustrated in figure 2, esters are also formed during subterminal oxidation of alkanes and therefore would likely be present in the polar metabolites of crude oil resulting from aerobic oxidation. Ester compounds presumed to be metabolites have been detected in groundwater impacted by fuel release sites (O'Reilly and others, 2015). Esters in the form of acyl glycerides would also be biosynthesized during microbial growth.

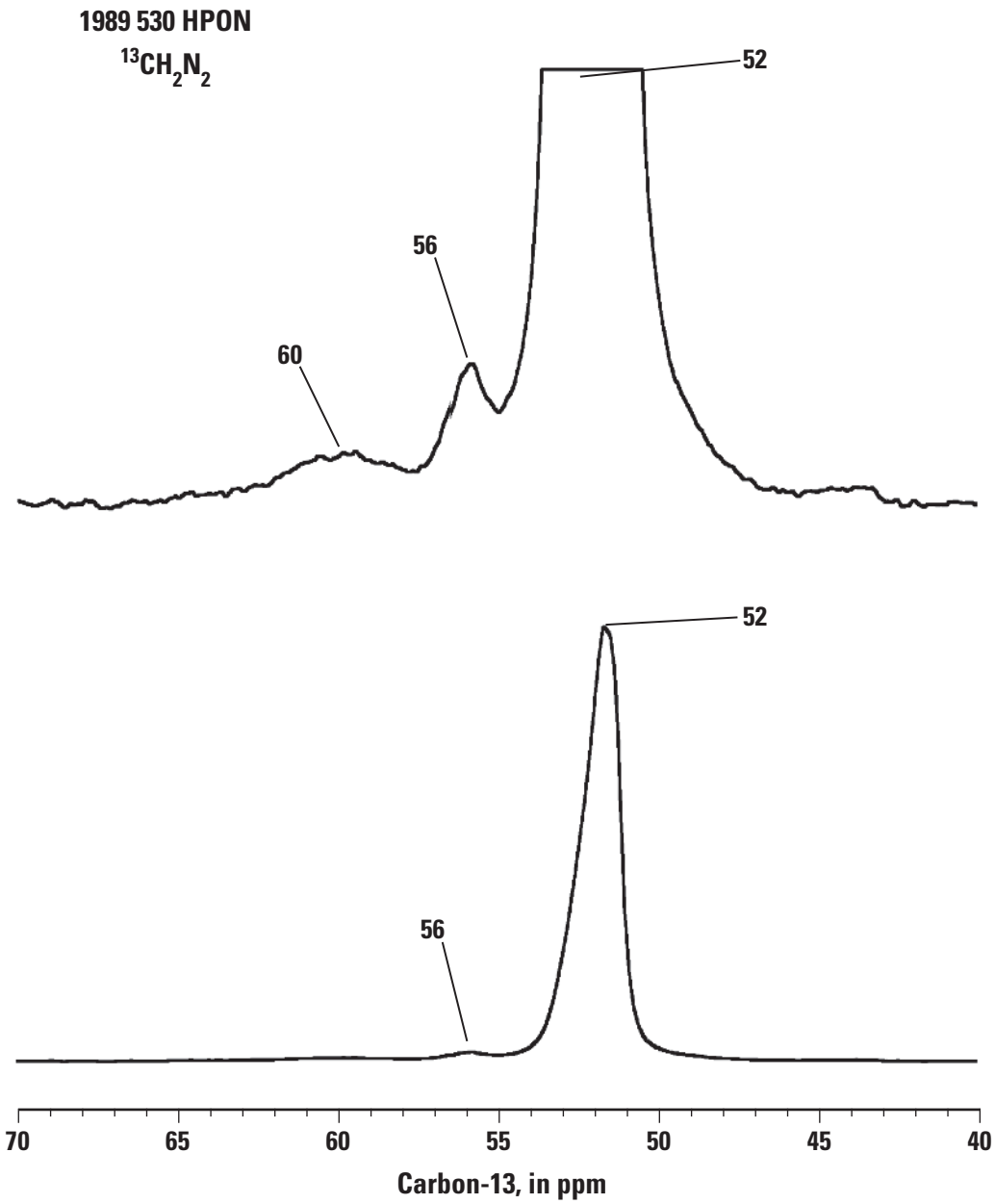

Figure 24. Liquid-state continuous decoupled carbon-13 nuclear magnetic resonance (NMR) spectrum of diazomethylated 1989 well 530 hydrophobic neutral (HPON) fraction. Line broadening = 1.0 hertz. The top spectrum is the vertical expansion, and the bottom spectrum is on scale. ($^{13}CH_2N_2$, diazomethane; ppm, parts per million)

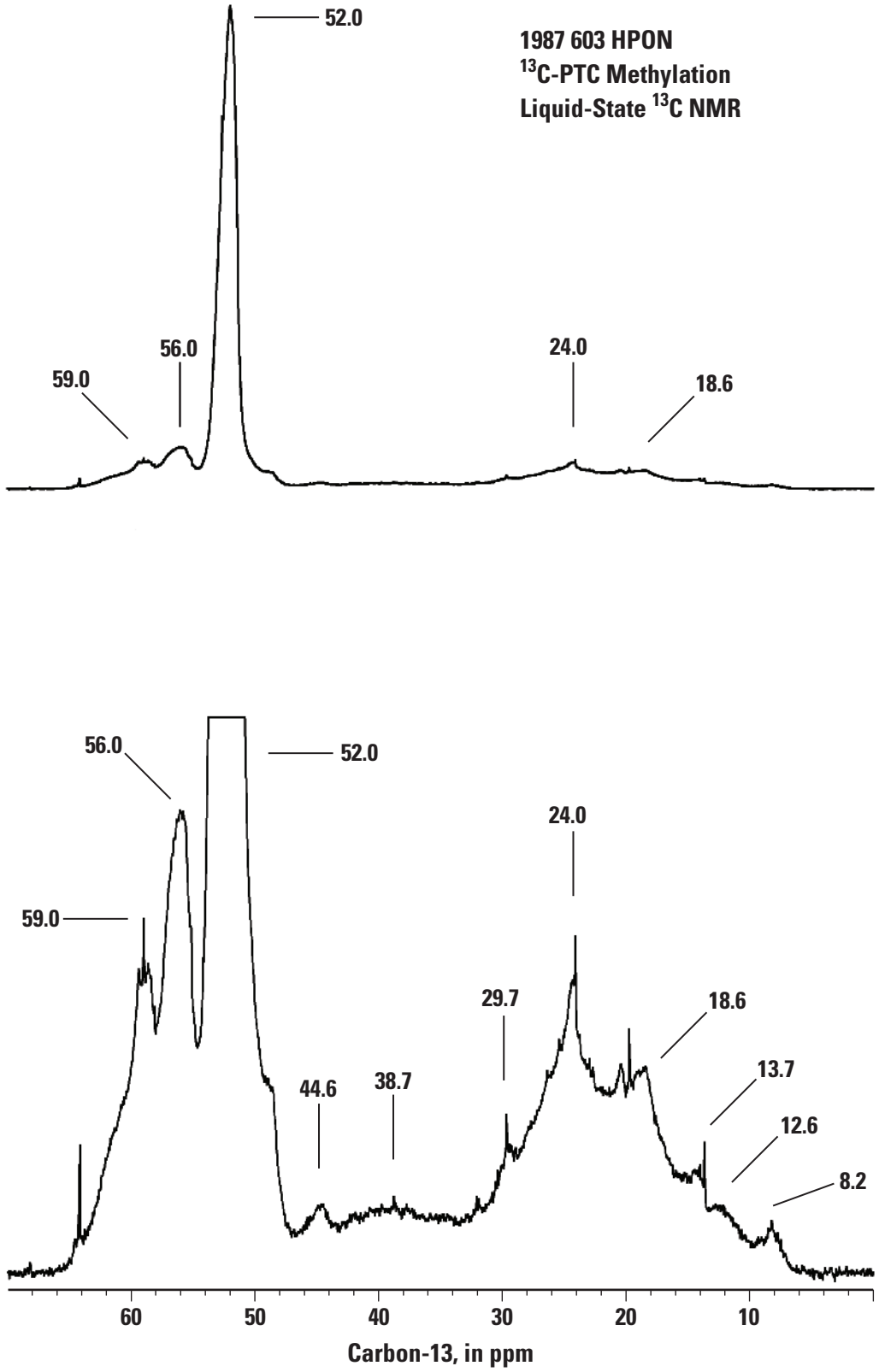

Figure 25. Liquid-state continuous decoupled carbon-13 nuclear magnetic resonance (NMR) spectrum of phase transfer catalysis (PTC)-methylated 1987 603 hydrophobic neutral (HPON) fraction. Line broadening = 1.0 hertz. The top spectrum is the vertical expansion, and the bottom spectrum is on scale. (^{13}C, carbon-13; ppm, parts per million)

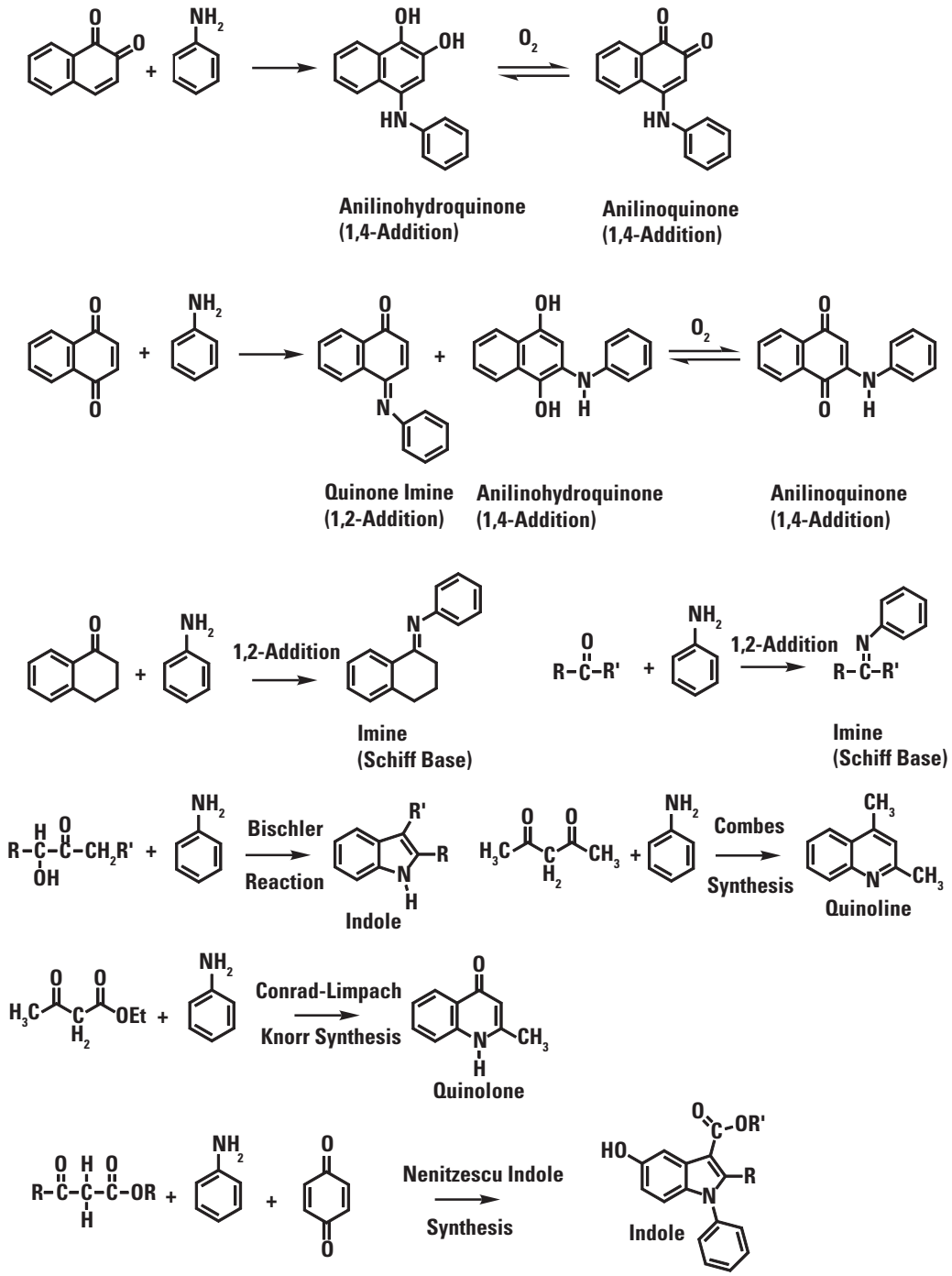

Figure 26. Reactions of aniline with carbonyl groups. (C, carbon; N, nitrogen, O, oxygen; R, attached group; R', attached group)

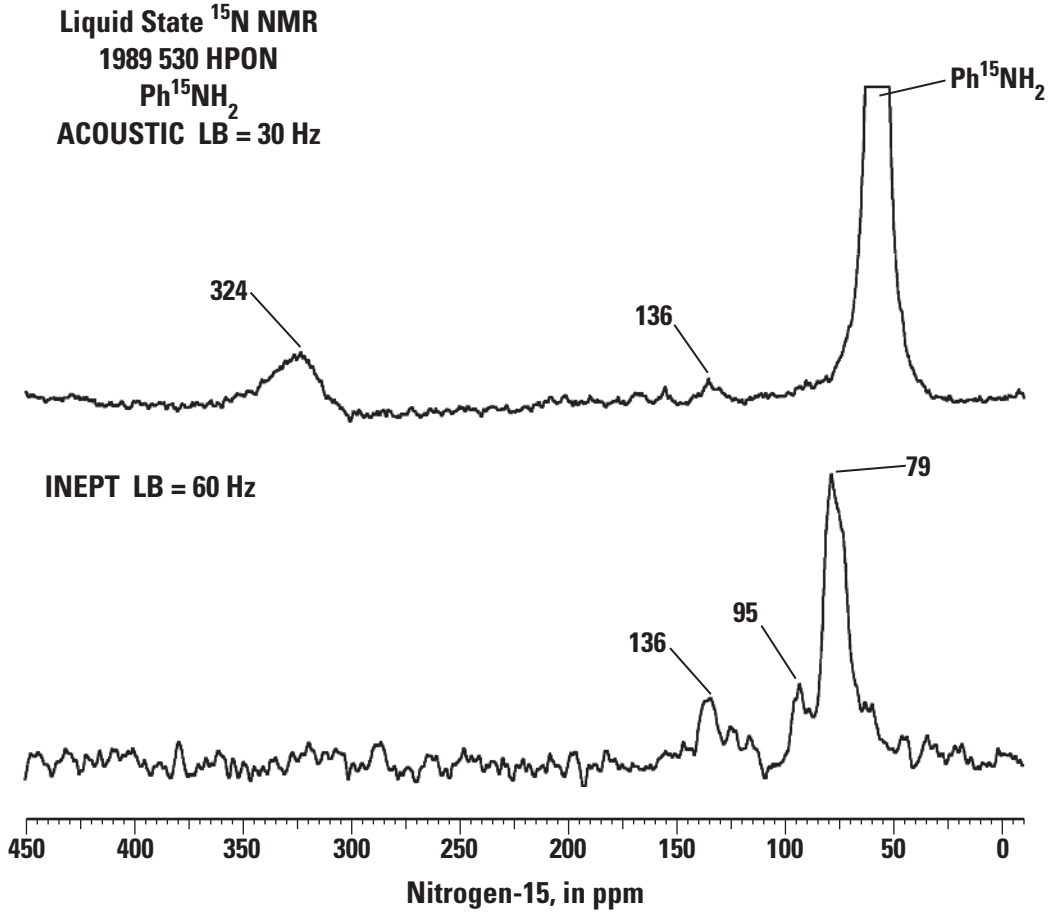

Figure 27. Liquid-state ACOUSTIC (alternating compound one eighties used to suppress transients in the coil) and INEPT (insensitive nuclei enhanced by polarization transfer) nitrogen-15 (^{15}N) nuclear magnetic resonance (NMR) spectra of 1989 well 530 hydrophobic neutral (HPON) fraction reacted with aniline. (Hz, hertz; LB, line broadening; $Ph^{15}NH_2$, aniline; ppm, parts per million)

Fourier Transform Ion Cyclotron Resonance Mass Spectrometry Analyses

Eight samples were analyzed by negative-mode (-) ESI FTICR-MS: 1987 310 HPOA and HPIA, 1986 530 HPOA and HPIA, 1987 603 HPOA and HPIA, and 1998 530 HPOA and HPON. Molecular formulas were reported in Islam and others (2016). Table 6 lists the number of assigned peaks for each sample. They range from 5,697 to 7,544 for 1987 603 HPIA and 1998 HPON, respectively, and the average molecular weights range from 416 for 1987 603 HPIA to 486 for 1987 310 HPOA. Carbon numbers ($C^{\#}$s) from the molecular formulas range from C_6 to C_{81} (table 6). The greater number of formulas detected in the contaminant well HPOA and HPIA fractions compared to their corresponding background well fractions is consistent with the additional input of oil-derived DOC into the groundwater.

Table 6 also subdivides the total number of molecular formulas into those containing oxygen, nitrogen, or sulfur, and those containing O and N; O and S; O, S, and N; and no oxygens. In all cases, the majority of molecular formulas contain oxygen, ranging from 88 to 93 of all assigned peaks. Consistent with elemental analyses, the well 530 and 603 HPOA and HPIA fractions have lower numbers of nitrogen-containing molecular formulas than their corresponding well 310 fractions. Most strikingly, the number of sulfur-containing molecular formulas is significantly greater in the contaminant well fractions, again consistent with their elemental sulfur contents. The distribution of sulfur-containing molecular formulas then is a major characteristic distinguishing the background from contaminant well DOC. The percentages of assigned molecular formulas containing no oxygens range from 7 to 12. These molecular formulas without oxygen are mainly compounds containing nitrogen or sulfur heteroatoms (table 6).

The numbers of matching molecular formulas between selected pairs of samples are listed in table 7. It must be emphasized that these matches do not take into account structural isomers (constitutional isomers) and therefore represent an upper limit on the number of individual structures common to each sample. Comparing the number of formula

Table 6. Number of peaks assigned with chemical formulas from the spectra obtained by negative-mode (-) electrospray ionization Fourier transform ion cyclotron resonance mass spectrometry, average molecular weights (Ave MW) of assigned peaks, range of carbon numbers (C#s) for assigned peaks, and number of molecular formulas containing oxygen (O), oxygen and nitrogen (O+N), nitrogen (N), oxygen and sulfur (O+S), sulfur (S), oxygen and nitrogen and sulfur (O+N+S), no oxygen, nitrogen without oxygen, and sulfur without oxygen.

[Data for sample 1998 530 HPON are from one replicate. HPIA, hydrophilic acid; HPOA, hydrophobic acid; HPON, hydrophobic neutral; No., number; %, percent]

Sample	No. of assigned peaks	Ave MW of assigned peaks	Range of C#	No. of O	No. of O+N	No. of N	No. of O+S	No. of S	No. of O+N+S	No. Without O	No. of N without O	No. of S without O
1987 310 HPOA	6,414	486	C_6–C_{76}	5,654 (88%)	3,383 (53%)	3,981 (62%)	637 (10%)	727 (11%)	0	760 (12%)	598 (9%)	90 (1%)
1987 310 HPIA	6,007	457	$C_{7-}C_{81}$	5,316 (89%)	3,451 (57%)	3,932 (65%)	646 (11%)	725 (12%)	0	691 (12%)	481 (8%)	79 (1%)
1987 603 HPOA	6,612	421	C_{10}–C_{65}	6,142 (93%)	1,454 (22%)	1,810 (27%)	2,307 (35%)	2,407 (36%)	0	470 (7%)	356 (5%)	100 (2%)
1987 603 HPIA	5,697	416	C_8–C_{76}	5,123 (90%)	2,346 (41%)	2,780 (49%)	1,510 (27%)	1,539 (27%)	0	574 (10%)	434 (8%)	29 (1%)
1986 530 HPOA	7,255	456	C_8–C_{74}	6,591 (91%)	2,358 (33%)	2,934 (40%)	2,299 (32%)	2,356 (33%)	0	664 (9%)	576 (8%)	57 (1%)
1986 530 HPIA	6,900	442	C_8–C_{63}	6,069 (88%)	3,327 (48%)	3,873 (56%)	1,221 (18%)	1,324 (19%)	0	831 (12%)	546 (8%)	103 (2%)
1998 530 HPOA	7,467	446	C_8–C_{76}	6,809 (91%)	2,206 (30%)	2,768 (37%)	2,452 (33%)	2,513 (34%)	0	658 (9%)	562 (8%)	61 (1%)
1998 530 HPON	7,643	430	C_{12}–C_{76}	7,087 (93%)	1,990 (26%)	2,336 (31%)	2,448 (32%)	2,592 (34%)	0	556 (7%)	346 (5%)	144 (2%)

Table 7. Number of matching molecular formulas between hydrophobic acid (HPOA) and hydrophilic acid (HPIA) fractions, percent (%) of formulas matched in each sample pair, and number of formulas unique to contaminant well fractions.

	Sample(s)
	Number of matching molecular formulas between sample pairs
1987 310 HPOA and 1987 310 HPIA	3,333
1986 530 HPOA and 1986 530 HPIA	2,915
1986 530 HPOA and 1998 530 HPOA	5,583
1987 603 HPOA and 1987 603 HPIA	2,271
1987 310 HPOA and 1986 530 HPOA	3,542
1987 310 HPOA and 1998 530 HPOA	3,411
1987 310 HPOA and 1987 603 HPOA	2,398
1987 310 HPIA and 1986 530 HPIA	4,075
1987 310 HPIA and 1987 603 HPIA	3,020
	Percent of molecular formulas matched in pair
1987 310 HPOA	52.0% in 1987 310 HPIA
1987 310 HPIA	55.5% in 1987 310 HPOA
1986 530 HPOA	40.2% in 1986 530 HPIA
1986 530 HPIA	42.2% in 1986 530 HPOA
1987 603 HPOA	34.3% in 1987 603 HPIA
1987 603 HPIA	39.9% in 1987 603 HPOA
	Number of molecular formulas unique to contaminant fraction
1986 530 HPOA and 1987 310 HPOA	3,713 (51.2%)
1986 530 HPIA and 1987 310 HPIA	2,825 (40.9%)
1987 603 HPOA and 1987 310 HPOA	421 (63.7%)
1987 603 HPIA and 1987 310 HPIA	162 (28.5%)
1998 530 HPOA and1987 310 HPOA	4,056 (54.3%)

matches between sets of HPOA and HPIA fractions from the same water sample provides insight into the process of how the DOC partitions between the XAD-8 and XAD-4 resins in the two-column array isolation procedure. Thus, 52 percent of the molecular formulas in 1987 310 HPOA are present in 1987 310 HPIA, 40.2 percent of molecular formulas in 1986 530 HPOA are present in 1986 530 HPIA, and 34.3 percent of molecular formulas in 1987 603 HPOA are present in 1987 603 HPIA. Again, these percentages represent an upper limit on the overlap of individual structures, as the number of structural isomers cannot be determined from the FTICR-MS data.

Subtracting the number of molecular formula matches between the background 1987 310 HPOA and each of the contaminant well HPOA fractions leaves 3,713, 4,214, and 4,056 molecular formulas unique (that is, oil derived) to the 1986 530 HPOA, 1987 603 HPOA, and 1998 530 HPOA samples, respectively. Likewise, subtracting the number of molecular formula matches between the background 1987 310 HPIA and the two contaminant HPIA fractions leaves 2,825 and 1,622 molecular formulas unique to the 1986 530 HPIA and 1987 603 HPIA samples, respectively. These numbers of unique molecular formulas represent a lower limit, as the number of structural isomers again are unknown. In this limited dataset, the lower proportion of unique, or oil derived, molecular formulas in the contaminant well HPIA samples compared to the HPOA samples is consistent with the general observation that the contaminant well HPIA samples have higher fractions of modern carbon (younger ^{14}C ages) than their corresponding HPOA samples. In other words, there is a greater concentration of oil-derived DOC isolates in the HPOA than in the HPIA fractions. These calculations rely on as yet unconfirmed assumptions that interannual changes in the composition of the background DOC are not significant, or that mixing of the background and oil-derived DOC does not effect an accelerated cometabolic biodegradation of the background DOC.

Analyses of molecular formulas derived from FTICR-MS data of crude oil and natural organic matter have been undertaken via a number of calculations and graphical representations, including aromaticity indices, nominal oxidation state of carbon determinations, van Krevelen diagrams, and more (Hur and others, 2010). Here, we report relative abundances of $O_{4\text{-}10}$, S_1, $S_1O_{1\text{-}10}$, $N_{1\text{-}4}$, $N_1O_{1\text{-}10}$, and $S_1O_{1\text{-}10}$ class compounds and DBE versus $C^{\#}$ plots for the $O_{4\text{-}10}$ class compounds to distinguish background from oil-derived DOC. Additional analyses of the FTICR-MS data are ongoing. The discussion that follows should be considered within the context of the quantitative limitations of (-) ESI FTICR referred to in the "Methods" section.

Distribution of Heteroatom-Containing Classes

Oxygen-Containing Classes

As discussed in the previous section, oxygen-containing compound classes were the most abundant detected by (-) ESI in the eight samples analyzed (figs. 28–30; Islam and others, 2016). The ranges of oxygen to carbon (O/C) ratios determined from the molecular formulas of the $O_{4\text{-}10}$ oxygen class compounds (all molecular formulas containing oxygen) reveal significant variation in the oxidation state and polarity among the molecules comprising the individual HPIA, HPOA, and HPON fractions (table 8). The lowest value of 0.06 occurs in the O_4 compound class of the 1987 603 HPOA while the highest value of 1.0 occurs in the O_{10} compound class of the 1998 530 HPON. Figure 28 shows that O_8, O_9, and O_{10} are the major classes for the 1987 310 HPOA fraction, whereas lower oxygen-containing species such as O_5, O_6, and O_7 are the major compound classes for the 1986 530 HPOA, 1998 530 HPOA, and 1987 603 HPOA fractions. For example, the relative abundance of the O_8 group was 25 percent for 1987 310 HPOA, but it was 13 percent for 1987 603 HPOA. Comparing the 1986 and 1998 530 HPOA fractions, 1986 has lower $O_{4\text{–}6}$ but higher $O_{8\text{–}10}$ relative abundances. These abundances suggest a relative increase from 1986 to 1998 in the concentration of oil constituents that have undergone only partial oxidation and would be consistent with the increase in DOC (from 21 to 24 mg C/L; table 1) and decrease in fraction modern carbon (from 0.2342 to 0.1610; table 3), coinciding with downgradient migration of the contaminant plume.

Differences in the distribution of the O_n species within the HPIA samples are less pronounced (fig. 29). The 1987 310 HPIA sample is predominated by the O_9, O_{10}, and O_8 compound classes, in that order, whereas the 1986 530 HPIA sample is predominated by the O_9, O_8, and O_{10}, and 1987 603 HPIA is predominated by the O_8, O_7, and O_9 compound classes. The 1986 530 and 1987 603 HPIA samples have greater proportions of O_6 and O_7 compound classes and lower proportions of O_9 and O_{10} compound classes than the 1987 310 HPIA sample.

Comparing the 1998 530 HPON and 1998 530 HPOA fractions, the HPON has O_5, O_4, and O_6 as its major classes, respectively, while its O_8, O_9, and O_{10} classes occur in significantly smaller proportions than the HPOA (fig. 30). For the HPOA fraction, O_6, O_7, and O_5 are the major compound classes, respectively (fig. 30).

The greater abundance of lower oxygen-containing species for contaminant well HPOA and HPIA samples (wells 530 and 603) compared to the background (well 310) is again attributable to the lower degree of oxidation for compounds originating from the oil. The elevated concentrations of DOC at wells 530 and 603 indicate that a significant proportion of the DOC is oil derived, so it is reasonable that the presence of DOC derived from parent hydrocarbons (including the oxygen-containing constituents of the aromatic, resin, and asphaltene fractions) that have undergone only partial oxidation shifts the distribution of oxygen species to lower numbers compared to well 310. Presumably, the 310 HPON would also show a greater abundance of higher oxygen-containing species than the 603 and 530 HPONs, and this item is of interest for future investigation.

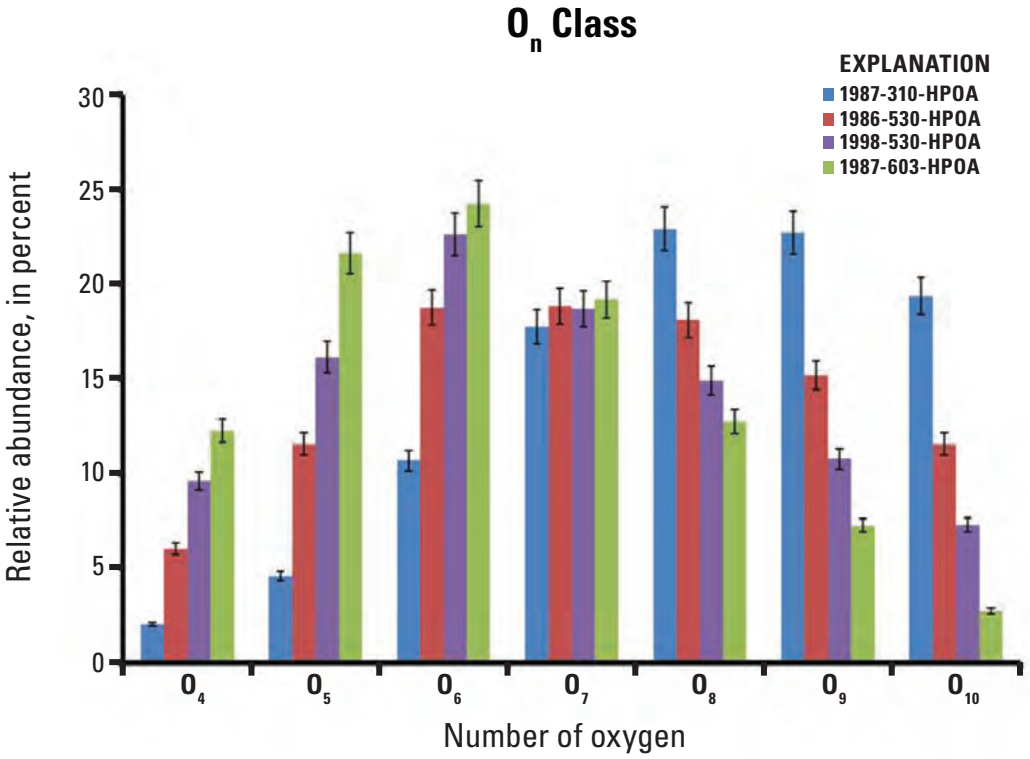

Figure 28. Distribution of O_n class compounds (compounds containing n number of oxygen atoms) in hydrophobic acid (HPOA) fractions determined by Fourier transform ion cyclotron resonance mass spectrometry (FTICR-MS). Figure is from Islam and others, 2016.

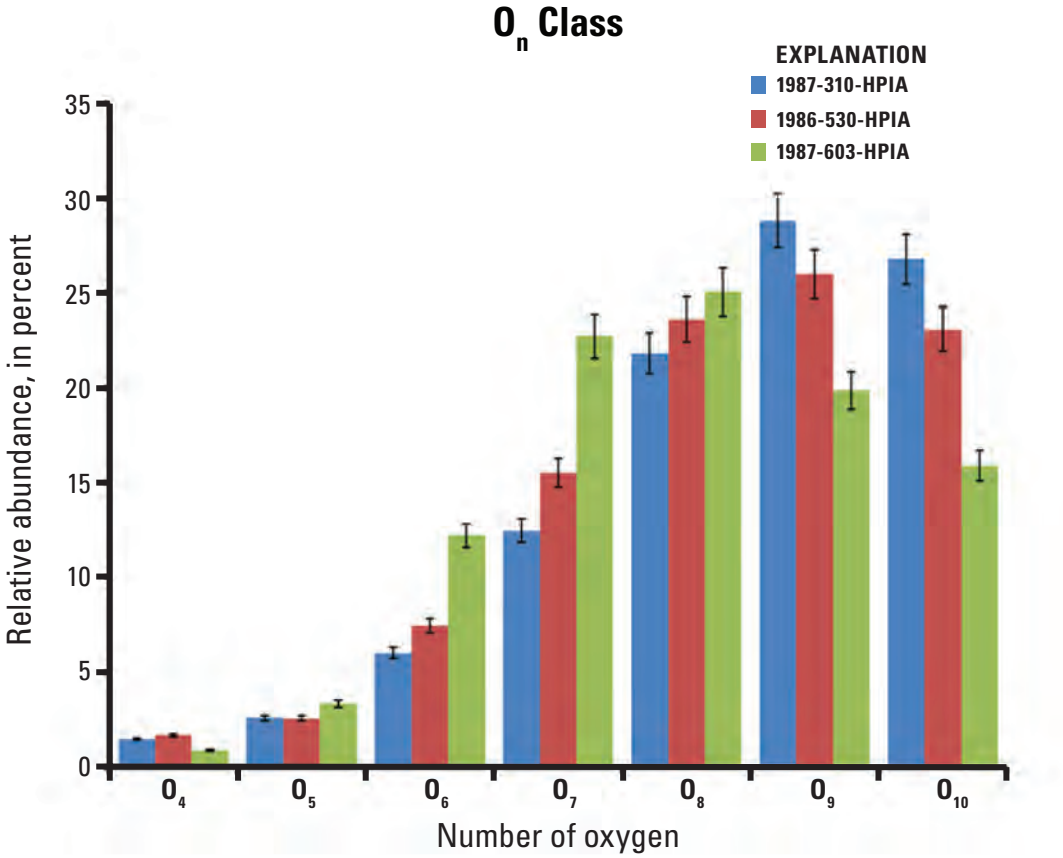

Figure 29. Distribution of O_n class compounds (compounds containing n number of oxygen atoms) in hydrophilic acid (HPIA) fractions determined by Fourier transform ion cyclotron resonance mass spectrometry (FTICR-MS). Figure is from Islam and others, 2016.

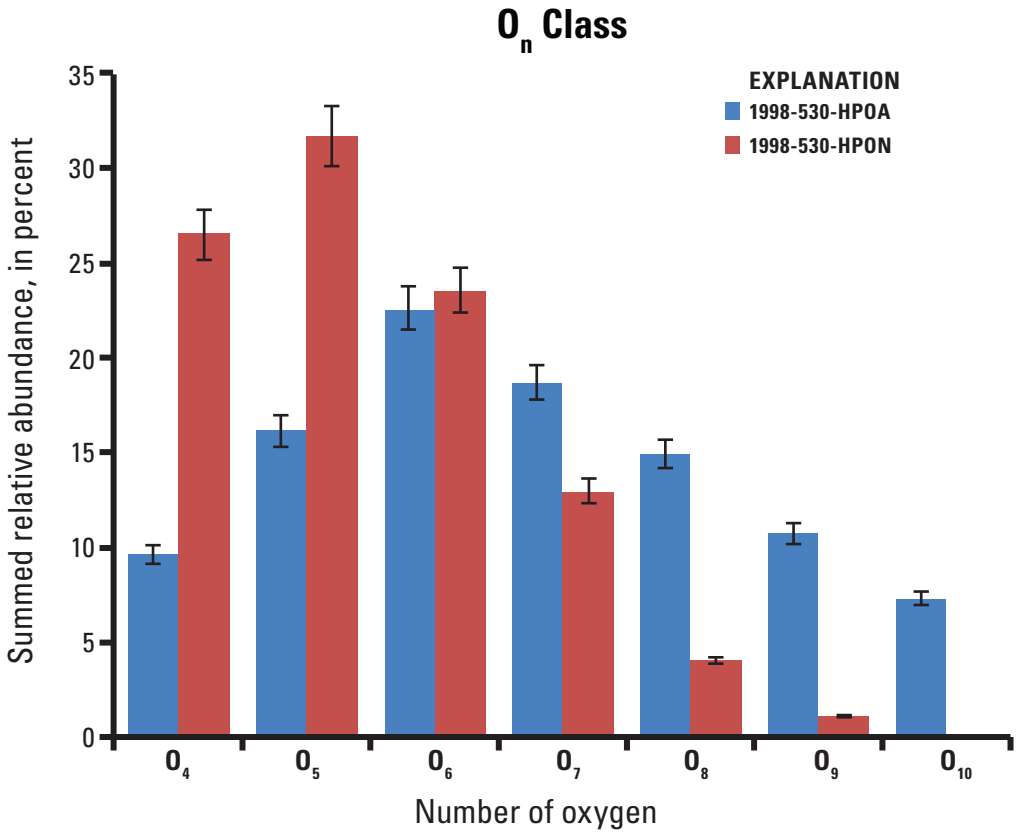

Figure 30. Distribution of O_n class compounds (compounds containing n number of oxygen atoms) in 1998 well 530 hydrophobic acid (HPOA) and hydrophobic neutral (HPON) fractions determined by Fourier transform ion cyclotron resonance mass spectrometry (FTICR-MS).

Table 8. Ranges of oxygen to carbon (O/C) ratios for oxygen class compounds containing n number of oxygen atoms (O_n) determined by Fourier transform ion cyclotron resonance mass spectrometry compared with O/C ratios of entire samples determined by elemental analysis.

[HPIA, hydrophilic acid; HPOA, hydrophobic acid; HPON, hydrophobic neutral; O_n, oxygen class compound with n number of oxygen atoms]

Sample	Ranges of oxygen to carbon (O/C) ratios							
	O_4	O_5	O_6	O_7	O_8	O_9	O_{10}	Elemental Analysis
1986 Well 530 HPOA	0.1–0.3	0.1–0.4	0.2–0.5	0.2–0.6	0.2–0.6	0.2–0.6	0.2–0.7	0.47
1986 Well 530 HPIA	0.09–0.2	0.1–0.4	0.09–0.5	0.2–0.7	0.2–0.8	0.2–0.8	0.3–0.8	0.74
1987 Well 603 HPOA	0.06–0.3	0.1–0.4	0.1–0.5	0.1–0.5	0.2–0.6	0.2–0.7	0.1–0.6	0.44
1987 Well 603 HPIA	0.1–0.2	0.1–0.4	0.1–0.5	0.2–0.6	0.2–0.7	0.2–0.8	0.3–0.9	0.78
1998 Well 530 HPON	0.1–0.2	0.1–0.3	0.1–0.5	0.1–0.5	0.2–0.5	0.2–0.5	0.2–0.3	0.36
1998 Well 530 HPOA	0.1–0.3	0.1–0.4	0.1–0.5	0.2–0.5	0.2–0.6	0.2–0.7	0.2–1.0	0.5
1987 Well 310 HPOA	0.1–0.3	0.1–0.4	0.1–0.5	0.2–0.6	0.2–0.7	0.2–0.7	0.2–0.7	0.66
1987 Well 310 HPIA	0.09–0.3	0.1–0.3	0.2–0.5	0.2–0.6	0.3–0.7	0.3–0.8	0.3–0.9	0.77

Sulfur-Containing Classes

The distribution of classes containing one sulfur atom (S_1) is shown in figure 31. The 1998 530 HPON fraction has the highest relative abundance of S_1 class compounds. The S_1 compound classes in general do not conform to any pattern distinguishing the background from contaminated wells, which contrasts with the S_1O_n compound classes where the differences are significant (figs. 32–35). The contaminant well HPOA samples all have greater concentrations of S_1O_n compounds than the background sample, especially with regard to the higher oxygenated species such as S_1O_8, S_1O_9, and S_1O_{10} (fig. 33). Within the contaminant well HPOA fractions, the S_1O_4, S_1O_5, and S_1O_6 compounds are notably higher in the well 603 (spray zone) sample than in the well 530 samples. The contaminant well HPIA samples also have a greater concentration of oxygenated sulfur species than the background sample, the S_1O_5, S_1O_6, S_1O_7, S_1O_8, S_1O_9, and S_1O_{10} species in particular (fig. 34). Although a corresponding HPON fraction from well 310 was unavailable for comparison, it is interesting to note that the 1998 530 HPON fraction also contains a significant concentration of S_1O_n class compounds, particularly $S_1O_{3–6}$ constituents (fig. 35).

The greater concentrations of S_1O_n class compounds in the contaminant well HPOA and HPIA fractions correlate with the elemental sulfur contents of these samples (table 2), all of which are greater than their corresponding background samples. In turn, the elevated elemental sulfur contents of the contaminant well HPOA and HPIA fractions can be attributed in part to the presence of S_1O_n class compounds. All four contaminant well HPON fractions have significant sulfur contents ranging from 2.85 percent for 1989 530 HPON to 6.28 percent for 1998 530 HPON.

The main sulfur-containing constituents in crude oil are thiols, sulfides, disulfides, sulfoxides, thiophenes, thioxanthones (Robson and others, 2017), in addition to resins and asphaltenes. The sulfur resides mainly in the aromatic, resin, and asphaltene fractions of the crude oil (table 2). Presumably, the S_1O_n compounds correspond primarily to the soluble partial degradation products of the sulfur-containing constituents in the crude oil. The S_1O_n compounds may derive from the aromatic, resin, or asphaltene fractions of the oil, or reflect an enrichment of sulfur-containing constituents of the oil in general that have not undergone complete biodegradation. Waldo and others (1991) suggested that organosulfide species in crude oil may undergo autoxidation to sulfoxides when exposed to oxic waters in shallow reservoirs. This pathway

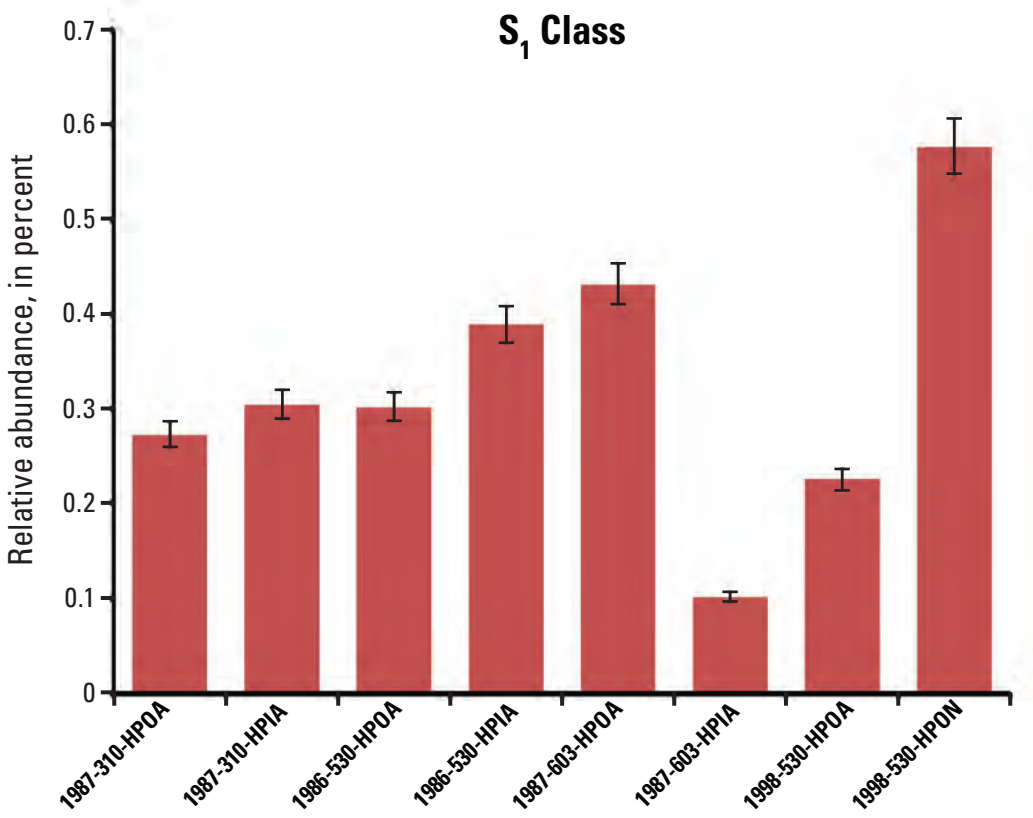

Figure 31. Distribution of S_1 class compounds (compounds containing one sulfur atom) in nonvolatile organic acid fractions determined by Fourier transform ion cyclotron resonance mass spectrometry (FTICR-MS). (HPIA, hydrophilic acid; HPOA, hydrophobic acid; HPON, hydrophobic neutral)

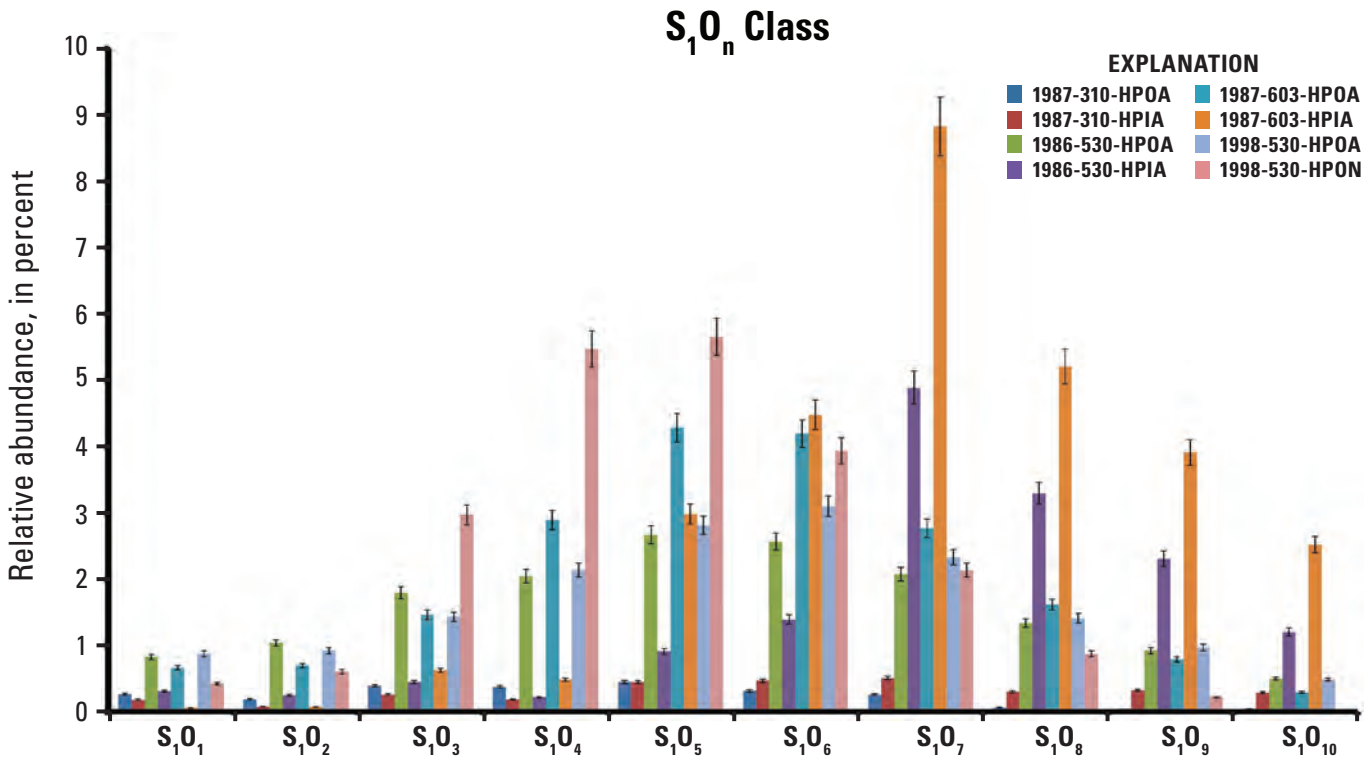

Figure 32. Distribution of S_1O_n class compounds (compounds containing one sulfur atom and n number of oxygen atoms) in nonvolatile organic acid (NVOA) fractions determined by Fourier transform ion cyclotron resonance mass spectrometry (FTICR-MS). Figure is from Islam and others (2016). (HPIA, hydrophilic acid; HPOA, hydrophobic acid; HPON, hydrophobic neutral)

is a potential nonmicrobial one that could account in part for the S_1O_n species in the well 603 samples isolated from oxic groundwater.

Sulfur-containing compounds have been diagnostic of oil contamination in other study sites. Degradation of oil samples from the 2007 South Korea M/V Hebei Spirit oil spill resulted in higher abundances of S_1O_1 class compounds (Islam and others, 2013; Islam and others, 2015). Sulfur-containing compounds and oxygenated sulfur species have been reported as constituents in water impacted by oil from the Athabasca oil sands (Headley and others, 2011; Barrow and others, 2014; Barrow and others, 2015; Headley and others, 2016; Vaughan and others, 2016).

Nitrogen-Containing Classes

The distribution of $N_{1\text{-}4}$ class compounds (compounds containing one to four nitrogens) is shown in figures 36–37. Compounds containing two nitrogens (N_2) are the major classes for both the background (310) and contaminant wells (530 and 603). Distributions of $N_1O_{1\text{-}10}$ class compounds (compounds containing one nitrogen and one to ten oxygens) are shown in figures 38–41. For both HPOA (fig. 38) and HPIA (fig. 40) fractions, there is no discernible pattern distinguishing the background from contaminant well samples. The N_1O_1 and N_1O_2 species are the most abundant for the background and contaminant well HPOA fractions (fig. 39). Among HPOA fractions, 1987 603 has the highest concentrations of $N_1O_{4\text{–}7}$ species. In the three HPIA fractions, the higher oxygenated $N_1O_{7\text{–}10}$ species are the most abundant (fig. 40). There is somewhat of a Gaussian distribution of the $N_1O_{1\text{–}10}$ class compounds for the 1998 530 HPON fraction (fig. 41), in which the N_1O_4 and N_1O_5 species have the greatest abundance. The distributions of $N_2O_{1\text{-}10}$ class compounds appear to distinguish the background from the contaminant HPOA and HPIA fractions (figs. 42–45). For both HPOA and HPIA fractions in the background and contaminant wells, the concentrations of N_2O_n species decrease with increasing numbers of oxygens from 1 through 10. The 1987 310 HPOA has the highest concentrations of $N_2O_{1\text{–}7}$ species among the HPOA fractions (fig. 43), while the 1987 310 HPIA (fig. 44) has the highest concentrations of $N_2O_{1\text{–}10}$ species among the HPIA fractions. For the most abundant $N_2O_{1\text{–}3}$ species, 1987 603 HPOA has the lowest concentrations among the HPOA fractions. Of the HPIA fractions, 1987 603 HPIA has the lowest concentrations for the entire suite of $N_2O_{1\text{–}10}$ class compounds. The most abundant N_2O_n species for the 1998 530 HPON fraction are N_2O_1, N_2O_2, and N_2O_6 in that order (fig. 45).

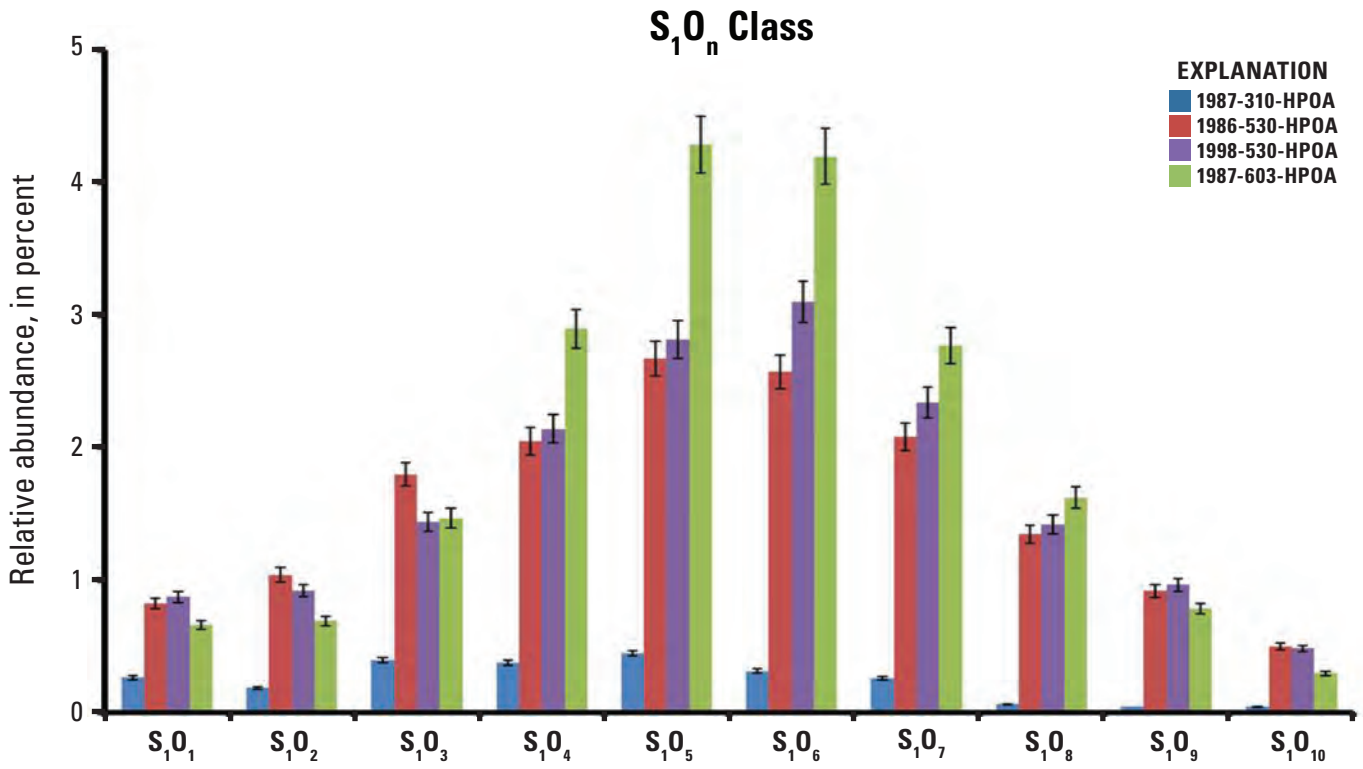

Figure 33. Distribution of S_1O_n class compounds (compounds containing one sulfur atom and n number of oxygen atoms) in hydrophobic acid (HPOA) fractions determined by Fourier transform ion cyclotron resonance mass spectrometry (FTICR-MS). Figure is from Islam and others (2016).

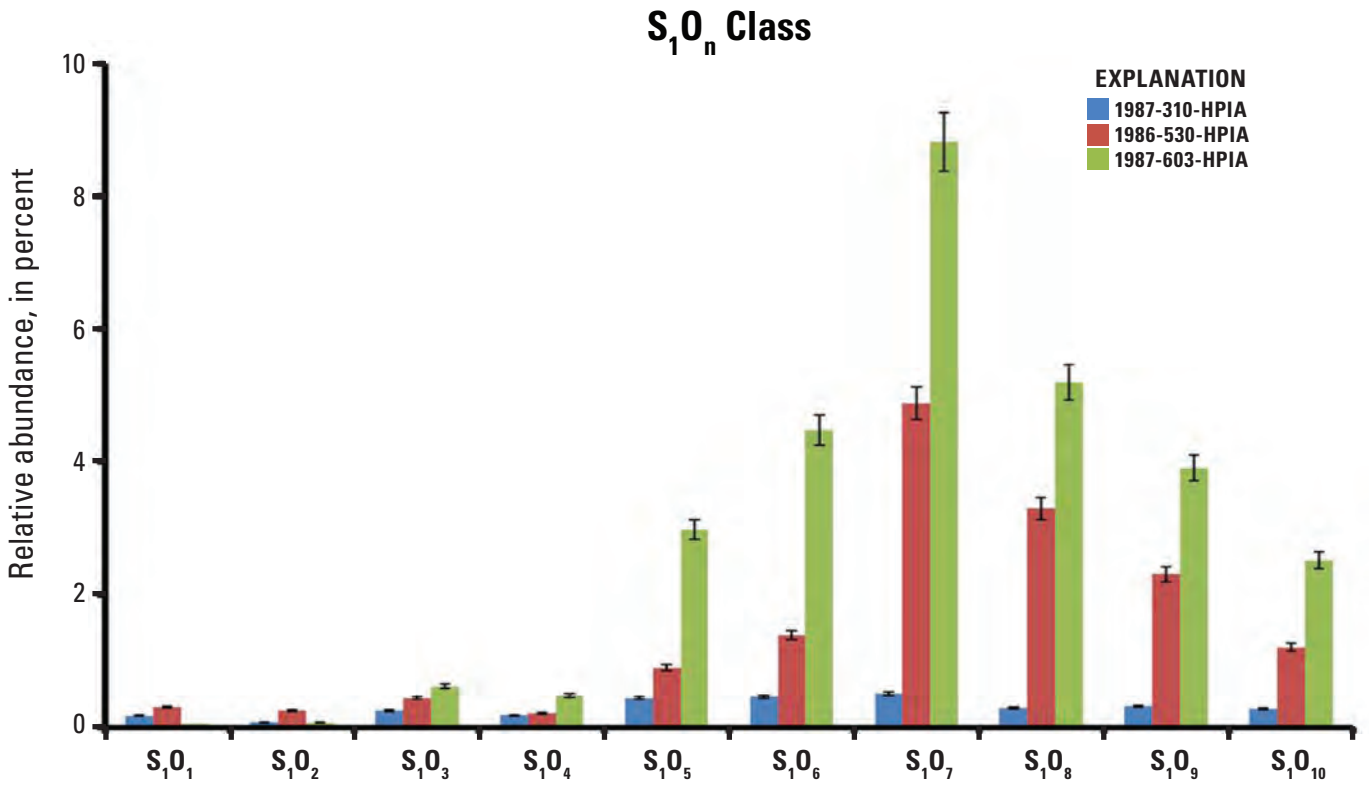

Figure 34. Distribution of S_1O_n class compounds (compounds containing one sulfur atom and n number of oxygen atoms) in hydrophilic acid (HPIA) fractions determined by Fourier transform ion cyclotron resonance mass spectrometry (FTICR-MS). Figure is from Islam and others (2016).

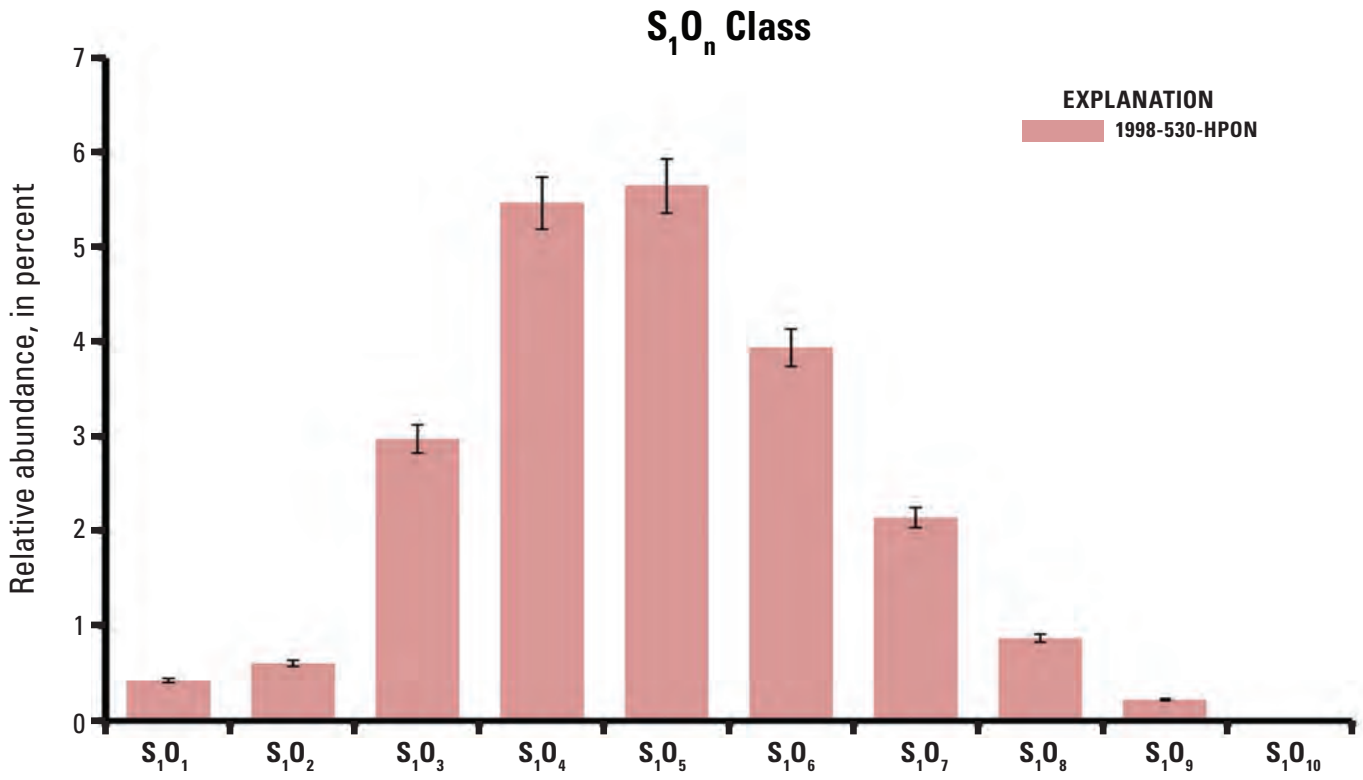

Figure 35. Distribution of S_1O_n class compounds (compounds containing one sulfur atom and n number of oxygen atoms) in the 1998 well 530 hydrophobic neutral (HPON) fraction determined by Fourier transform ion cyclotron resonance mass spectrometry (FTICR-MS). Figure is from Islam and others (2016).

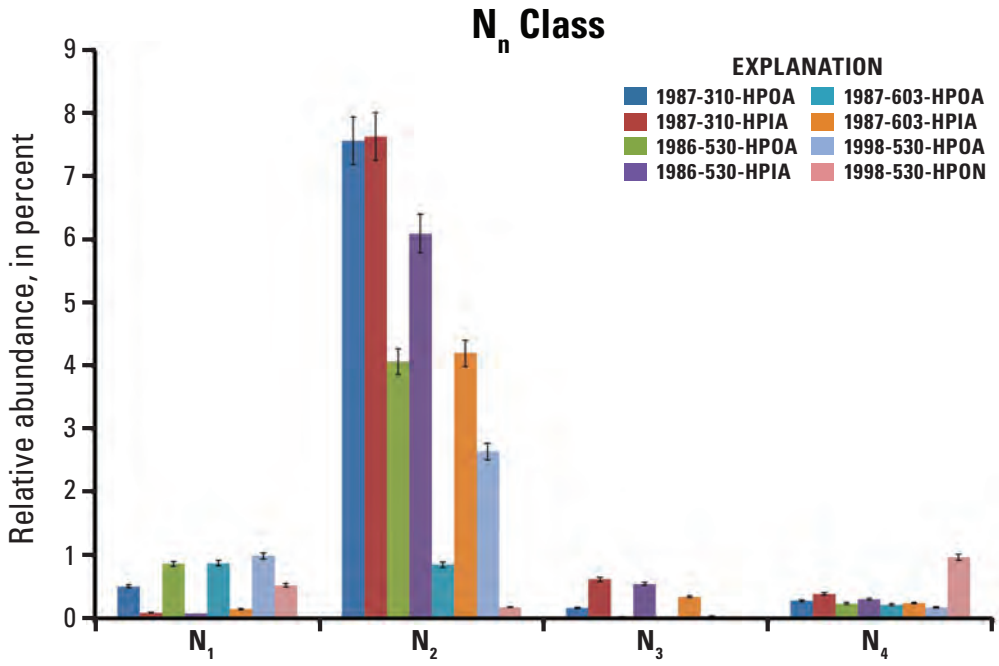

Figure 36. Distribution of N_n class compounds (compounds containing n number of nitrogen atoms) in nonvolatile organic acid (NVOA) fractions determined by Fourier transform ion cyclotron resonance mass spectrometry (FTICR-MS). (HPIA, hydrophilic acid; HPOA, hydrophobic acid; HPON, hydrophobic neutral)

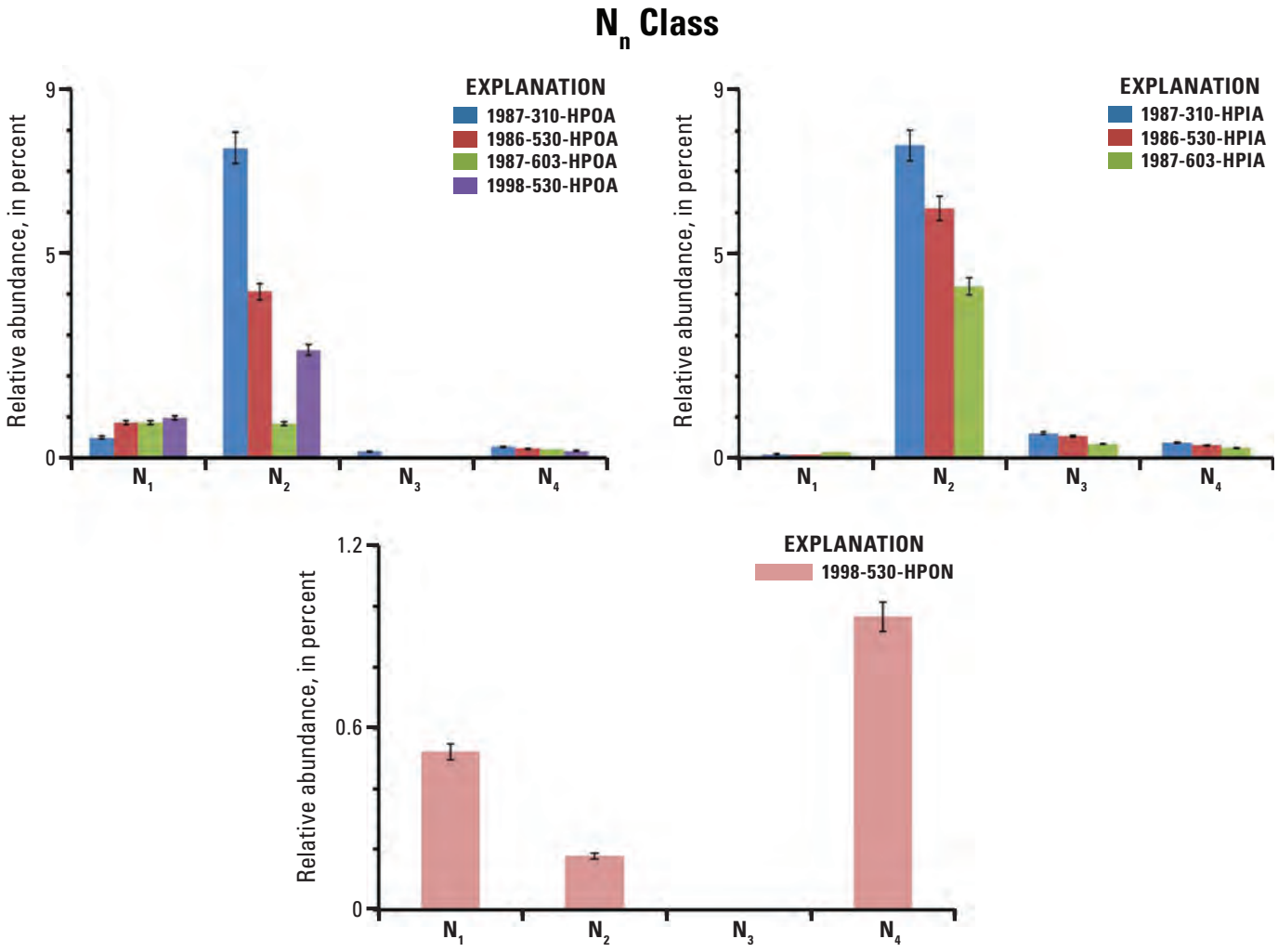

Figure 37. Distribution of N_n class compounds (compounds containing n number of nitrogen atoms) in hydrophobic acid (HPOA), hydrophilic acid (HPIA), and hydrophobic neutral (HPON) fractions determined by Fourier transform ion cyclotron resonance mass spectrometry (FTICR-MS).

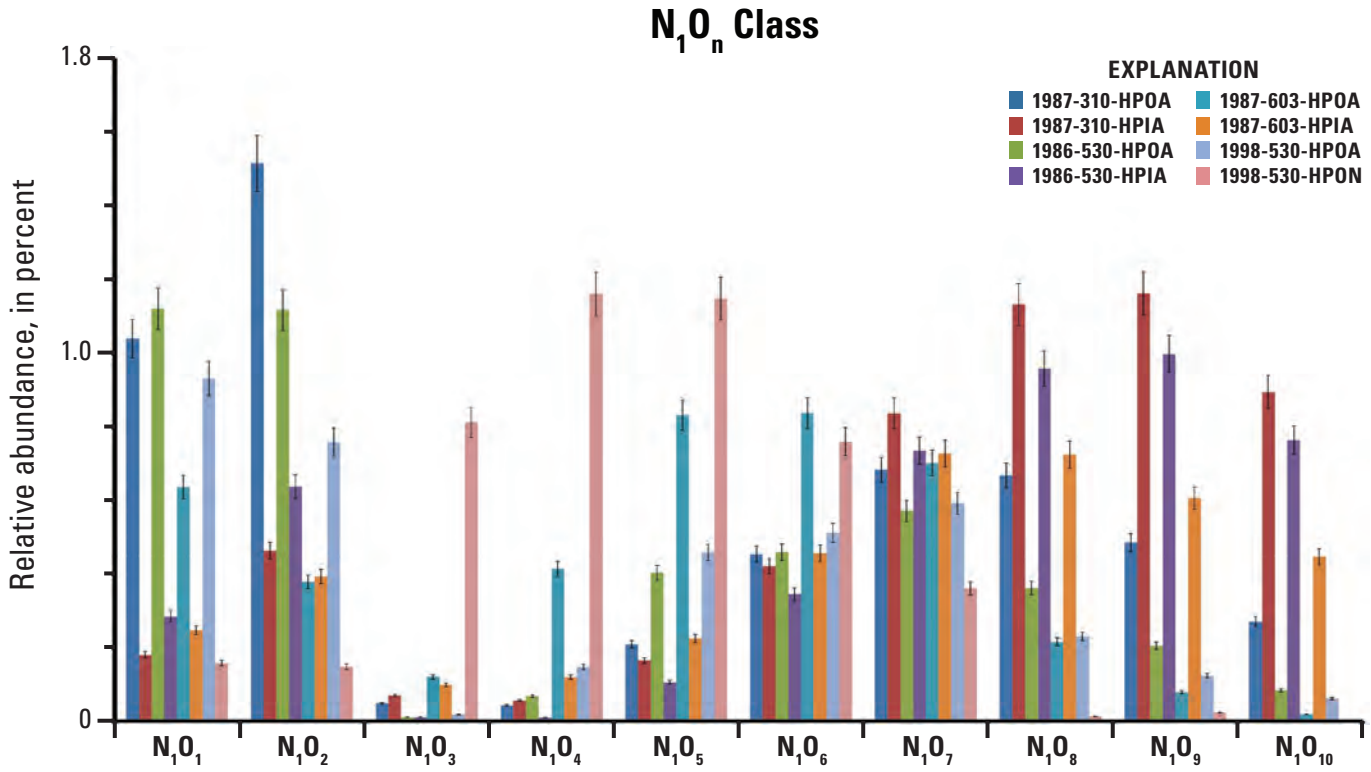

Figure 38. Distribution of N_1O_n class compounds (compounds containing one nitrogen atom and n number of oxygen atoms) in nonvolatile organic acid (NVOA) fractions determined by Fourier transform ion cyclotron resonance mass spectrometry (FTICR-MS). (HPIA, hydrophilic acid; HPOA, hydrophobic acid)

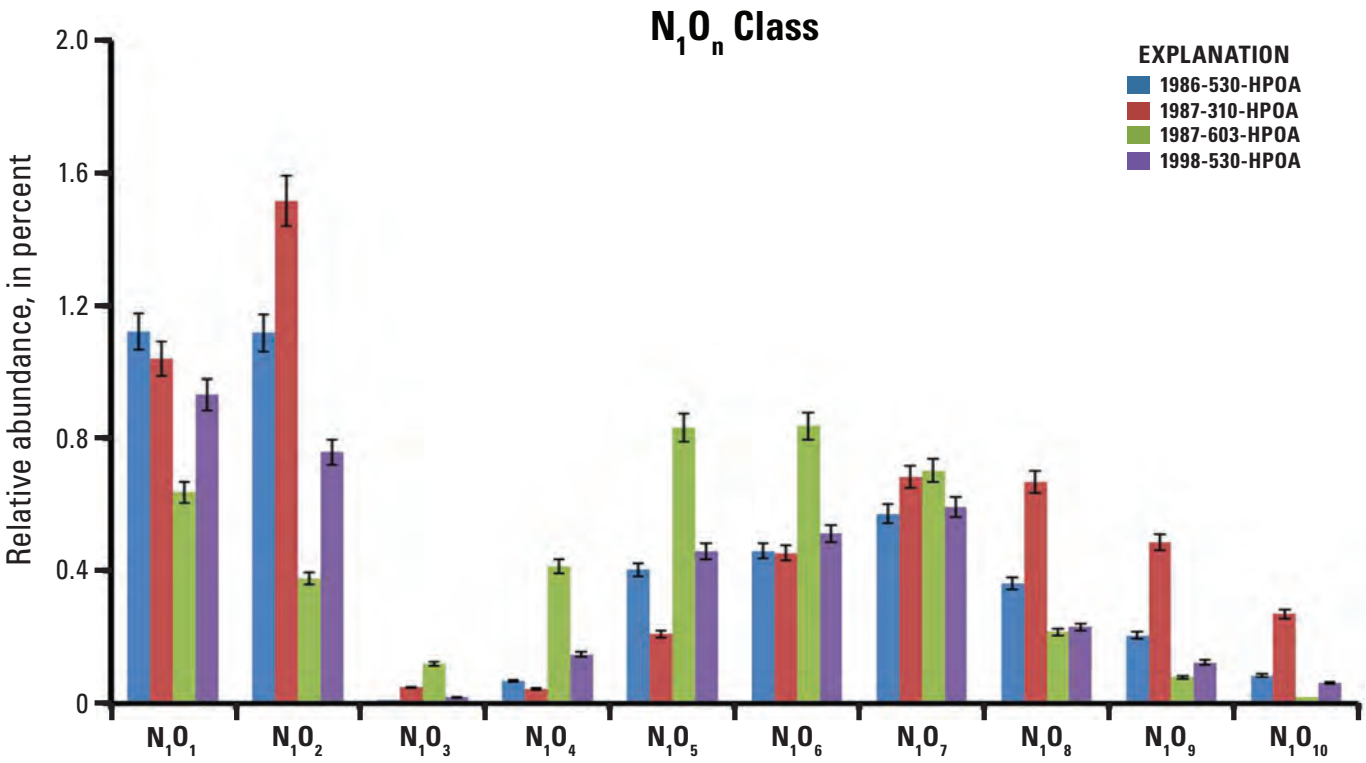

Figure 39. Distribution of N_1O_n class compounds (compounds containing one nitrogen atom and n number of oxygen atoms) in hydrophobic acid (HPOA) fractions determined by Fourier transform ion cyclotron resonance mass spectrometry (FTICR-MS). Figure is from Islam and others (2016).

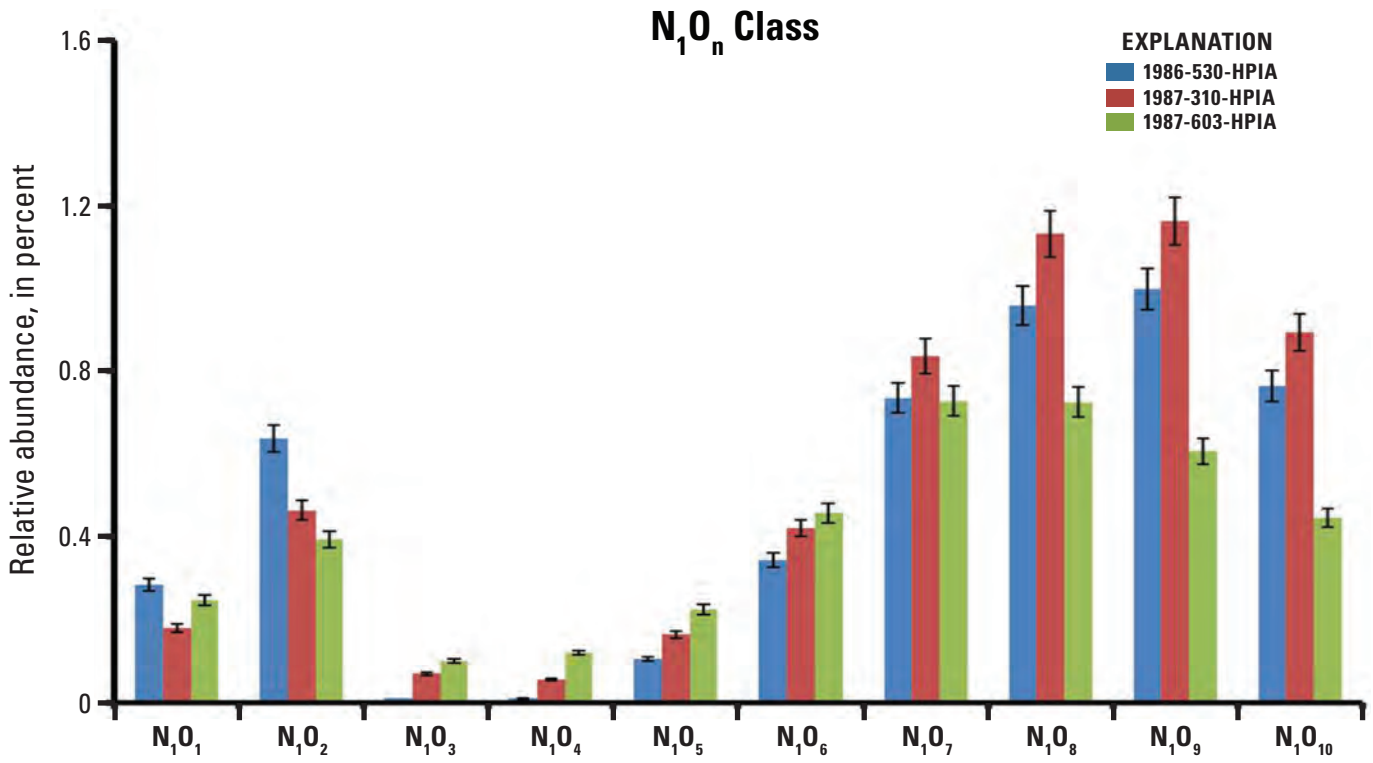

Figure 40. Distribution of N_1O_n class compounds (compounds containing one nitrogen atom and n number of oxygen atoms) in hydrophilic acid (HPIA) fractions determined by Fourier transform ion cyclotron resonance mass spectrometry (FTICR-MS). Figure is from Islam and others (2016).

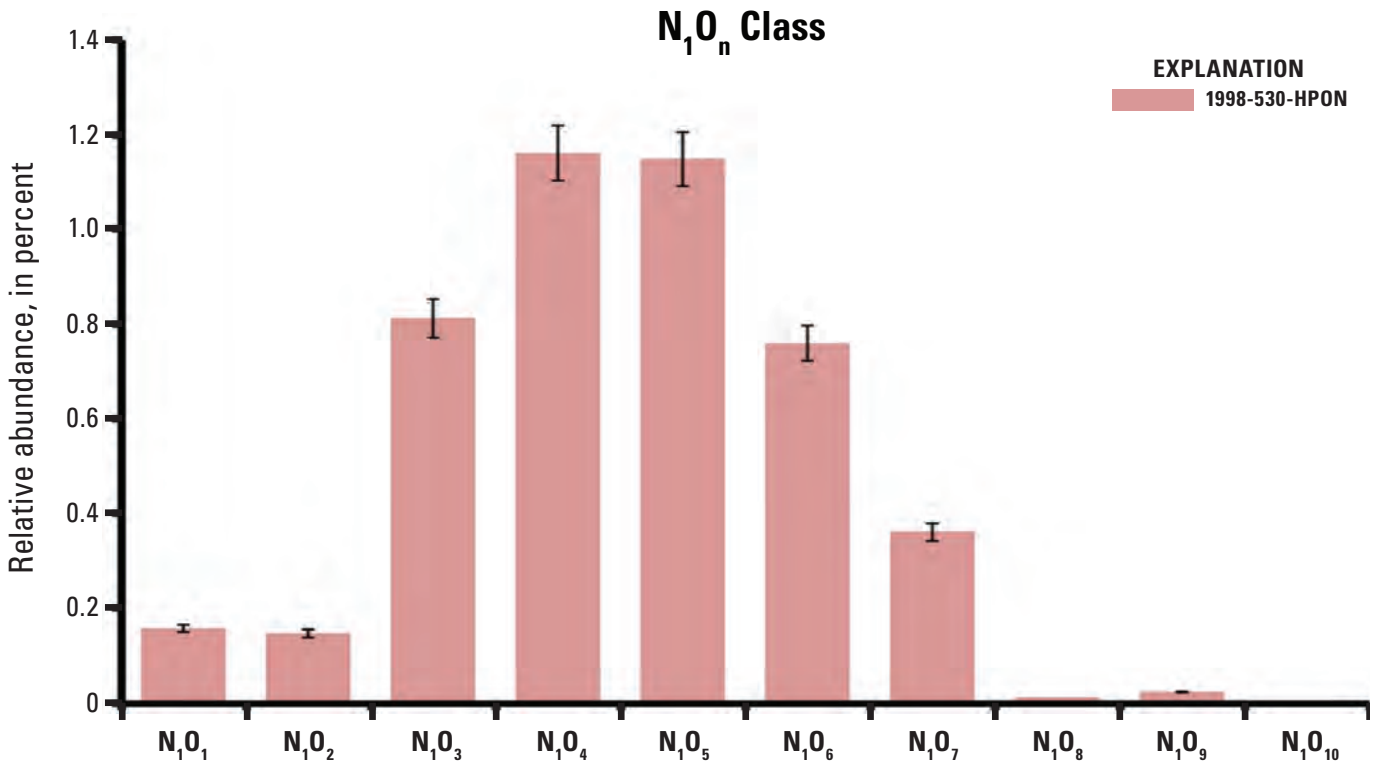

Figure 41. Distribution of N_1O_n class compounds (compounds containing one nitrogen atom and n number of oxygen atoms) in the 1998 well 530 hydrophobic neutral (HPON) fraction determined by Fourier transform ion cyclotron resonance mass spectrometry (FTICR-MS).

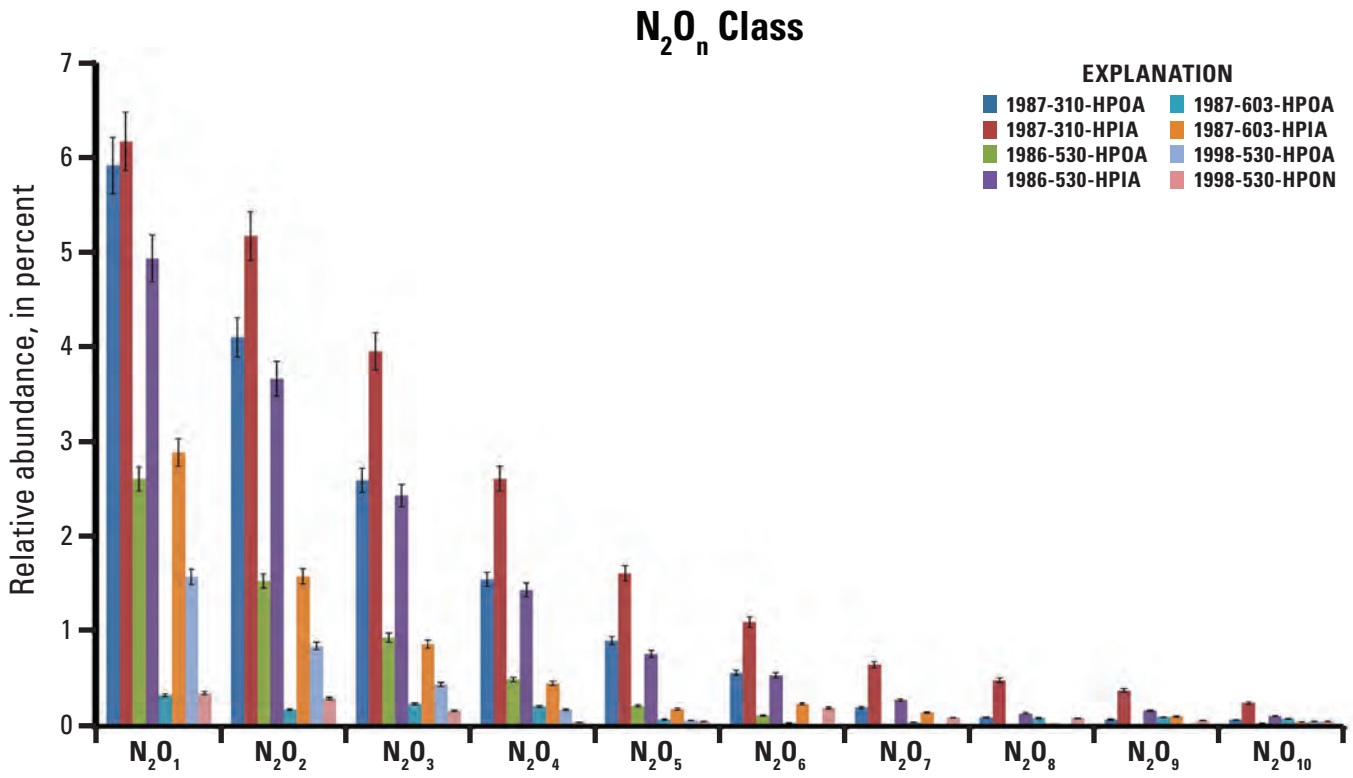

Figure 42. Distribution of N_2O_n class compounds (compounds containing two nitrogen atoms and n number of oxygen atoms) in nonvolatile organic acid (NVOA) fractions determined by Fourier transform ion cyclotron resonance mass spectrometry (FTICR-MS). (HPIA, hydrophilic acid; HPOA, hydrophobic acid; HPON, hydrophobic neutral)

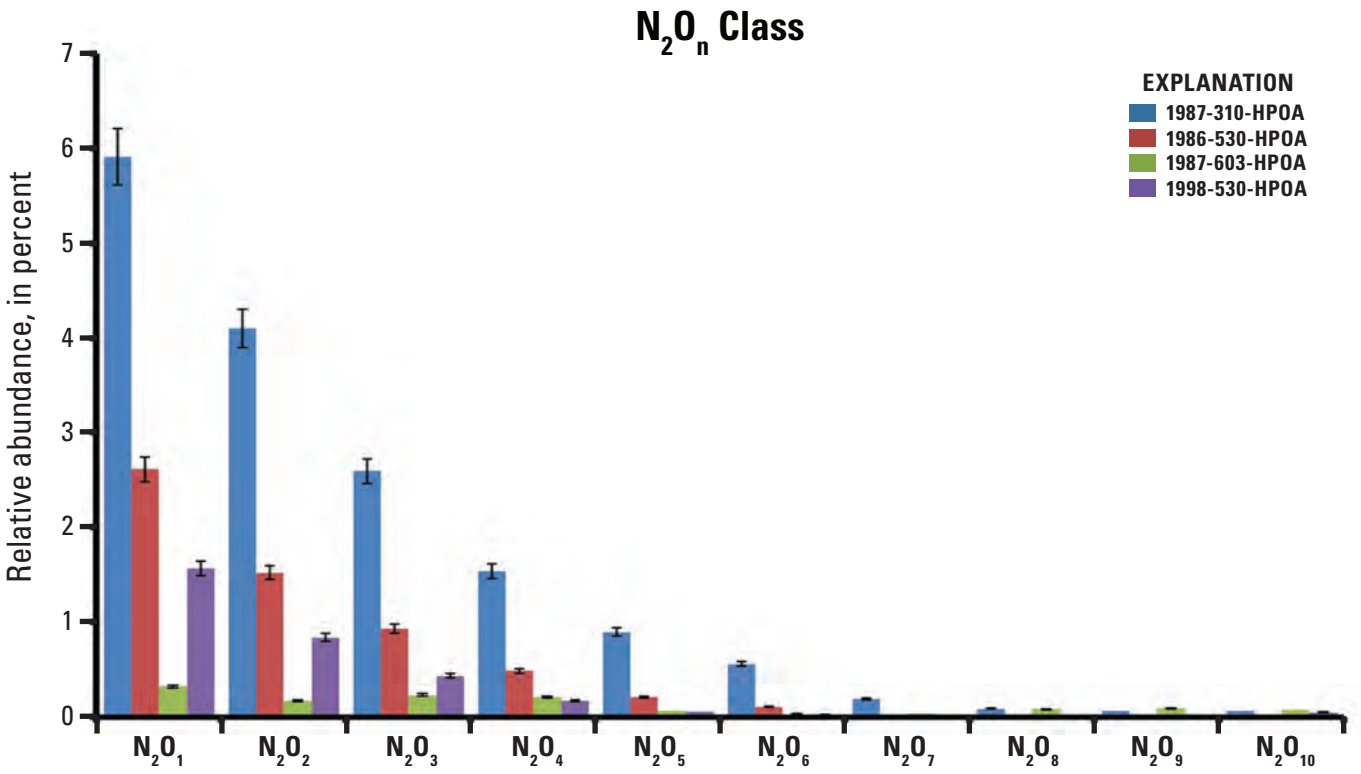

Figure 43. Distribution of N_2O_n class compounds (compounds containing two nitrogen atoms and n number of oxygen atoms) in hydrophobic acid (HPOA) fractions determined by Fourier transform ion cyclotron resonance mass spectrometry (FTICR-MS).

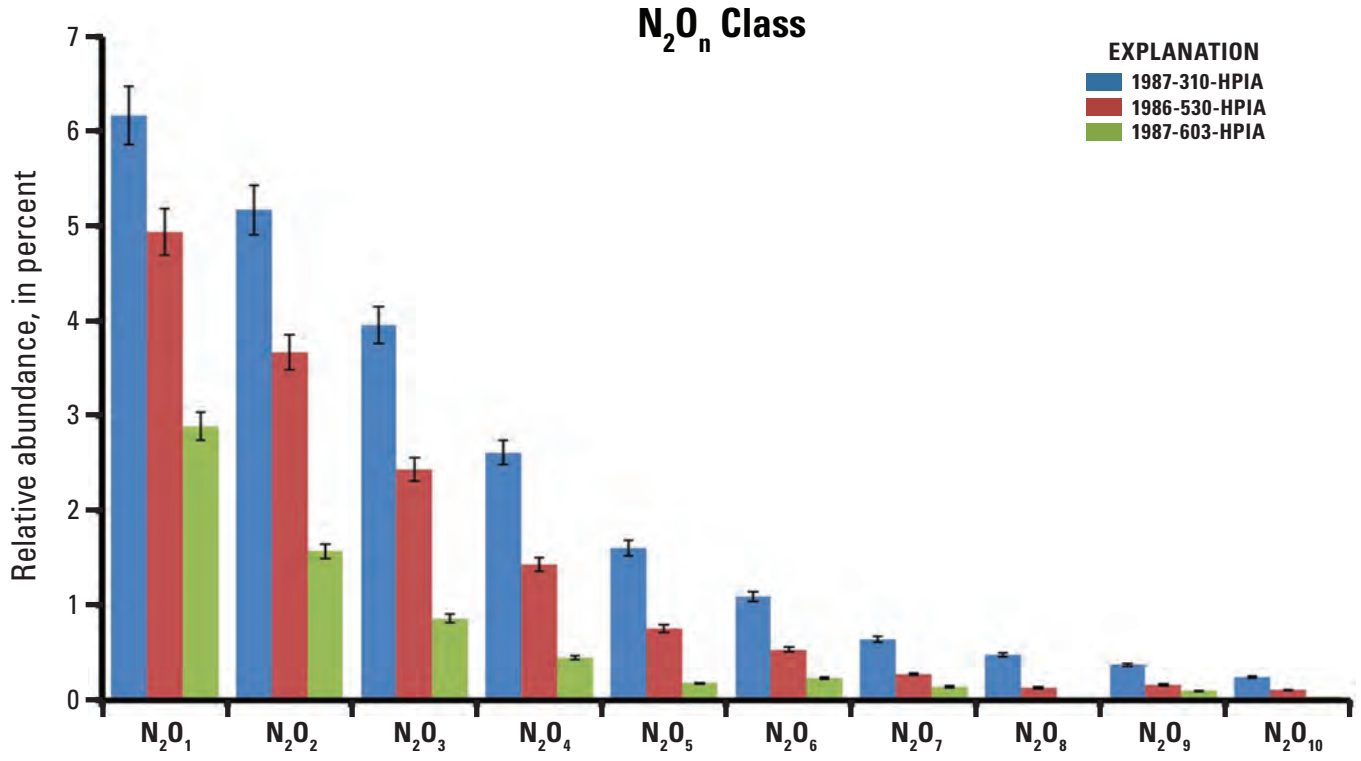

Figure 44. Distribution of N_2O_n class compounds (compounds containing two nitrogen atoms and n number of oxygen atoms) in hydrophilic acid (HPIA) fractions determined by Fourier transform ion cyclotron resonance mass spectrometry (FTICR-MS).

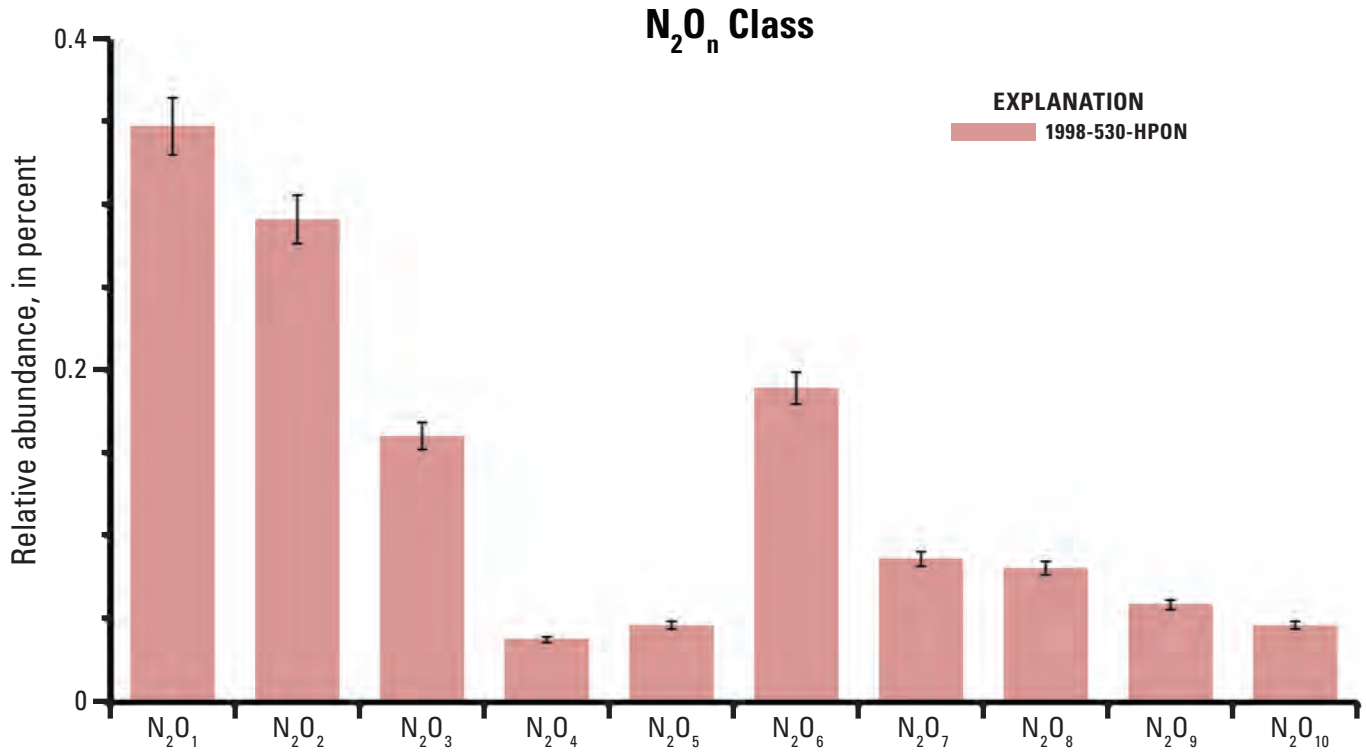

Figure 45. Distribution of N_2O_n class compounds (compounds containing two nitrogen atoms and n number of oxygen atoms) in the 1998 well 530 hydrophobic neutral (HPON) fraction determined by Fourier transform ion cyclotron resonance mass spectrometry (FTICR-MS).

Double Bond Equivalent Versus Carbon Number Plots

Plots of double bond equivalents (DBE) versus carbon numbers ($C^{\#}$s) in the O_4–O_{10} compound classes (all molecular formulas containing oxygen) are shown in figures 46–52 for the HPOA samples and in figures 53–59 for the HPIA samples. The 1998 530 HPOA and HPON plots are compared in figures 60–65. Ranges of DBEs and ranges of $C^{\#}$s are listed in table 9. Average DBEs and average $C^{\#}$s are listed in table 10.

Double Bond Equivalent Versus Carbon Number Plots—Comparison of Hydrophobic Acid Fractions

In general, the background well 310 HPOA fraction has maximum intensities at carbon number less than 20 ($<C_{20}$) for all O_4–O_{10} classes in the DBE versus $C^{\#}$ plots. Vertical lines were drawn at C_{20} to help illustrate this observation (figs. 46–65). Table 11 lists the minimum values of DBEs for a molecular formula to contain one aromatic ring (DBE=4) or one saturated ring (DBE=1) for various combinations of carboxylic acid, ketone, and alcohol or ether (A/E) oxygens. Not all possible permutations of oxygen functionalities are included, but rather the likely combinations determined from the NMR data. For this analysis, horizontal lines were drawn at DBE values of 6, 7, 8, and 9 for the $O_{4–5}$, $O_{6–7}$, $O_{8–9}$, and O_{10} class compounds, respectively, to distinguish between two general categories of molecular formulas: those containing an aromatic or saturated ring and those comprised strictly of aliphatic structures (figs. 46–65). Confirmation of these assignments will require calculation of aromaticity indices for all the molecular formulas identified. Using this designation, the majority of compounds in the DBE versus $C^{\#}$ plots appear to contain an aromatic or saturated ring for all oxygen class compounds in the 310 HPOA fraction. The background 310 HPOA fraction is differentiated from the contaminant well 530 and 603 well HPOA fractions in several respects among the O_4–O_{10} compound classes. Contaminant well HPOA fractions exhibit peak intensities not present in the background 310 HPOA fraction for a number of oxygen compound classes in the DBE versus $C^{\#}$ plots. There appear to be two general classes for these potentially oil-derived constituents: (1) C_{20}–C_{30} compounds containing an aromatic or saturated ring (indicated in black circles; table 12) and (2) C_{12}–C_{23} aliphatic compounds (indicated in rectangles; table 12). In particular, for the O_5, O_6, O_7, O_8, O_9, and O_{10} compound classes, the well 530 HPOA samples have higher concentrations of $C^{\#}$ greater than 20 ($>C_{20}$) compounds containing an aromatic or saturated ring than the well 310 HPOA fraction. In the case of 1986 530 HPOA, the O_{10} class compounds appear to contain aliphatic components up to C_{30} that may be oil derived. The fractions exhibiting these potentially oil-derived constituents are listed in table 12 for each of the oxygen compound classes.

Table 9. Ranges of double bond equivalent (DBE) and carbon number (C#) values for $O_{4\text{-}10}$ compound classes (compounds containing four to ten oxygen atoms).

[HPIA, hydrophilic acid; HPOA, hydrophobic acid; HPON, hydrophobic neutral; O_n, where O is oxygen and n is the number of atoms]

Sample	DBE	C#	DBE	C#	DBE	C#	DBE	C#	DBE	C#	DBE	C#	DBE	C#
	O_4	O_4	O_5	O_5	O_6	O_6	O_7	O_7	O_8	O_8	O_9	O_9	O_{10}	O_{10}
1987 310 HPOA	2.5–27.5	13–39	3.5–16.5	14–35	3.5–16.5	12–31	4.5–16	11–32	1.5–16.5	12–36	0.5–17.5	12–37	1.5–18.5	13–40
1987 310 HPIA	3.5–37.5	14–44	4.5–29.5	13–38	4.5–27.5	11–31	4.5–26.5	11–32	5–14.5	11–29	4.5–16.5	11–28	3.5–15.5	12–30
1986 530 HPOA	2.5–26.5	13–40	2.5–16.5	11–30	3.5–16.5	11–31	3.5–15.5	11–32	1.5–16.5	12–34	0.5–17.5	12–37	1.5–18.5	13–40
1986 530 HPIA	3.5–34.5	14–43	3.5–16.5	12–32	3.5–25.5	11–31	3.5–17.5	10–30	3.5–16.5	10–29	3.5–17.5	11–30	4.5–16.5	12–30
1998 530 HPOA	2.5–25.5	13–39	2.5–18.5	11–36	3.5–17.5	11–37	3.5–17.5	12–35	4.5–18.5	12–36	1.5–18.5	11–38	1.5–20.5	13–39
1998 530 HPON	1.5–22.5	14–36	2.5.–20.5	13–38	3.5–21.5	12–38	4.5–21.5	13–39	4.5–20.5	14–37	2.5–19.5	16–38	10.5–19.5	31–39
1987 603 HPOA	3.5–23.5	13–33	3.5–21.5	13–35	3.5–20.5	12–35	4.5–20.5	12–35	4.5–20.5	12–37	5.5–20.5	13–36	2.5–20.5	15–35
1987 603 HPIA	4.5–27.5	11–37	4.5–13.5	12–24	3.5–14.5	11–25	3.5–17.5	11–31	4.5–16.5	11–30	4.5–17.5	11–30	5.5–17.5	12–30

Table 10. Average double bond equivalent (DBE) and carbon number (C#) values for $O_{4\text{-}10}$ class compounds (compounds with four to ten oxygen atoms).

[HPIA, hydrophilic acid; HPOA, hydrophobic acid; HPON, hydrophobic neutral; —, not determined]

Sample	DBE	C#	DBE	C#	DBE	C#	DBE	C#	DBE	C#	DBE	C#	DBE	C#
	O_4	O_4	O_5	O_5	O_6	O_6	O_7	O_7	O_8	O_8	O_9	O_9	O_{10}	O_{10}
1987 310 HPOA	11.93	22.1	9.37	19.4	8.8	19.1	8.9	19.2	9.2	19.5	9.8	20.6	10.5	22.3
1987 310 HPIA	12	21.1	9.7	18.1	9	17.6	8.6	17.3	8.4	17.2	8.6	17.4	8.9	17.4
1986 530 HPOA	8.7	19.9	8	19.6	8.1	20	8.8	20.8	9.2	21.5	9.8	22.5	10.5	23.6
1986 530 HPIA	9.4	19.6	8.2	17.8	7.7	17	7.6	16.9	7.7	17.1	8.2	17.47	8.7	18.7
1998 530 HPOA	8.4	19.9	8.6	19.8	8.6	20.1	9.4	21	10	21.9	10.6	23.1	—	—
1998 530 HPON	9.9	22.4	10.4	23.8	10.6	24.7	11.1	25.8	11.6	27.1	12.8	30.4	—	—
1987 603 HPOA	9.8	20.6	9.7	20.6	9.9	21	10.5	21.2	10.3	22.8	11.5	23.9	12.3	25.6
1987 603 HPIA	9.8	18.7	8	16.6	7.5	15.9	7.6	16	7.9	16.4	8.6	17.8	9.4	19.5

Table 11. Minimum double bond equivalent (DBE) values for molecular formulas to contain one aromatic or one saturated ring for combinations of carboxylic acid, ketone, and alcohol or ether oxygens.

[A, minimum value of DBEs for one aromatic ring (4 DBE); B, minimum value of DBEs for one saturated ring (1 DBE); O_n, oxygen with n number of atoms; A/E, alcohol or ether oxygens]

Compound class	Combinations of oxygen-containing functional groups				
	Minimum value of DBEs				
O_{10}	5 Carboxyl	4 Carboxyl 2 ketone	4 Carboxyl 1 ketone 1 A/E	4 Carboxyl 2 A/E	3 Carboxyl 4 ketone
	A=9 DBE B=6 DBE	A=10 DBE B=7 DBE	A=9 DBE B=6 DBE	A=8 DBE B=5 DBE	A=11 DBE B=8 DBE
O_9	4 Carboxyl 1 A/E	4 Carboxyl 1 ketone	3 Carboxyl 3 ketone	3 Carboxyl 2 ketone 1 A/E	3 Carboxyl 1 ketone 2 A/E
	A=8 DBE B=5 DBE	A=9 DBE B=6 DBE	A=10 DBE B=7 DBE	A=9 DBE B=6 DBE	A=8 DBE B=5 DBE
O_8	4 Carboxyl	3 Carboxyl 2 ketone	3 Carboxyl 1 ketone 1 A/E	3 Carboxyl 2 A/E	2 Carboxyl 4 ketone
	A=8 DBE B=5 DBE	A=9 DBE B=6 DBE	A=8 DBE B=5 DBE	A=7 DBE B=4 DBE	A=10 DBE B=7 DBE
O_7	3 Carboxyl 1 A/E	3 Carboxyl 1 ketone	2 Carboxyl 3 ketone	2 Carboxyl 2 ketone 1 A/E	2 Carboxyl 1 ketone 2 A/E
	A=7 DBE B=4 DBE	A=8 DBE B=5 DBE	A=9 DBE B=6 DBE	A=8 DBE B=5 DBE	A=7 DBE B=4 DBE
O_6	3 Carboxyl	2 Carboxyl 2 ketone	2 Carboxyl 1 ketone 1 A/E	2 Carboxyl 2 A/E	
	A=7 DBE B=4 DBE	A=8 DBE B=5 DBE	A=7 DBE B=4 DBE	A=6 DBE B=3 DBE	
O_5	2 Carboxyl 1 A/E	2 Carboxyl 1 ketone	1 Carboxyl 3 ketone	1 Carboxyl 2 ketone 1 A/E	
	A=6 DBE B=3 DBE	A=7 DBE B=4 DBE	A=8 DBE B=5 DBE	A=7 DBE B=4 DBE	
O_4	2 Carboxyl	1 Carboxyl 2 ketone	1 Carboxyl 1 ketone 1 A/E	1 Carboxyl 2 A/E	
	A=6 DBE B=3 DBE	A=7 DBE B=4 DBE	A=6 DBE B=3 DBE	A=5 DBE B=2 DBE	

Table 12. Contaminant well hydrophobic acid (HPOA) fractions showing potentially oil-derived constituents as evident from double bond equivalent versus carbon number (DBE vs C#) plots.

[C_n, number of carbons per molecule; O_n, compound class with n number of oxygen atoms]

Compound class	Aromatic or saturated ring C_{20}–C_{30}	Aliphatic C_{12}–C_{23}
O_4	1998 530 HPOA	1986 530 HPOA
		1998 530 HPOA
O_5		1986 530 HPOA
		1987 603 HPOA
		1998 530 HPOA
O_6	1987 603 HPOA	1986 530 HPOA
		1987 603 HPOA
		1998 530 HPOA
O_7	1987 603 HPOA	1987 603 HPOA
	1998 530 HPOA	1986 530 HPOA
		1998 530 HPOA
O_8	1987 603 HPOA	1986 530 HPOA
	1998 530 HPOA	1998 530 HPOA
O_9	1986 530 HPOA	1986 530 HPOA
	1987 603 HPOA	
	1998 530 HPOA	
O_{10}	1986 530 HPOA	1986 530 HPOA
	1987 603 HPOA	
	1998 530 HPOA	

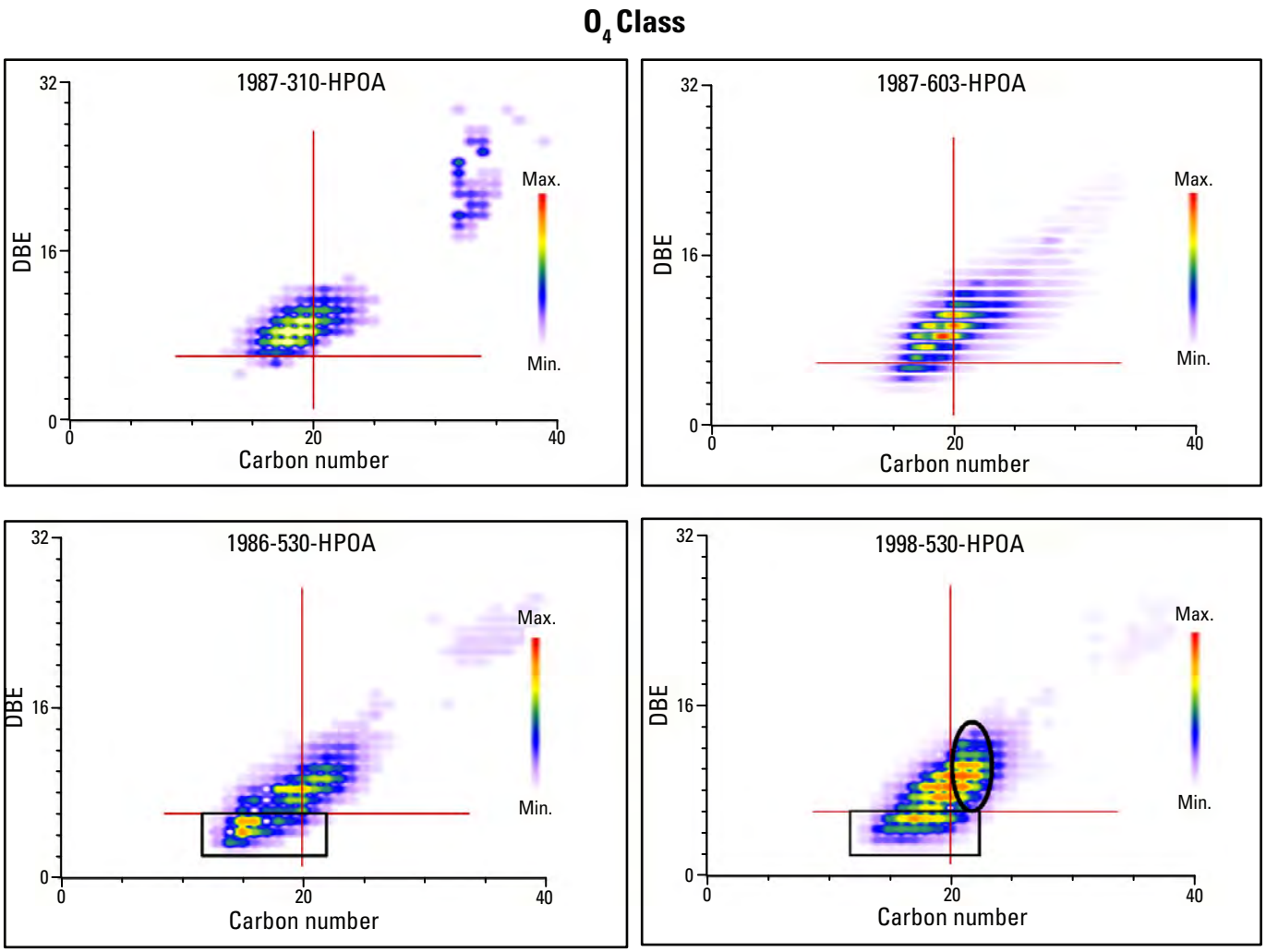

Figure 46. Double bond equivalent (DBE) versus carbon number (C#) plots for O_4 class compounds (compounds containing four oxygen atoms) in hydrophobic acid (HPOA) fractions. Rectangles denote molecular formulas potentially derived from aliphatic constituents of oil. Ovals denote molecular formulas potentially derived from aromatic or saturated ring constituents of oil. (Max., maximum; Min., minimum)

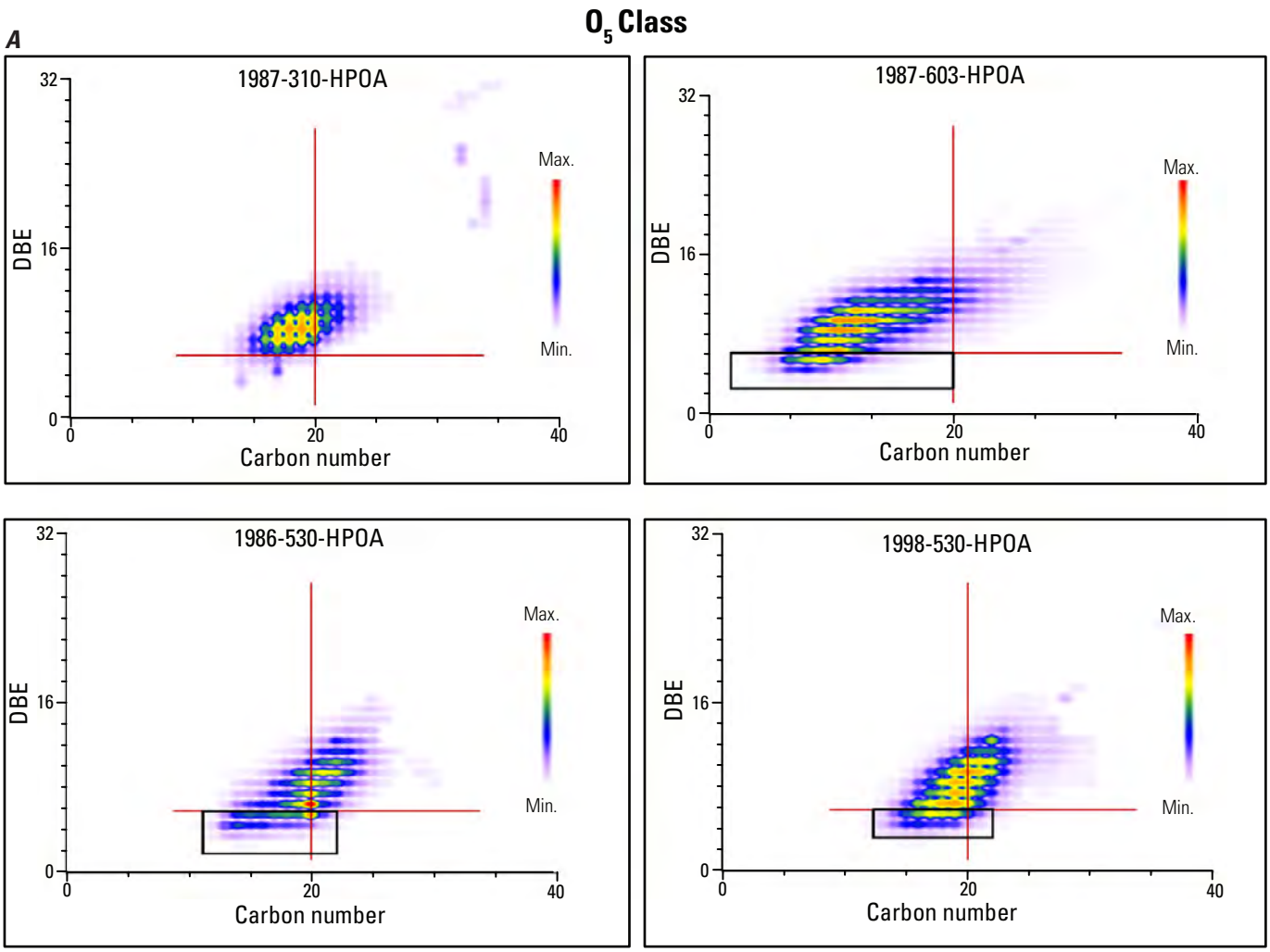

Figure 47. A, Double bond equivalent (DBE) versus carbon number ($C^{\#}$) plots for O_5 class compounds (compounds containing five oxygen atoms) in hydrophobic acid (HPOA) fractions. Rectangles denote molecular formulas potentially derived from aliphatic constituents of oil. *B*, DBE versus carbon number plots with DBE bar graphs for O_5 class compounds in HPOA fractions. Figure is from Islam and others (2016). (Max., maximum; Min., minimum)

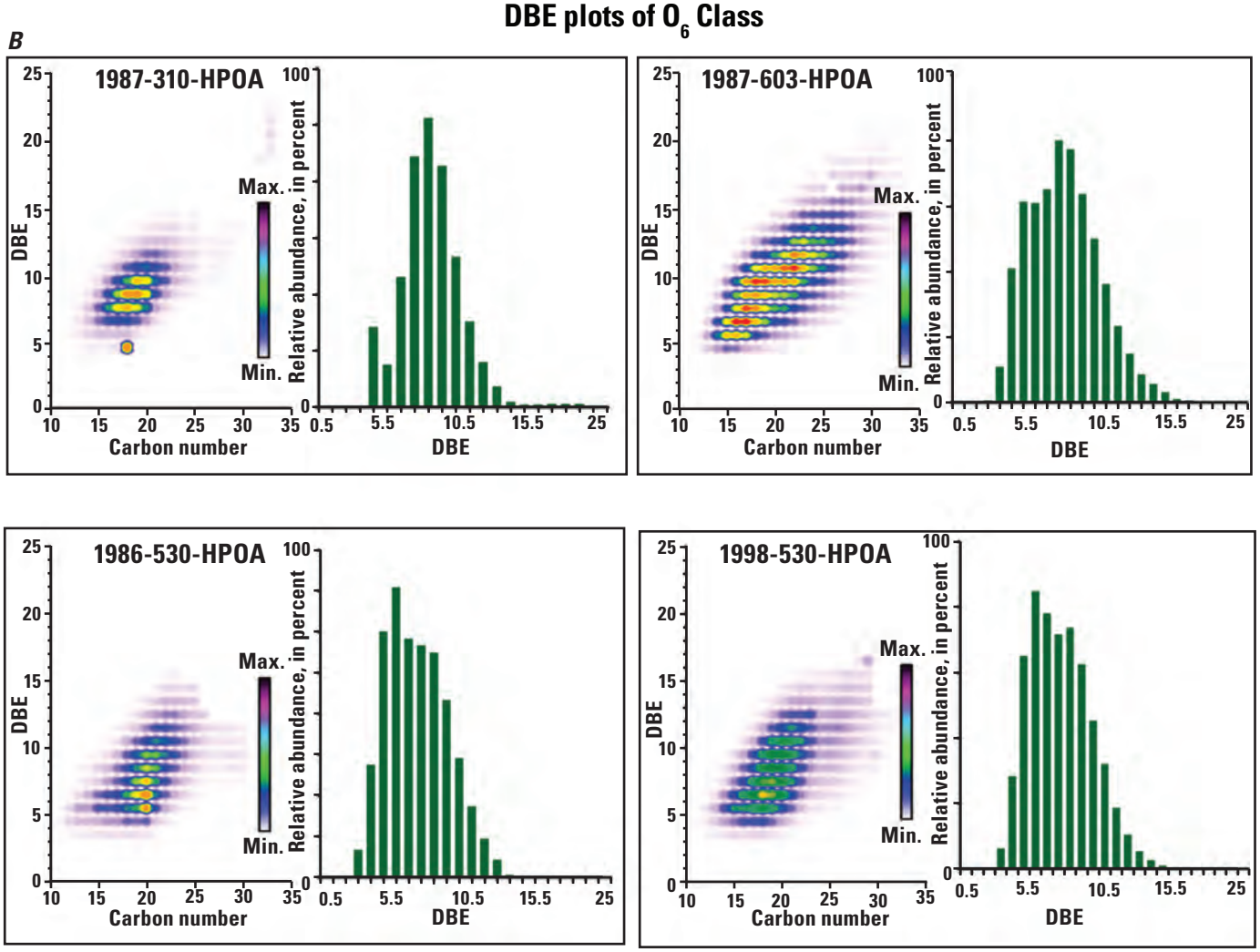

Figure 47.—Continued

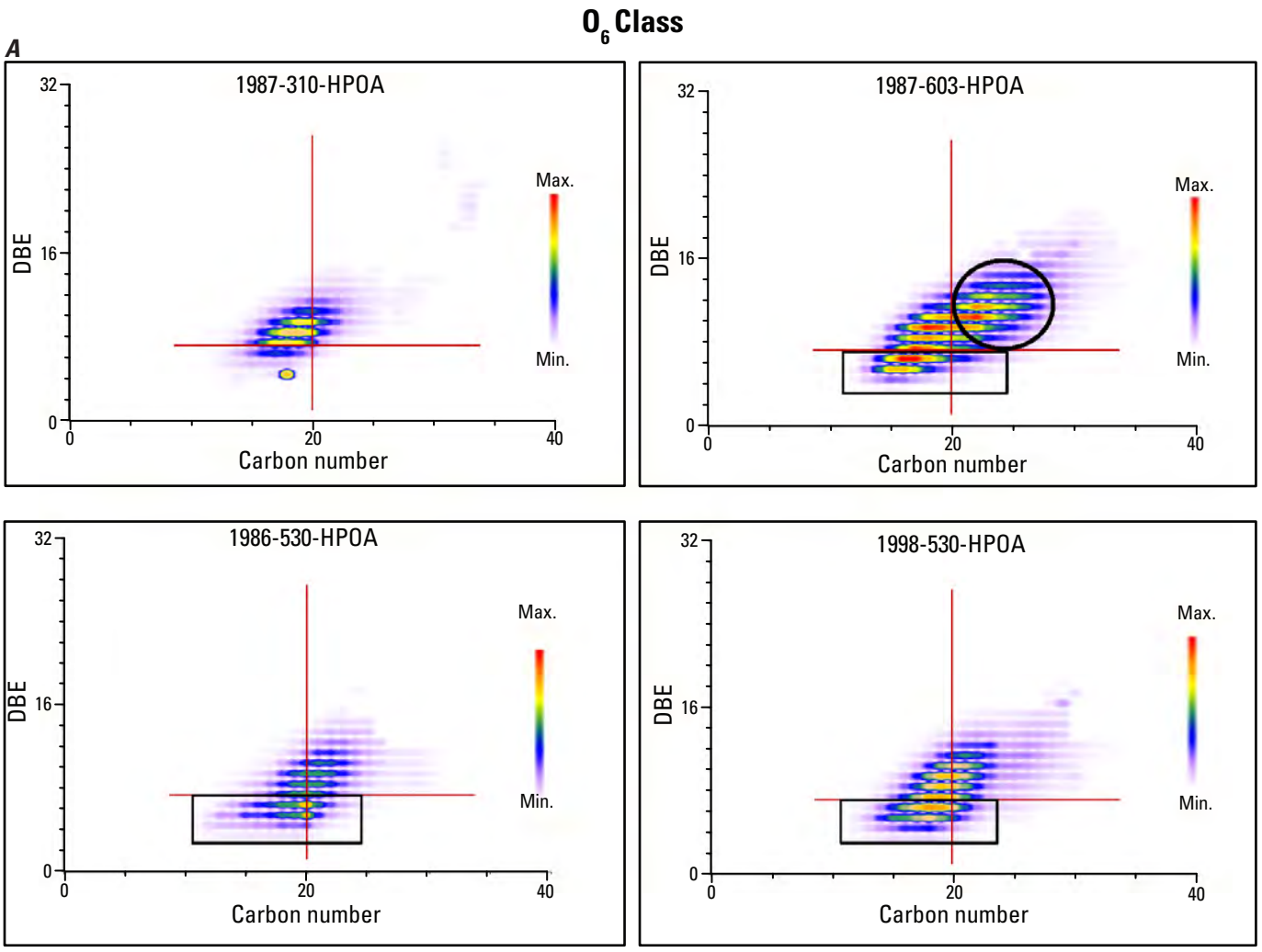

Figure 48. *A*, Double bond equivalent (DBE) versus carbon number ($C^{\#}$) plots for O_6 class compounds (compounds containing six oxygen atoms) in hydrophobic acid (HPOA) fractions. Rectangles denote molecular formulas potentially derived from aliphatic constituents of oil. Ovals denote molecular formulas potentially derived from aromatic or saturated ring constituents of oil. *B*, DBE versus carbon number plots with DBE bar graphs for O_6 class compounds in HPOA fractions. Figure is from Islam and others (2016). (Max., maximum; Min., minimum)

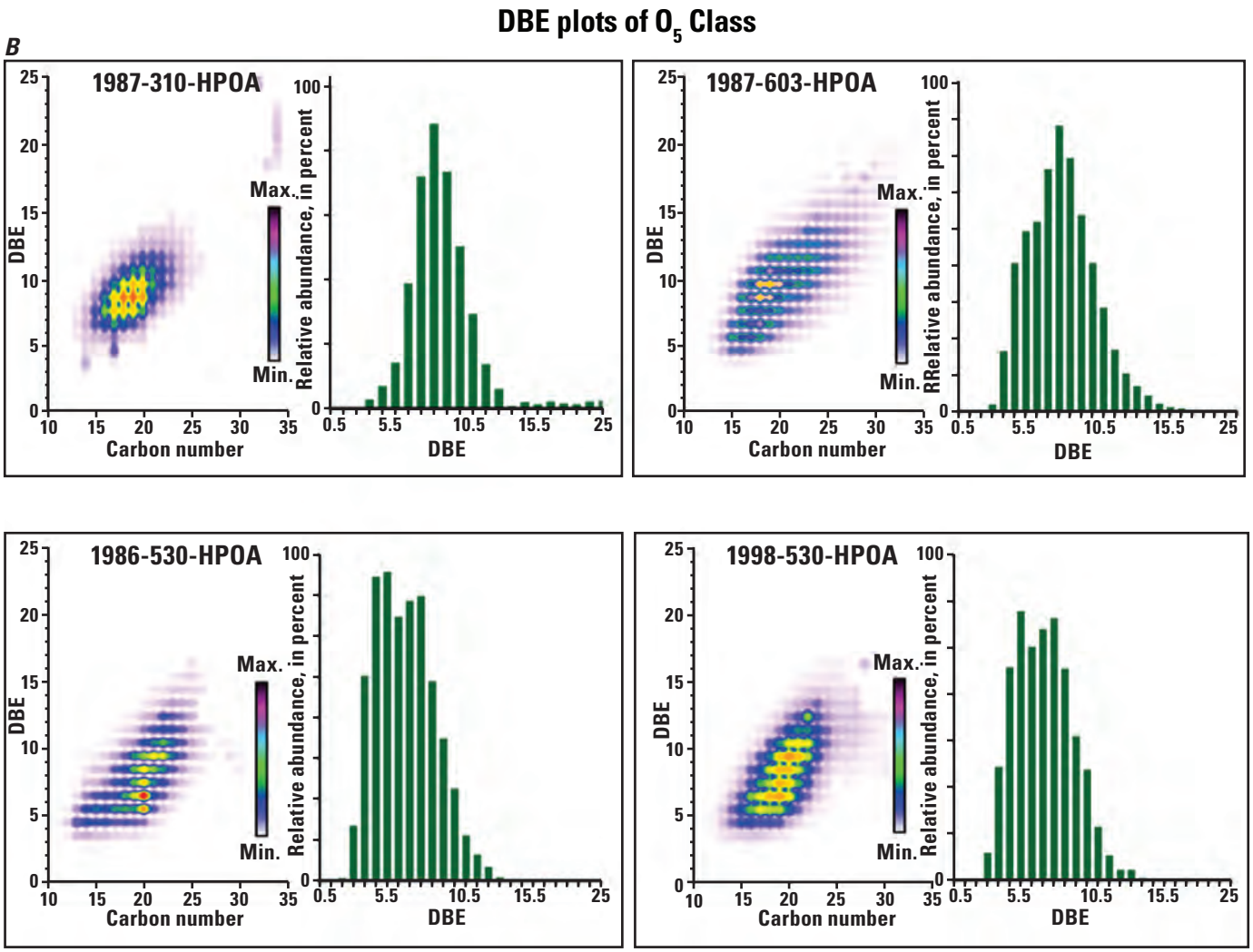

Figure 48.—Continued

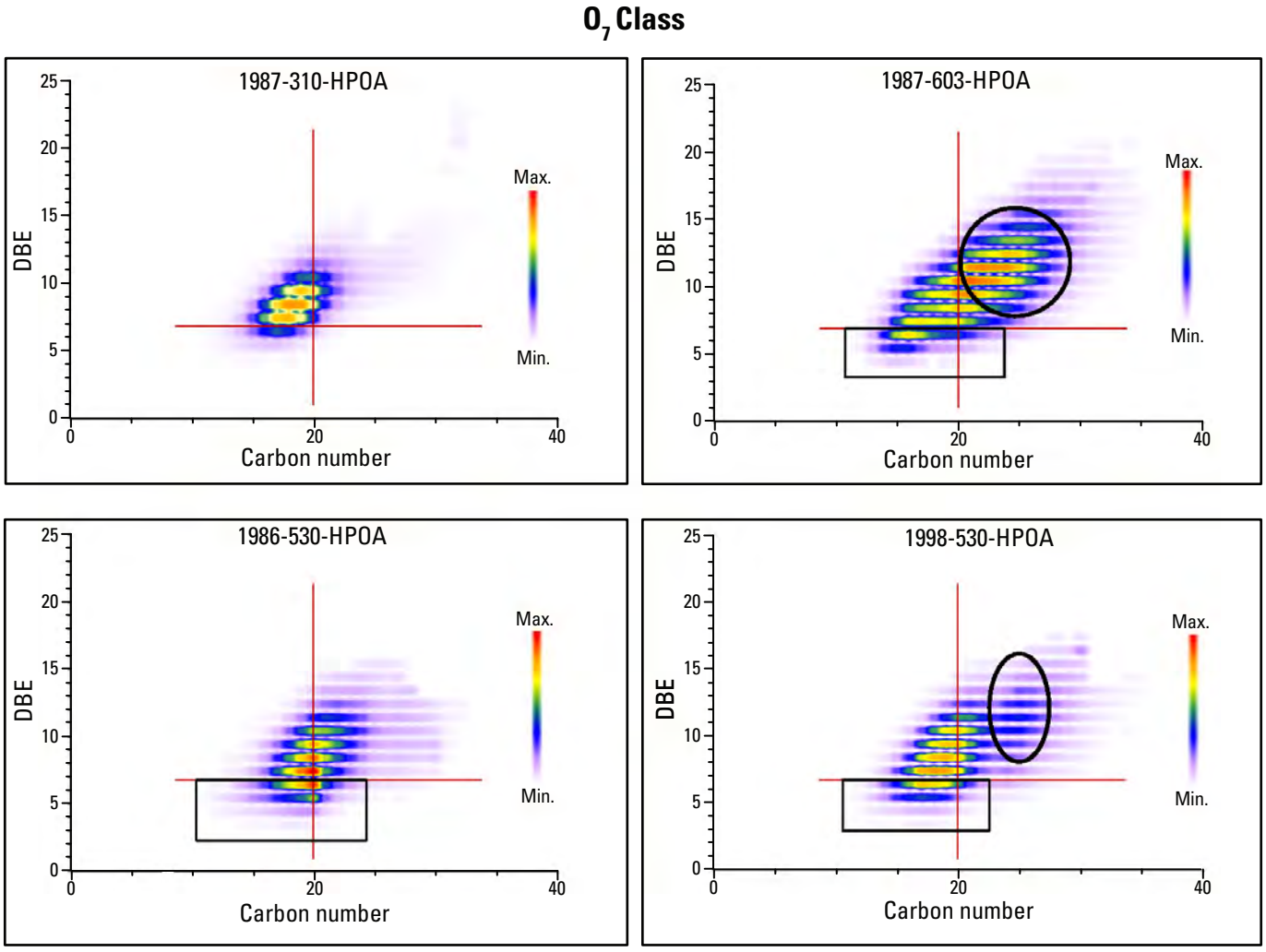

Figure 49. Double bond equivalent versus carbon number ($C^{\#}$) plots for O_7 class compounds (compounds containing seven oxygen atoms) in hydrophobic acid (HPOA) fractions. Rectangles denote molecular formulas potentially derived from aliphatic constituents of oil. Ovals denote molecular formulas potentially derived from aromatic or saturated ring constituents of oil. (Max., maximum; Min., minimum)

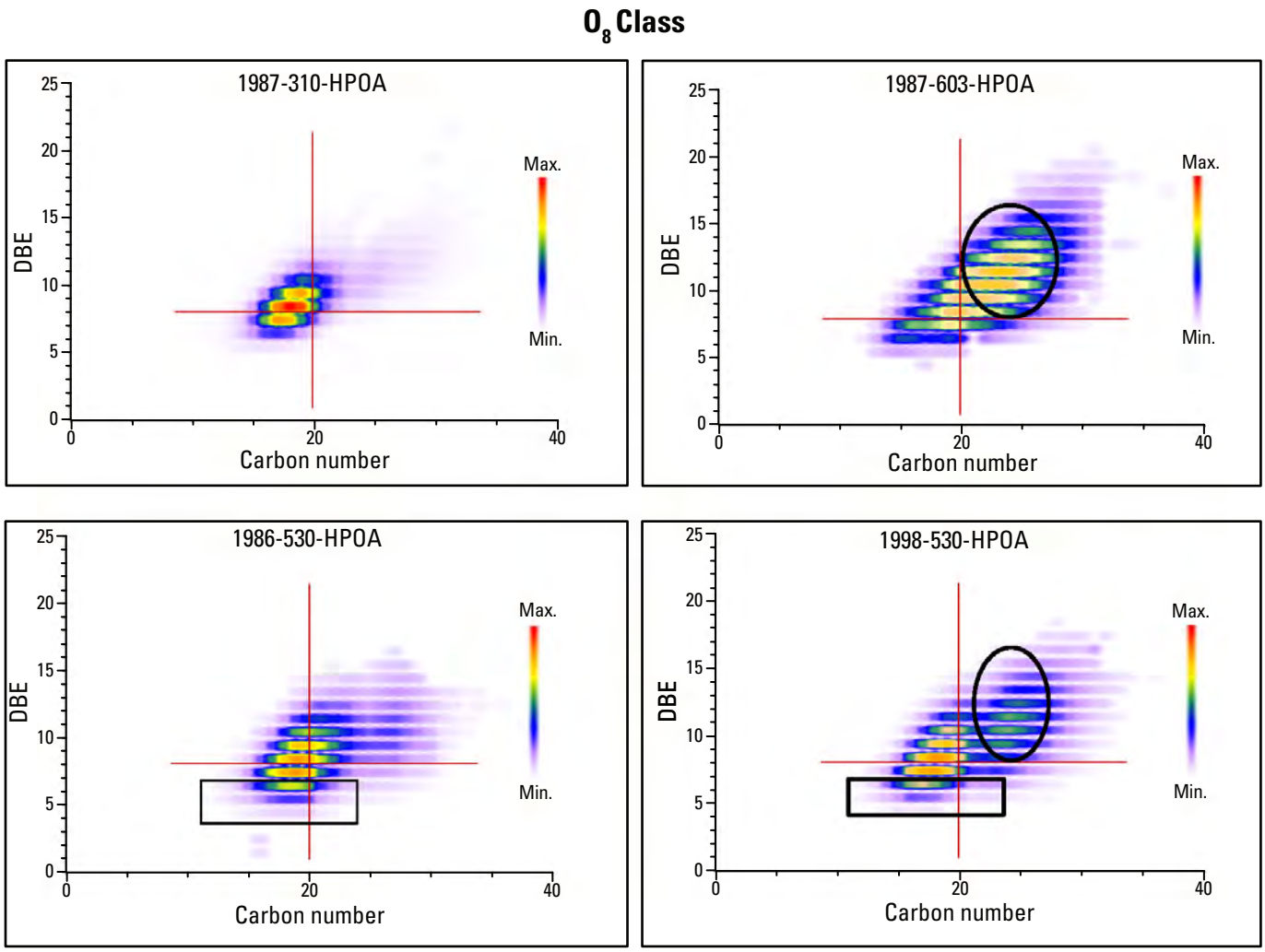

Figure 50. Double bond equivalent DBE versus carbon number ($C^{\#}$) plots for O_8 class compounds (compounds containing eight oxygen atoms) in hydrophobic acid (HPOA) fractions. Rectangles denote molecular formulas potentially derived from aliphatic constituents of oil. Ovals denote molecular formulas potentially derived from aromatic or saturated ring constituents of oil. (Max., maximum; Min., minimum)

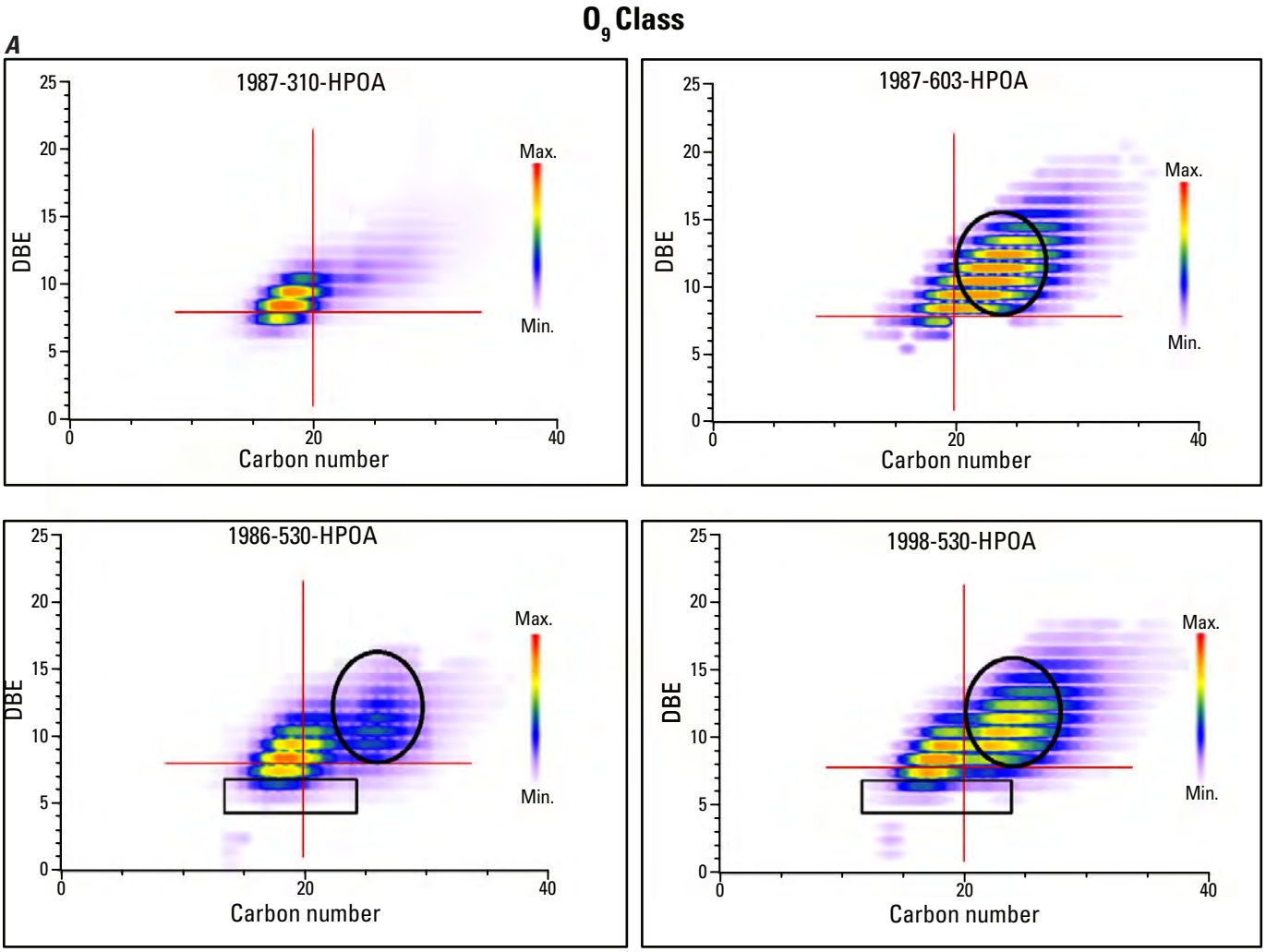

Figure 51. *A*, Double bond equivalent (DBE) versus carbon number (C#) plots for O_9 class compounds (compounds containing nine oxygen atoms) in hydrophobic acid (HPOA) fractions. Ovals denote molecular formulas potentially derived from aromatic or saturated ring constituents of oil. *B*, DBE versus carbon number plots with DBE bar graphs for O_9 class compounds in HPOA fractions. Figure is from Islam and others (2016). (Max., maximum; Min., minimum)

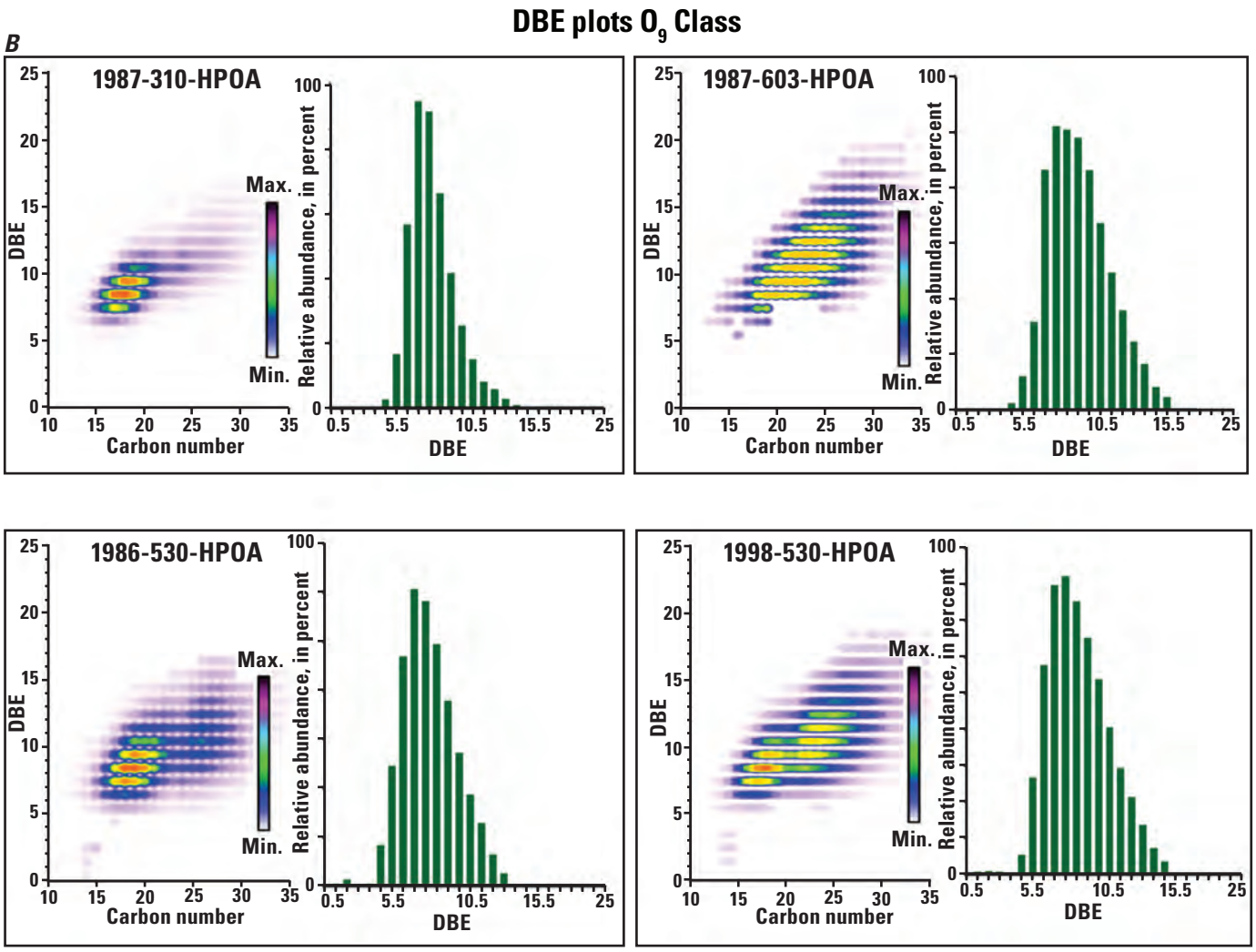

Figure 51.—Continued

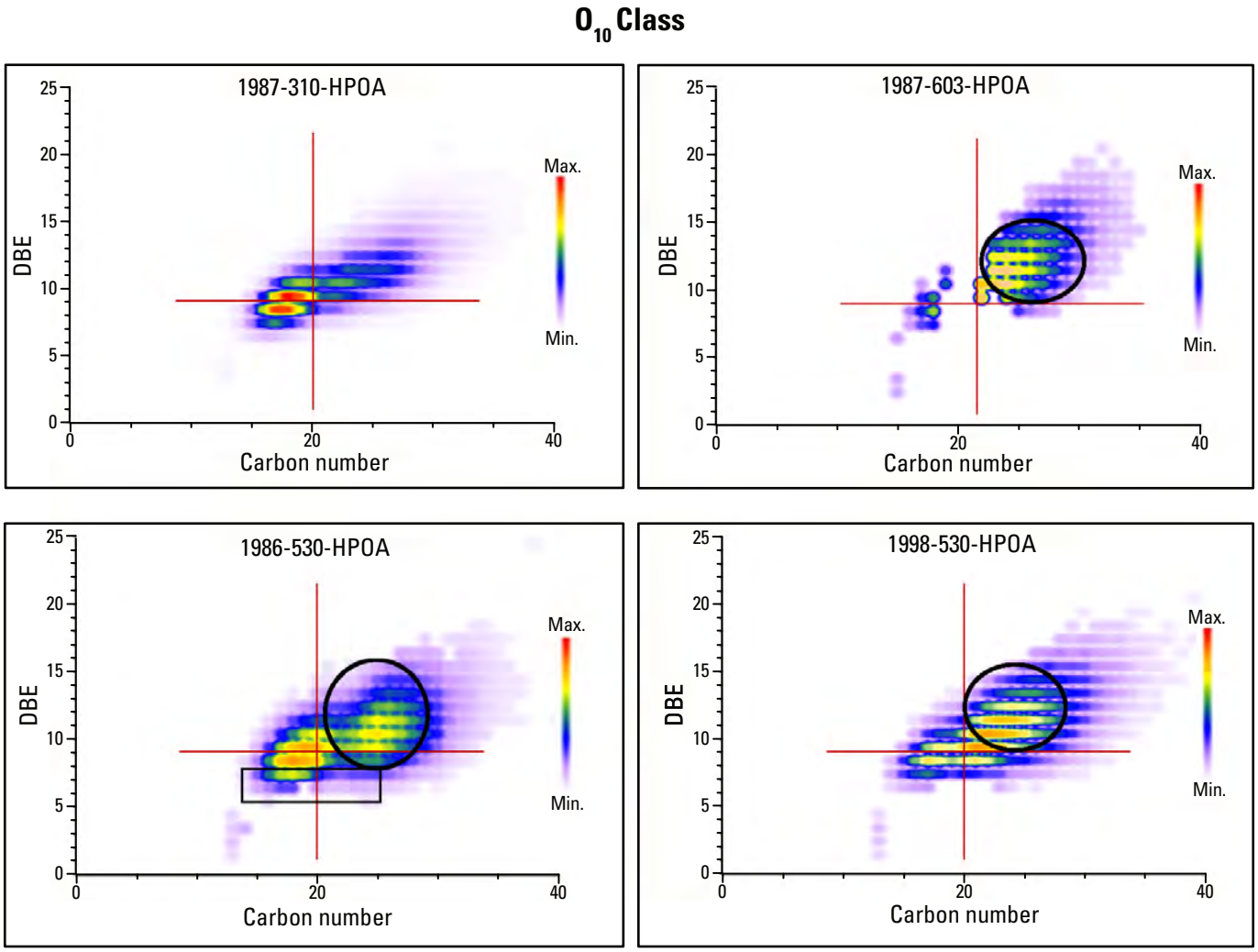

Figure 52. Double bond equivalent (DBE) versus carbon number (C#) plots for O_{10} class compounds (compounds containing 10 oxygen compounds) in hydrophobic acid (HPOA) fractions. Ovals denote molecular formulas potentially derived from aromatic or saturated ring constituents of oil. (Max., maximum; Min., minimum)

The spray zone well 603 HPOA fraction is in turn differentiated from both the well 310 and 530 HPOA samples. In the O_5 class, 603 HPOA has significantly greater concentrations of low molecular weight ($<C_{20}$) compounds containing an aromatic or saturated ring than the 310 and 530 fractions. In the O_6, O_7, O_8, and O_9 classes, well 603 has greater concentrations of $>C_{20}$ compounds containing an aromatic or saturated ring than the well 310 and 530 HPOA fractions.

The DBE versus $C^{\#}$ plots show the broader range of DBEs for the contaminant well HPOA fractions more clearly than is discernible from tables 8 and 9. As an example, for the O_6 compound classes in figure 48, molecular formulas with DBEs of 7.5, 8.5, and 9.5 are most abundant in 1987 310 HPOA, whereas those with DBEs of 5.5, 6.5, 7.5, 8.5, and 9.5 are most abundant in 1986 530 HPOA and 1998 530 HPOA, and those with DBEs of 6.5, 7.5, 8.5, 9.5, 10.5, and 11.5 are most abundant in 1987 603 HPOA. Variations in the range and distribution of DBEs between the background and contaminant HPOA fractions are likewise evident in the O_9 and O_5 compound classes (figs. 51 and 47, respectively). Once again, the increased range and abundances of DBEs in conjunction with molecular formulas that contain an expanded range of $C^{\#}$s reflect the contribution of partial oxidation products from the crude oil.

Double Bond Equivalent Versus Carbon Number Plots—Comparison of Hydrophilic Acid Fractions

There is somewhat of a consistent relationship among the three HPIA fractions for the O_4 through O_7 class compounds (figs. 53–59). The majority of compounds in the well 310 HPIA fraction are less than C_{20} and contain an aromatic or saturated ring. The majority of compounds in the well 603 HPIA fraction are also less than C_{20} but appear to have contributions of oil-derived aliphatic compounds in the O_6 and O_7 classes (table 13; figures 53–59). The 1986 530 HPIA fraction has significant concentrations of $>C_{20}$ compounds in the O_4 through O_7 classes, likely oil-derived compounds containing an aromatic or saturated ring. It also contains oil-derived aliphatic compounds in the O_4 through O_7 classes.

The majority of the O_8, O_9, and O_{10} class compounds in the 310 HPIA fraction also have carbon numbers less than C_{20}, whereas the O_9 class of the 603 HPIA and the O_{10} class of both the 603 and 530 HPIA fractions have significant concentrations of compounds with carbon numbers greater than C_{20}. The proportion of aliphatic structures appears to increase with all three fractions with the increase in oxygen atoms from O_8 to O_{10}. Oil-derived aliphatic compounds appear to be present in the O_8 and O_9 classes of the 530 and 603 HPIA and O_{10} class of the 530 HPIA fractions. As a general observation, the presence of oil-derived aliphatic compounds in the approximate range of C_{11} to C_{22} (table 13) and expanded ranges of DBEs and $C^{\#}$s distinguish the contaminant from background HPIA fractions (table 13).

Double Bond Equivalent Versus Carbon Number Plots—Comparison of 1998 530 Hydrophobic Neutral and Hydrophobic Acid Fractions

Comparison of the DBE versus $C^{\#}$ plots for the 1998 530 HPOA and HPON samples reveals another significant relationship between the two fractions: the HPON molecular formulas contain both higher average carbon numbers and higher average DBE values in all O_4–O_9 compound classes than the HPOA (figs. 60–65; table 10). The former is consistent with the 1986 dataset where the 1986 530 HPON fraction has a higher average carbon per molecule number (C/M=22) than the 1986 530 HPOA fraction (C/M=19), as determined by VPO and elemental analysis (table 2). The higher average carbon numbers of the 1998 530 HPON do not translate into a higher average molecular weight (table 6), as the HPON is less oxygenated than the HPOA. The majority of compounds in the HPON DBE versus $C^{\#}$ plots appear to contain aromatic or saturated rings for all oxygen class compounds (figs. 60–65). Additionally, maximum peak intensities in the DBE versus $C^{\#}$ plots occur above C_{20} for all oxygen compound classes in the HPON fraction (figs. 60–65).

Factors Separating Well 603 and 530 Fractions

Principal component analyses from the FTICR-MS data demonstrated that the well 1987 310, 1987 603, and 1986 and 1998 530 HPOA samples could be separated into three groups (Islam and others, 2016), as could the well 1987 310, 1987 603, and 1986 530 HPIA fractions. The data reveal some specific differences that may account for the separation of well 603 from well 530 in terms of the contaminant HPOA fractions. Compared to the 1986 and 1998 530 HPOA fractions, the 1987 603 HPOA fraction has (1) a greater proportion of $>C_{20}$, O_6, O_7, O_8, and O_9 class compounds, (2) a significantly higher proportion of S_1O_4, S_1O_5, and S_1O_6 species (fig. 33), and (3) a lower proportion of $N_2O_{1–3}$ species (fig. 43). The 1987 603 HPOA appears to have oil-derived C_{12}–C_{23} aliphatic compounds within the O_5 and O_6 compound classes, whereas the 1986 530 has them within the $O_{4–10}$ classes, and the 1998 530 HPOA has them within the $O_{4–8}$ classes. Within the contaminant well HPIA fractions, 1987 603 has higher concentrations of $S_1O_{5–10}$ and lower concentrations of $N_2O_{1–10}$ species than 1986 530 (figs. 34–44).

The compositional differences in DOC between well 603 in the spray zone and well 530 downgradient from the oil body likely result from the different pathways contamination was introduced into the groundwater (see the “Site Description” section) resulting in diverging degradation patterns. Oil-derived DOC in well 603 results from aerobic biodegradation and possibly photodegradation, whereas in well 530 from a combination primarily of anaerobic with some aerobic biodegradation.

Table 13. Contaminant well hydrophilic acid (HPIA) fractions showing potentially oil-derived constituents as evident from double bond equivalent versus carbon number (DBE vs C#) plots.

[O_n, compound class with n number of oxygen atoms; C_n, number of carbons per molecule; —, not detected]

Compound class	Aliphatic C_{11}–C_{22}
O_4	—
O_5	1986 530 HPIA
	1987 603 HPIA
O_6	1986 530 HPIA
	1987 603 HPIA
O_7	1986 530 HPIA
	1987 603 HPIA
O_8	1986 530 HPIA
	1987 603 HPIA
O_9	1986 530 HPIA
	1987 603 HPIA
O_{10}	1986 530 HPIA

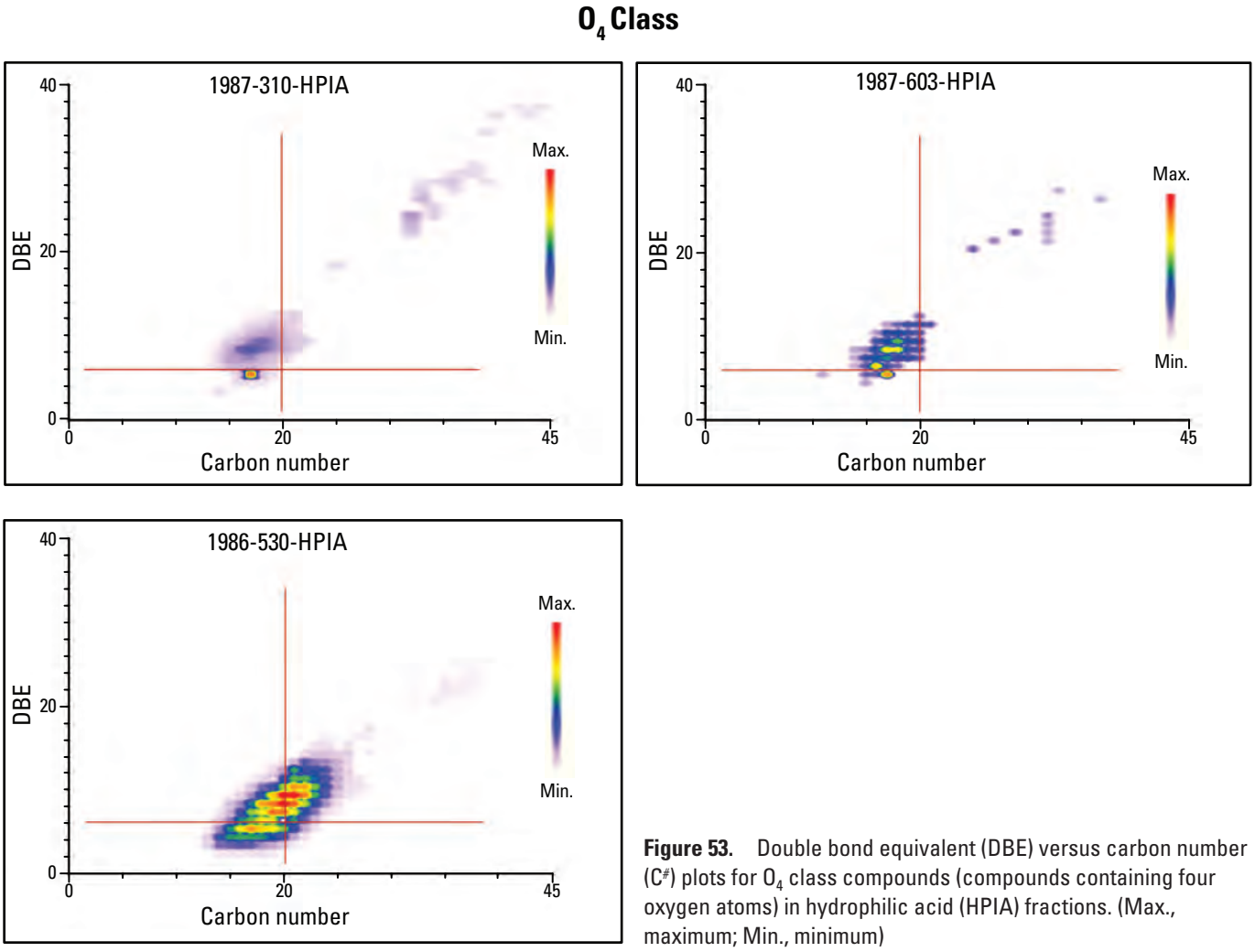

Figure 53. Double bond equivalent (DBE) versus carbon number (C#) plots for O_4 class compounds (compounds containing four oxygen atoms) in hydrophilic acid (HPIA) fractions. (Max., maximum; Min., minimum)

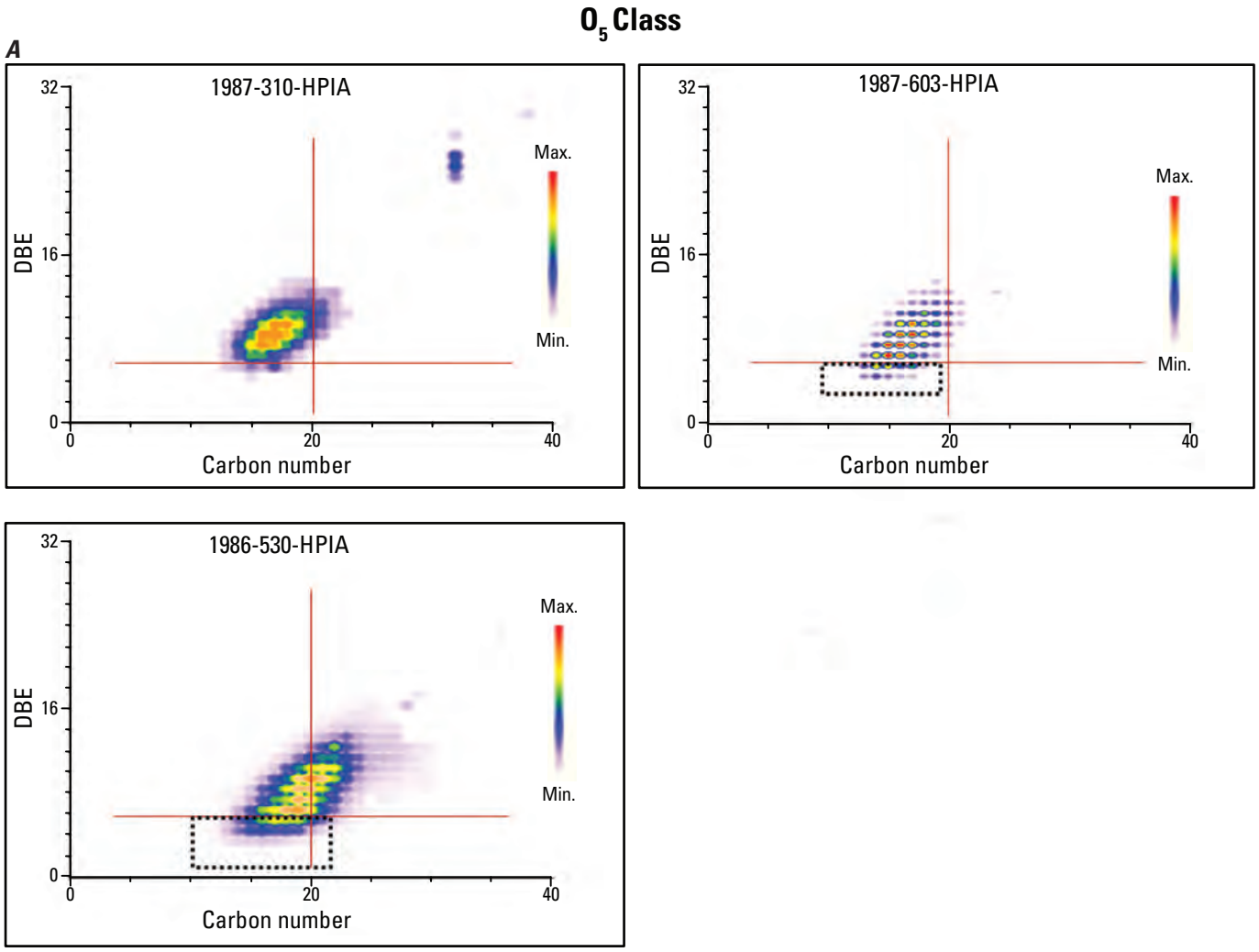

Figure 54. *A*, Double bond equivalent (DBE) versus carbon number (C#) plots for O_5 class compounds (compounds containing five oxygen atoms) in hydrophilic acid (HPIA) fractions. Rectangles denote molecular formulas potentially derived from aliphatic constituents of oil. *B*, DBE versus carbon number plots with DBE bar graphs for O_5 class compounds in HPIA fractions. Figure is from Islam and others (2016). (Max., maximum; Min., minimum)

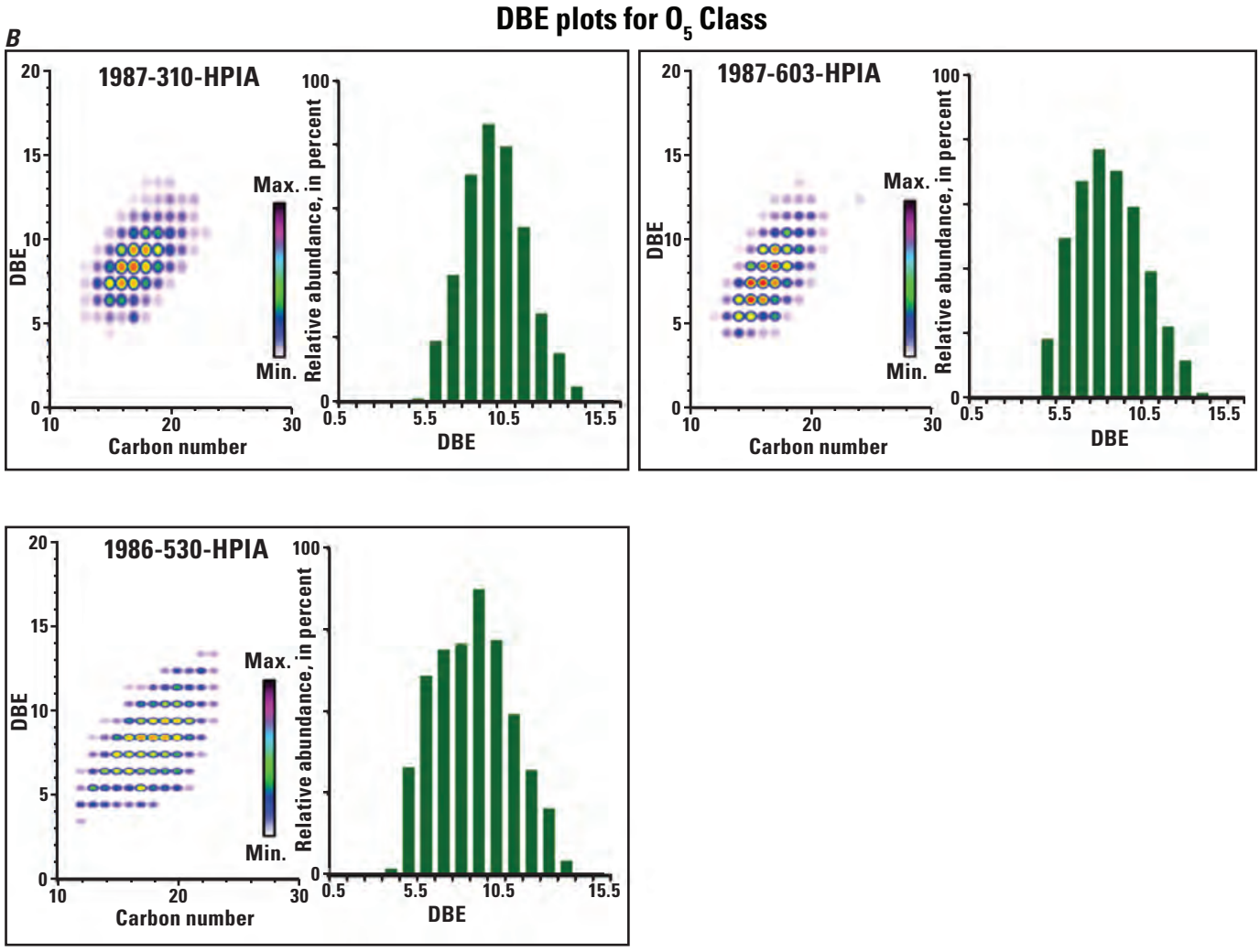

Figure 54.—Continued

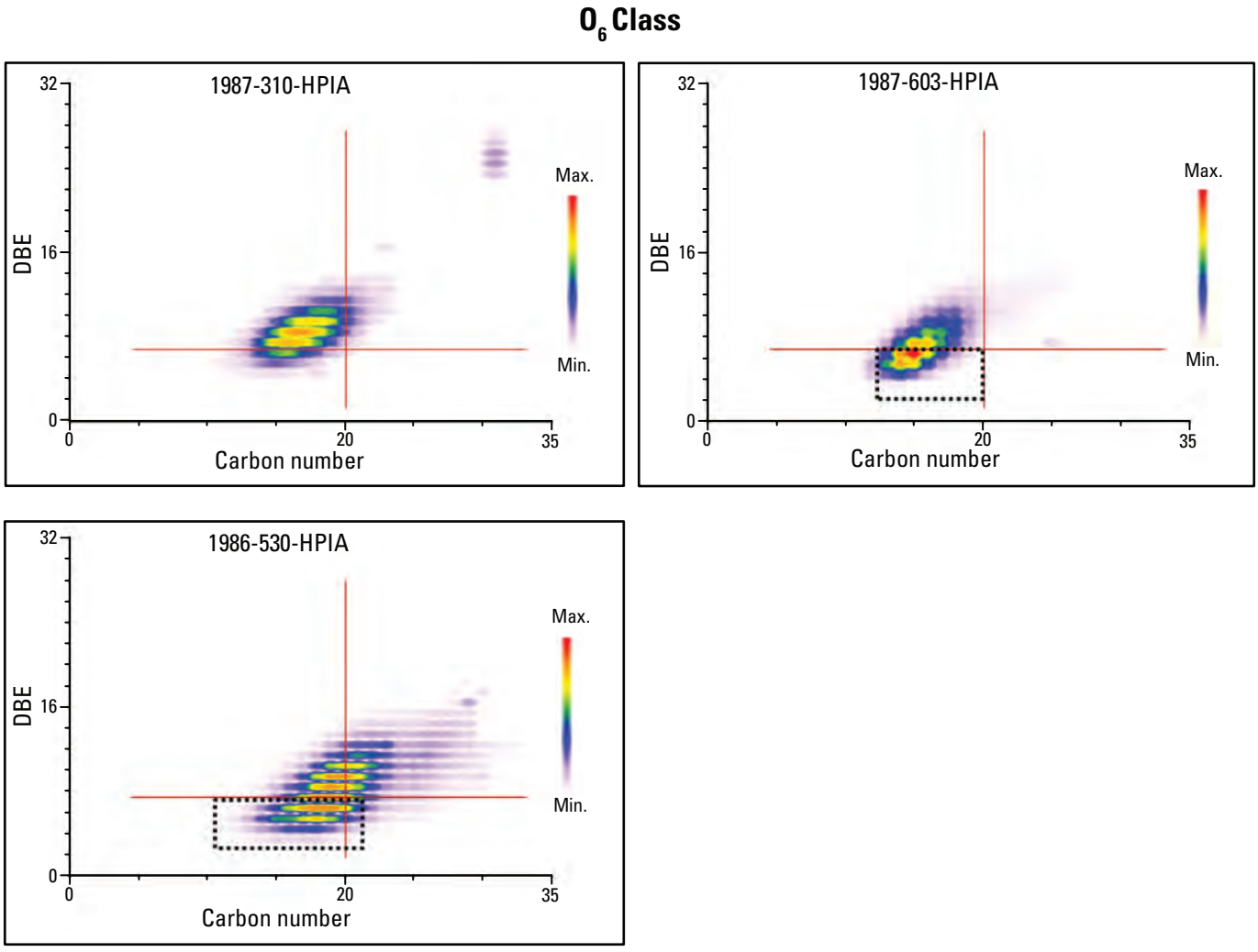

Figure 55. Double bond equivalent (DBE) versus carbon ($C^{\#}$) number plots for O_6 class compounds (compounds containing six oxygen atoms) in hydrophilic acid (HPIA) fractions. Rectangles denote molecular formulas potentially derived from aliphatic constituents of oil. (Max., maximum; min, minimum)

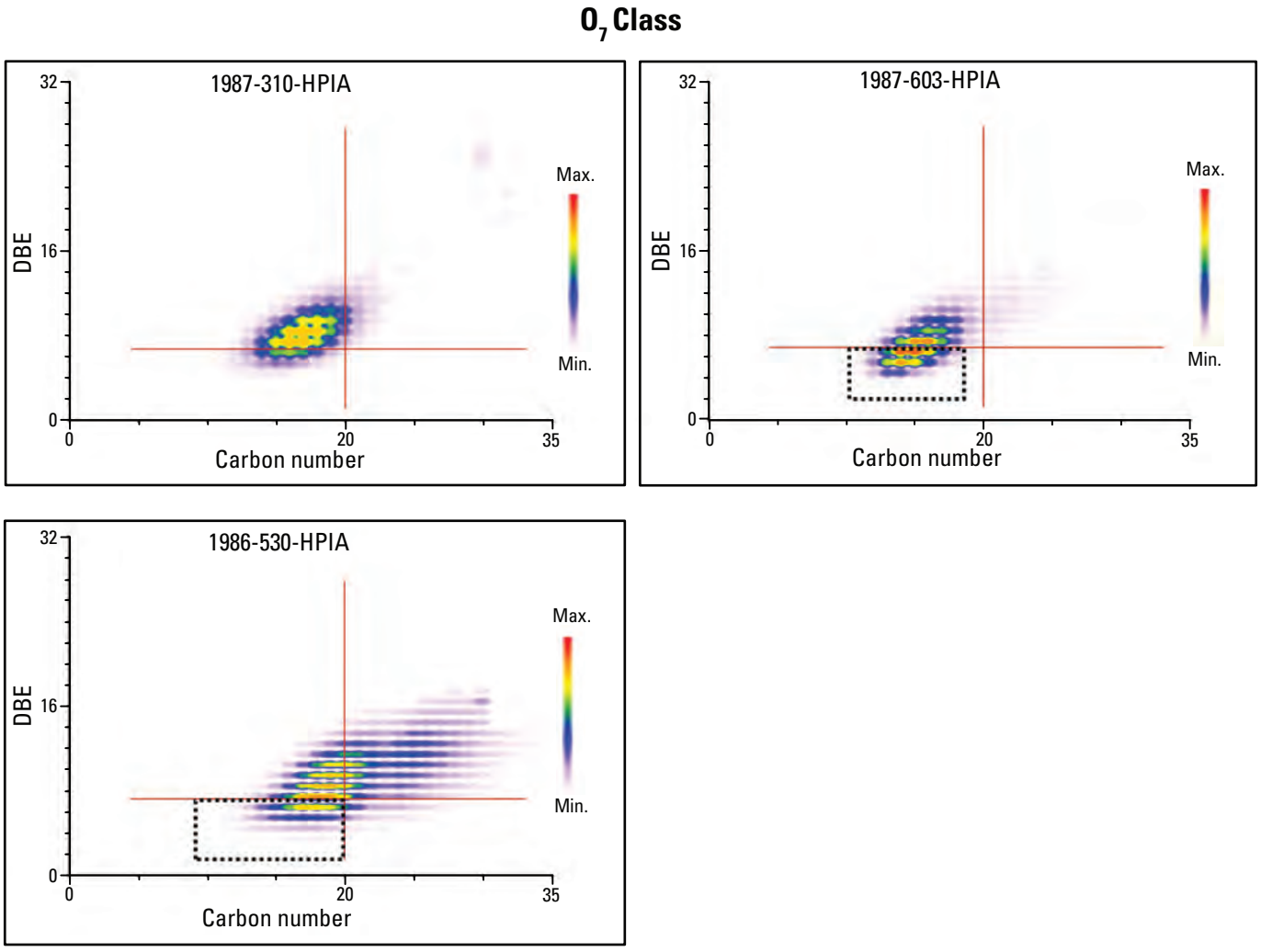

Figure 56. Double bond equivalent (DBE) versus carbon number (C#) plots for O_7 class compounds (compounds containing seven oxygen atoms) in hydrophilic acid (HPIA) fractions. Rectangles denote molecular formulas potentially derived from aliphatic constituents of oil. (Max., maximum; Min., minimum)

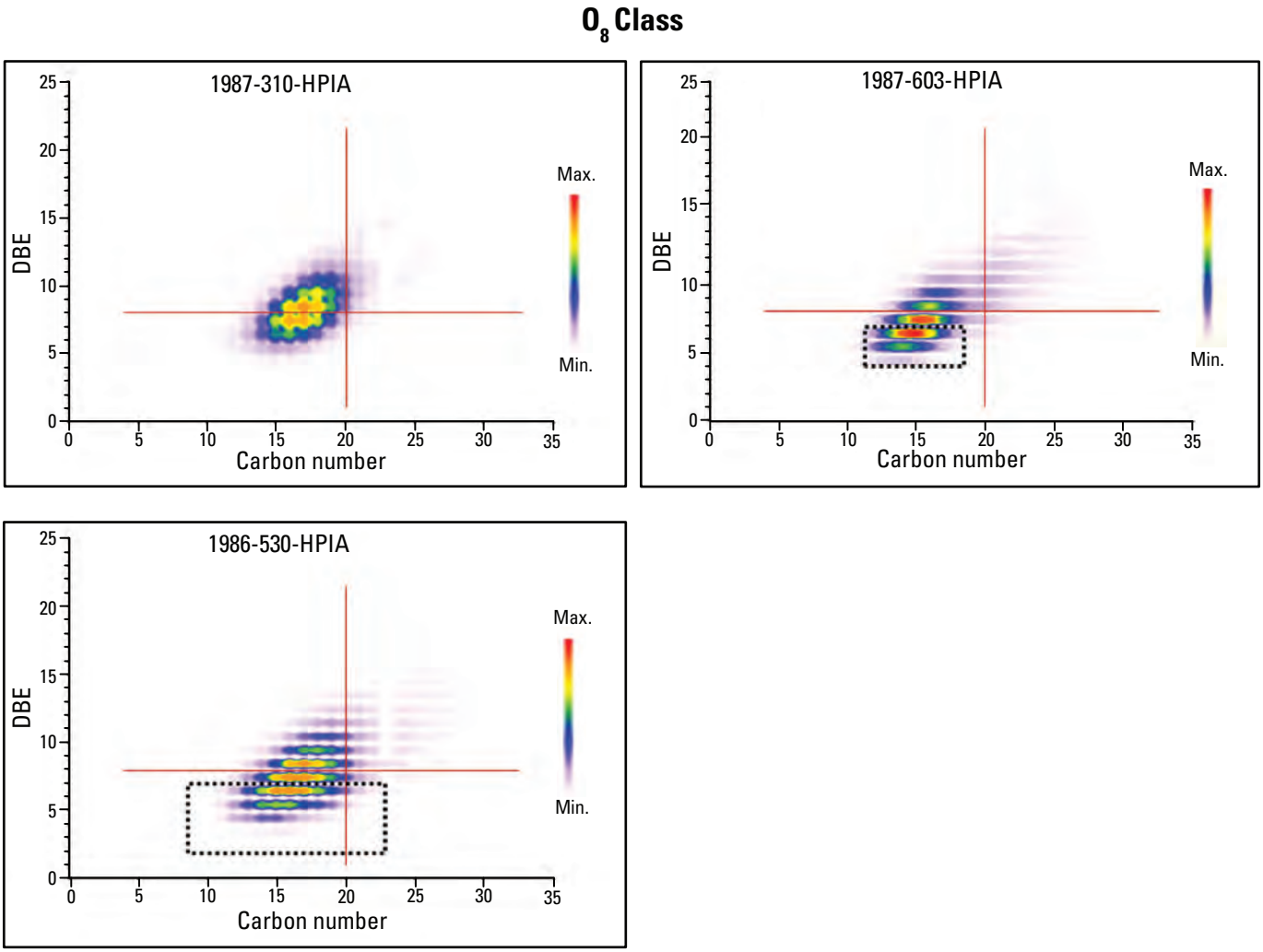

Figure 57. Double bond equivalent (DBE) versus carbon number (C#) plots for O_8 class compounds (compounds containing eight oxygen atoms) in hydrophilic acid (HPIA) fractions. Rectangles denote molecular formulas potentially derived from aliphatic constituents of oil. (Max., maximum; Min., minimum)

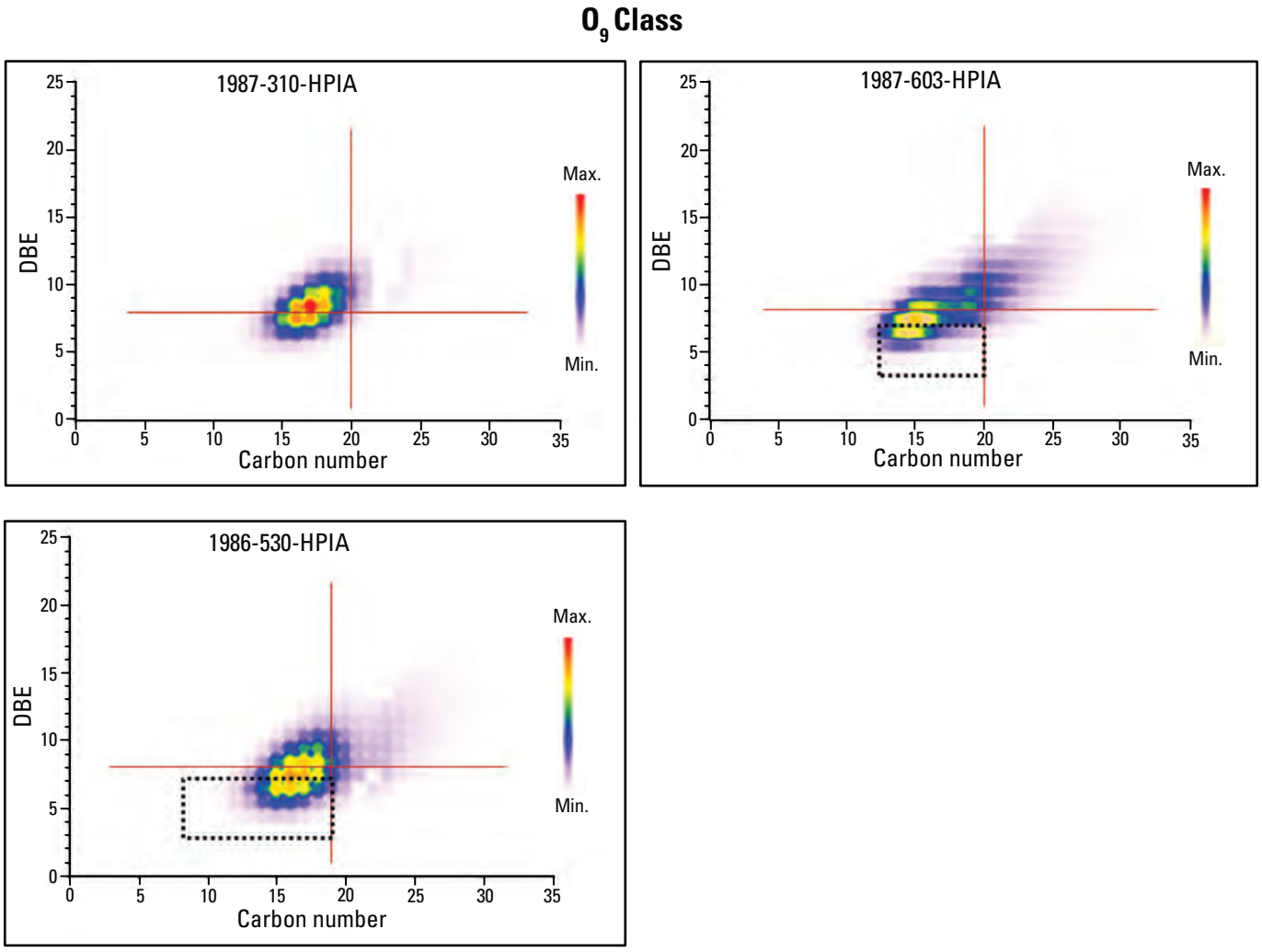

Figure 58. Double bond equivalent (DBE) versus carbon number (C#) plots for O_9 class compounds (compounds containing nine oxygen atoms) in hydrophilic acid (HPIA) fractions. Rectangles denote molecular formulas potentially derived from aliphatic constituents of oil. (Max., maximum; Min., minimum)

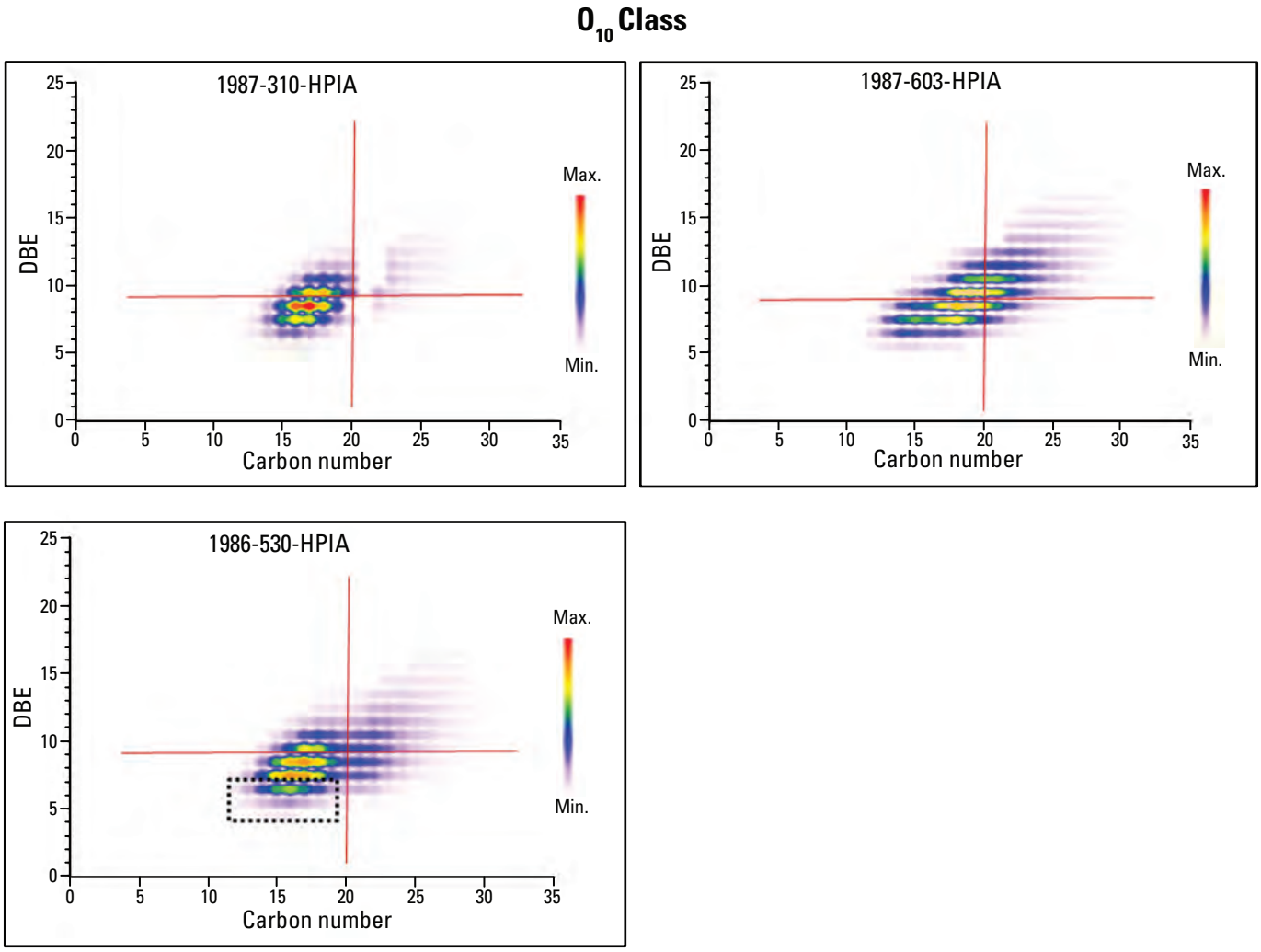

Figure 59. Double bond equivalent (DBE) versus carbon number ($C^{\#}$) plots for O_{10} class compounds (compounds containing 10 oxygen atoms) in hydrophilic acid (HPIA) fractions. Rectangles denote molecular formulas potentially derived from aliphatic constituents of oil. (Max., maximum; Min., minimum)

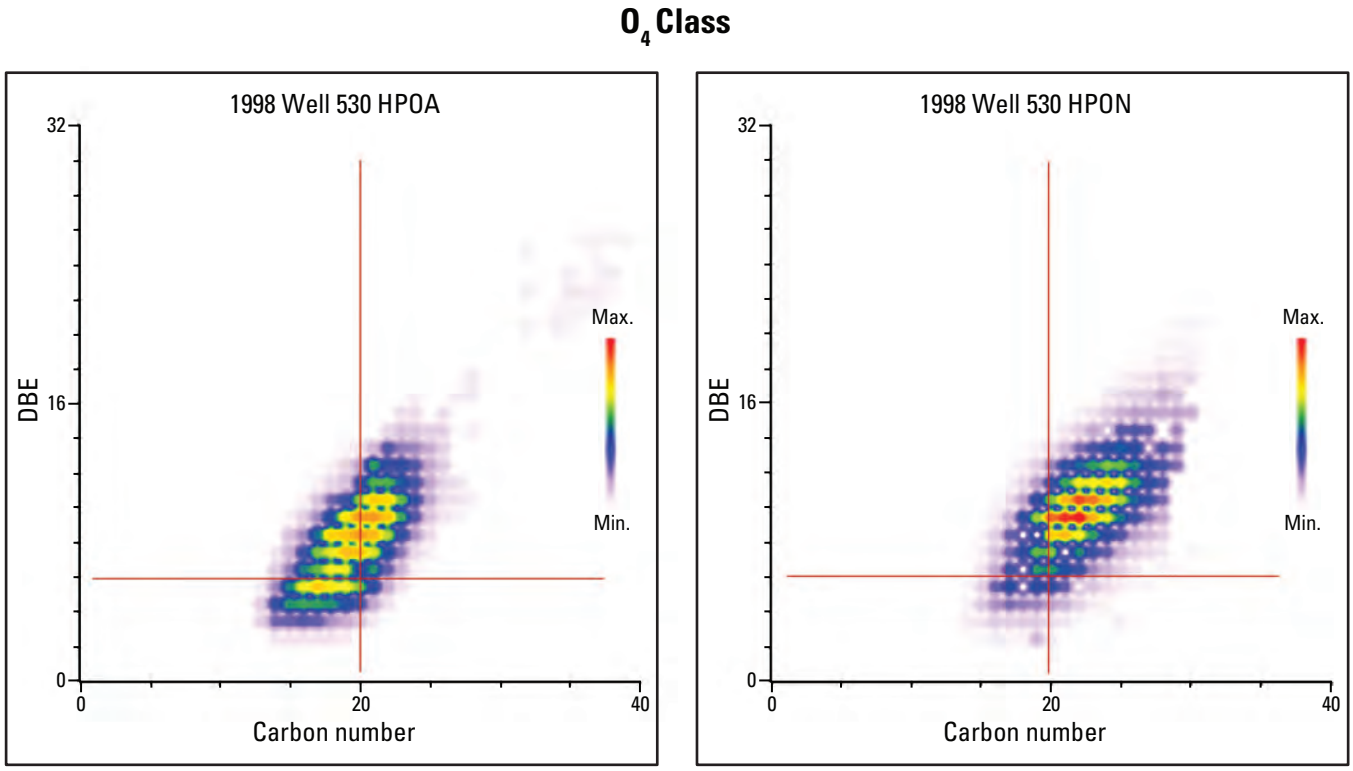

Name	Average DBE	Average carbon number
1998 Well 530 HPOA	8.4	19.9
1998 Well 530 HPON	9.9	22.4

Figure 60. Comparison of double bond equivalent (DBE) versus carbon number (C#) plots of O_4 class compounds (compounds containing four oxygen atoms) in the 1998 well 530 hydrophobic acid (HPOA) and hydrophobic neutral (HPON) fractions. (Max., maximum; Min., minimum)

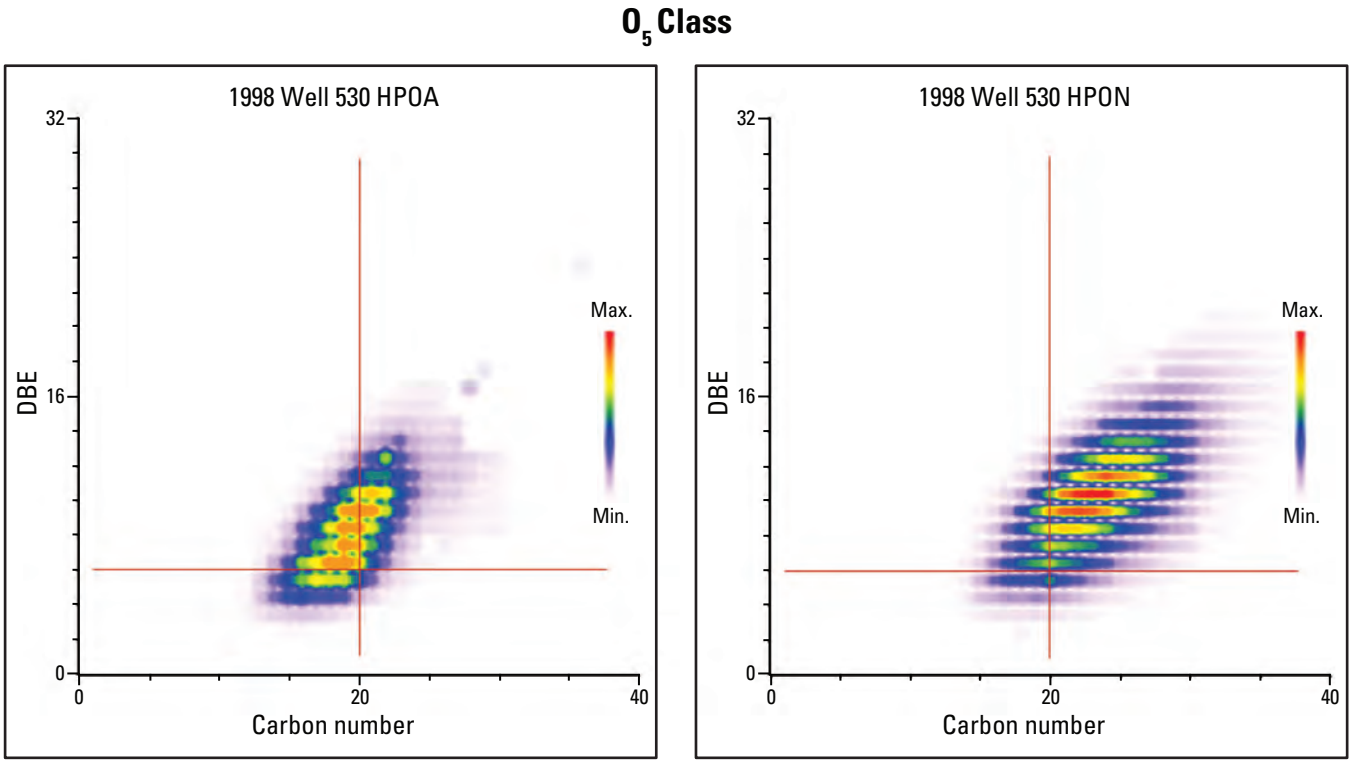

Name	Average DBE	Average carbon number
1998 Well 530 HPOA	8.6	19.8
1998 Well 530 HPON	10.4	23.8

Figure 61. Comparison of double bond equivalent (DBE) versus carbon number (C#) plots of O_5 class compounds (compounds containing five oxygen atoms) in the 1998 well 530 hydrophobic acid (HPOA) and hydrophobic neutral (HPON) fractions. (Max., maximum; Min., minimum)

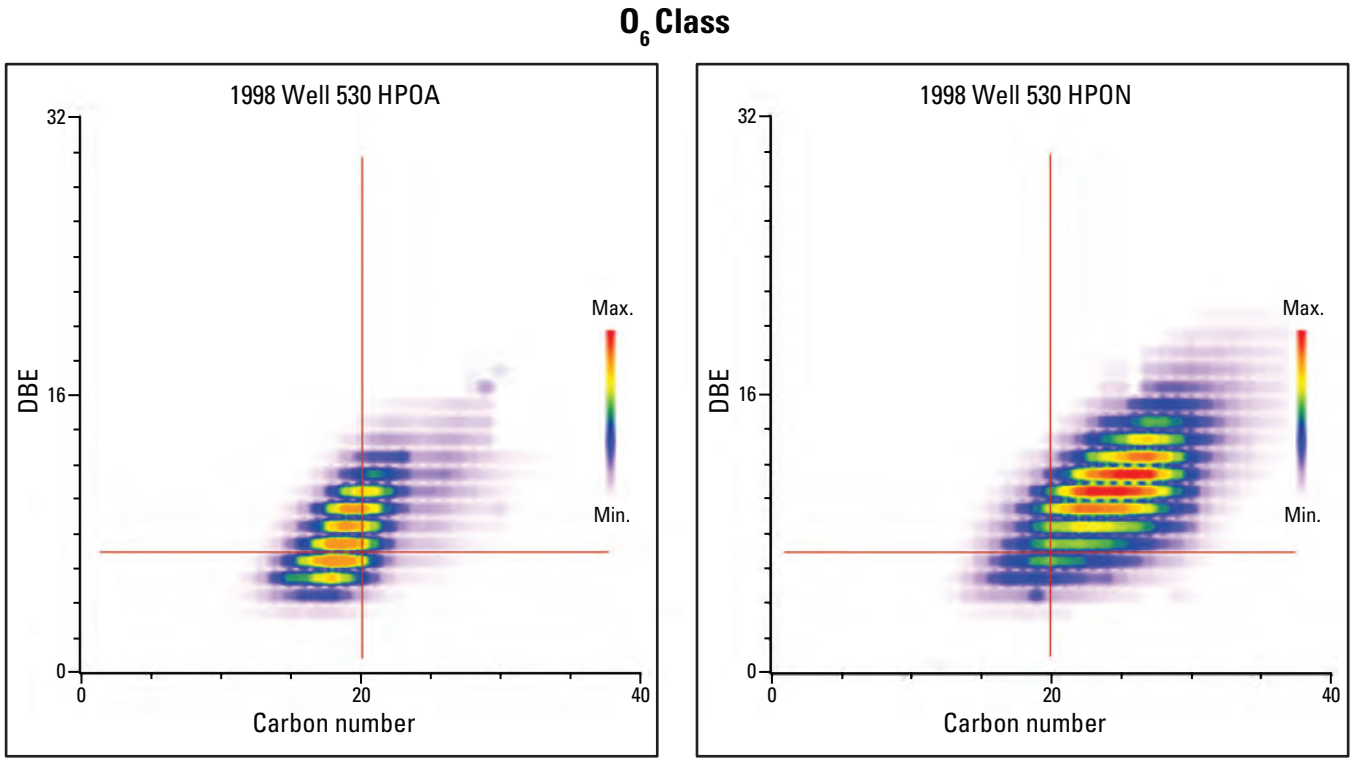

Name	Average DBE	Average carbon number
1998 Well 530 HPOA	8.6	20.1
1998 Well 530 HPON	10.6	24.7

Figure 62. Comparison of double bond equivalent (DBE) versus carbon number (C#) plots ofO_6 class compounds (compounds containing six oxygen atoms) in the 1998 well 530 hydrophobic acid (HPOA) and hydrophobic neutral (HPON) fractions. (Max., maximum; Min., minimum)

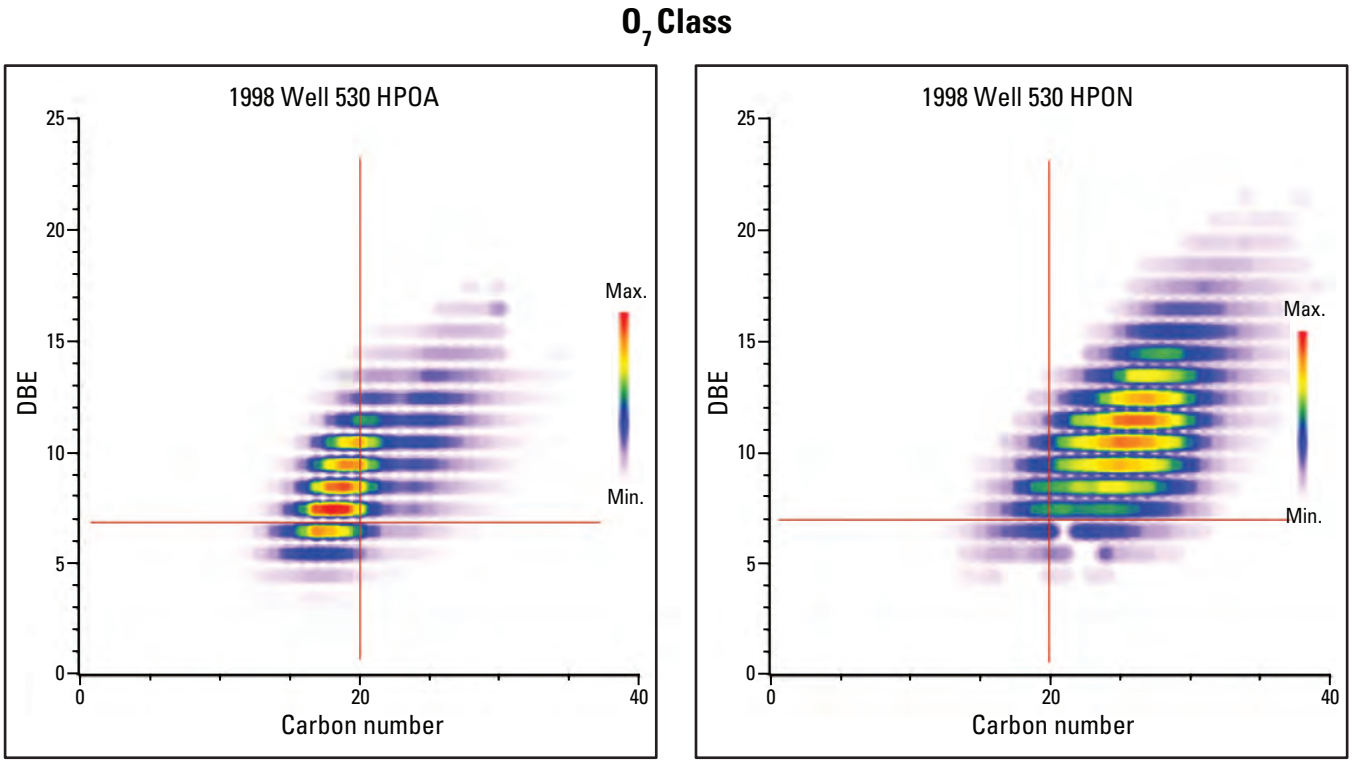

Name	Average DBE	Average carbon number
1998 Well 530 HPOA	9.4	21.0
1998 Well 530 HPON	11.1	25.8

Figure 63. Comparison of double bond equivalent (DBE) versus carbon number (C#) plots of O_7 class compounds (compounds containing seven oxygen atoms) in the 1998 well 530 hydrophobic acid (HPOA) and hydrophobic neutral (HPON) fractions. (Max., maximum; Min., minimum)

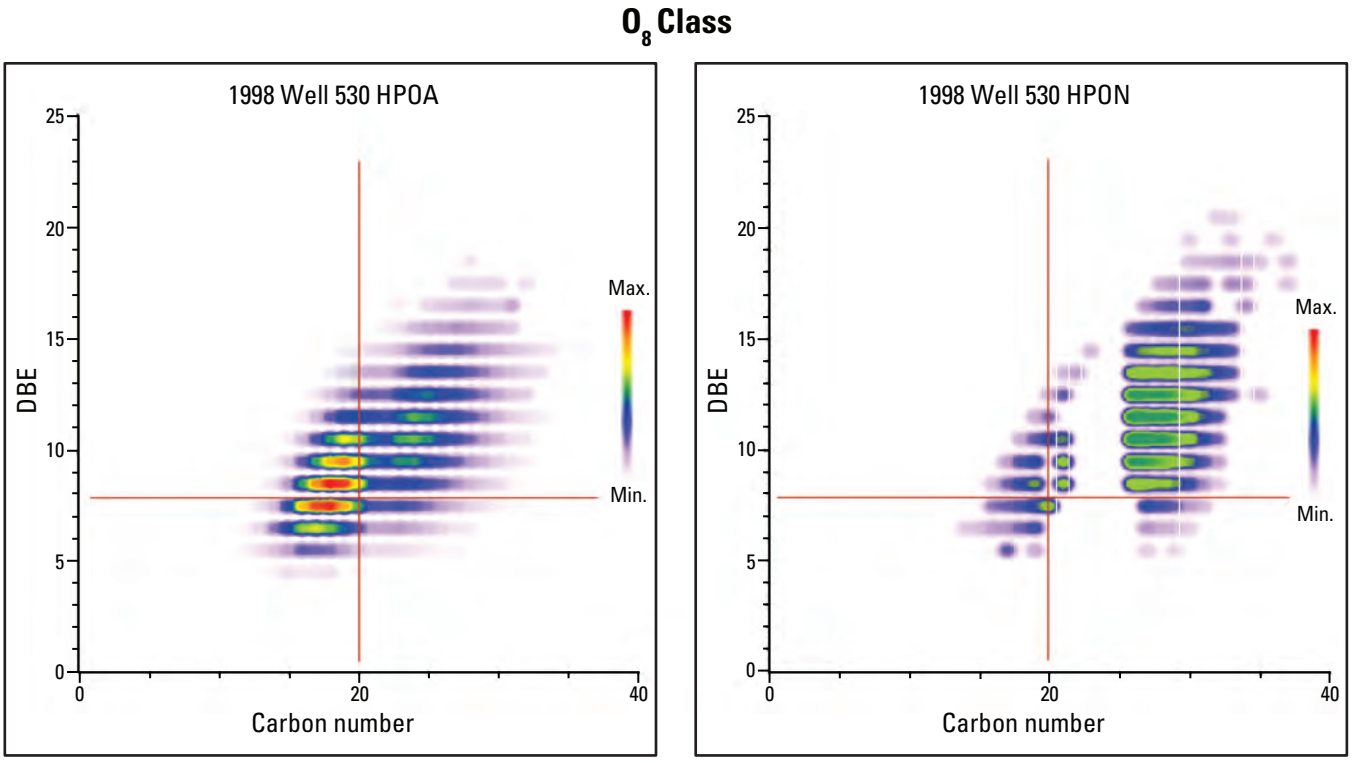

Name	Average DBE	Average carbon number
1998 Well 530 HPOA	10.0	21.9
1998 Well 530 HPON	11.6	27.1

Figure 64. Comparison of double bond equivalent (DBE) versus carbon number (C#) plots of O_8 class compounds (compounds containing eight oxygen atoms) in the 1998 well 530 hydrophobic acid (HPOA) and hydrophobic neutral (HPON) fractions. (Max., maximum; Min., minimum)

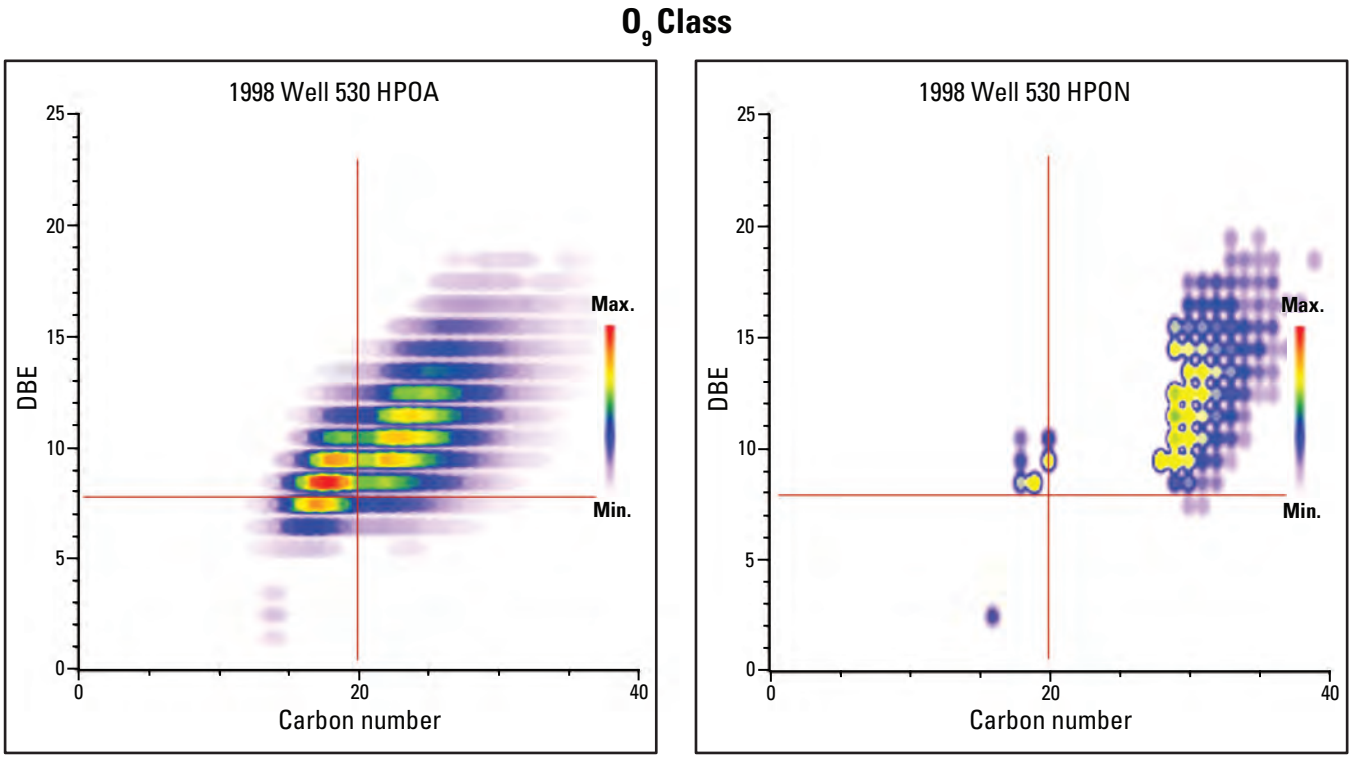

Name	Average DBE	Average carbon number
1998 Well 530 HPOA	10.6	23.1
1998 Well 530 HPON	12.8	30.4

Figure 65. Comparison of double bond equivalent (DBE) versus carbon number ($C^{\#}$) plots of O_9 class compounds (compounds containing nine oxygen atoms) in 1998 well 530 hydrophobic acid (HPOA) and hydrophobic neutral (HPON) fractions. (Max., maximum; Min., minimum)

Discussion

Synthesis of Data

All of the analyses indicate that the presence of oil-derived constituents distinguishes the contaminant well from the background well DOC. Fortuitously at the Bemidji site, as the background DOC in the shallow aquifer is post bomb, ^{14}C ages unequivocally serve as a tracer for the occurrence of oil-derived DOC in contaminated wells. The values of fraction modern carbon indicate that the order of decreasing contribution from the oil among the three DOC fractions in contaminant wells is HPON followed by HPOA followed by HPIA.

Hydrophobic Acid Fractions

Among the HPOA fractions, values for percent oxygen and O/C ratios from elemental analyses and percent carbon bonded to oxygen from ^{13}C NMR analyses are all less in the contaminant wells than in the background well. The latter difference is primarily in the lower O-alkyl carbon contents and secondarily in lower carboxyl/amide carbons of the contaminant well HPOA fractions. FTICR-MS analyses further reveal that $O_{5–7}$ are the major compound classes from the contaminant wells compared to $O_{8–10}$ for the background. The lower oxygen contents and predominance of lower oxygen-containing species in the contaminant well fractions are consistent with a contribution of crude oil constituents that have undergone partial oxidation. Contaminant well HPOA fractions are also distinguished from background in their greater elemental sulfur contents, particularly with their greater concentrations of $S_1O_{4–10}$ species. In terms of nitrogen, on the other hand, the contaminant well fractions have lower elemental nitrogen contents and, in particular, lower concentrations of $N_2O_{1–7}$ species. ^1H NMR spectra of the 1986 well 530 and 1987 well 603 fractions indicated a contribution to the DOC from the methyl-substituted aromatic constituents of the oil (Thorn and Aiken, 1998). In the contaminant well fractions, DBE versus $C^{\#}$ plots show oil-derived compounds containing

aromatic or saturated rings in the approximate range C_{20} to C_{30} among the $O_{4–10}$ class species and oil-derived aliphatic compounds in the approximate range C_{12} to C_{23} among the $O_{5–10}$ species.

Hydrophilic Acid Fractions

Among the HPIA fractions, the percent oxygen and O/C ratios do not differ significantly, while the proportion of O-alkyl carbons decreases from background to contaminant wells. The contaminant well fractions are again distinguished from background by their greater elemental sulfur contents and greater concentrations of $S_1O_{5–10}$ class compounds. The contaminant well fractions have lower elemental nitrogen contents and lower concentrations of N_2O_{1-10} class compounds than background. The contaminant well HPIA fractions (1986 530 and 1987 603) also have a contribution from the polar metabolites of methyl-substituted aromatic constituents of the oil, indicated by ^{1}H NMR peaks at 2.1–2.2 ppm (Thorn and Aiken, 1998). Finally, DBE versus $C^{\#}$ plots indicate oil-derived aliphatic compounds in the approximate range from C_{11} to C_{22} among the $O_{5–10}$ species in the contaminant well fractions.

Hydrophobic Neutral Fractions

As the fraction-containing constituents least altered from the crude oil, the HPON fraction from contaminated wells merits additional focus in future studies and analyses. A combination of characterization data, including the presence of cyclic ketones, distributions of alkyl and aromatic carbons, and elemental sulfur contents, indicates the HPON fraction contains partial oxidation products from several classes of crude oil constituents. These products include compounds from the aromatic, resin, and asphaltene fractions of the oil, including alkylaromatic and sulfur-containing constituents from these classes, as well as aliphatic and alicyclic compounds.

Comparison of 1986–1989 and 1998 Samples

The elemental, radiocarbon, and ^{13}C NMR analyses allow a partial time-course comparison between the 1986–1989 and 1998 well 530 and 603 samples. A comparison of FTICR-MS data is only available for the 1986 and 1998 well 530 HPOA fractions. Carbon-13 NMR provides the most direct information on the distribution of functional groups within the NVOA fractions. The overall similarities of the spectra for the well 603 and 530 samples suggest that a steady state in the composition of the partial oxidation products in each of the two zones existed between 1986–1989 and 1998. Specifically, the individual spectra within each set (1986 and 1998 530 HPOA [fig. 17], 1986 and 1998 530 HPIA [fig. 18], 1989 and 1998 530 HPON [fig. 20], and 1987 and 1998 603 HPOA [fig. 19]) bear a strong resemblance to one another. Within the 1986 and 1998 530 HPOA, 1989 and 1998 530 HPON, and 1987 and 1998 603 HPON pairs, the percent oxygen and the O/C ratios are close to one another (table 1). However, sulfur and nitrogen contents vary except for in the 1987 and 1998 603 HPOA fractions, where the percent nitrogen and carbon to nitrogen (C/N) ratios are similar.

For both the 1986 and 1998 530 HPOA fractions, O_5, O_6, and O_7 were the major oxygen compound classes (fig. 28). The relative abundances of the S_1O_{1-10} class compounds for the two fractions track closely with one another (fig. 33). The 530 HPOA fractions from both years show evidence of oil-derived aliphatic compounds in the range from C_{12} to C_{23} among the O_{4-8} class compounds and oil-derived compounds containing aromatic or saturated rings in the range from C_{20} to C_{30} for O_{9-10} class compounds. Principal component analysis placed the 1986 and 1998 well 530 HPOA fractions in the same grouping, separate from the background well 310 and spray zone well 603 HPOA fractions (Islam and others, 2016).

Analyses of DOC isolated from wells downgradient of the oil body in 2016 have reproduced several of the features reported in this study, including the presence of carboxylic acids of oil constituents containing aromatic and saturated rings, significant concentrations of molecular formulas containing sulfur, and average molecular weights ranging between ~ 400 and 500 Daltons (Podgorski and others, 2021). Additionally, oil-derived condensed aromatic compounds were detected as far downgradient as 254 m.

Inconsistency of Data with Microbial Biosynthesis Hypothesis

O'Reilly (2018), O'Reilly and others (2019), and Mohler and others (2020) have claimed that the contribution of partial oxidation products (polar metabolites) of petroleum constituents to the NVOAs isolated from contaminated wells in this study is overstated. They argued that compounds with molecular formulas unique to the contaminated wells may be comprised instead of biomolecules, for example, proteins, nucleotides and nucleic acids, carbohydrates, lipids, biosurfactants (primarily glycolipids [Das and Chandran, 2011]), and so forth, that were resynthesized by microorganisms from low weight metabolites of the petroleum. They specifically cited C_9 to C_{18} fatty acids as an example. The implication of this hypothesis is that, in contrast to partial oxidation products, the biomolecules would not pose a toxicity hazard to organisms. A complete response to this assertion is beyond the scope of the present report, but some general counterpoints are presented here, which build on the original rebuttal to the hypothesis by Podgorski and others (2018b).

To begin with, biomolecules synthesized from low molecular weight substrates would first exist within living or expired bacteria that reside in the particulate or colloidal, not the dissolved phase, of the groundwater organic matter. Extracellular enzymes produced from the bacteria would also occur in the colloidal phase. Solid-state CP/MAS ^{13}C NMR spectra of groundwater colloids have not been widely

reported, but the few published are distinguishable from the ^{13}C NMR spectra of the contaminant well NVOAs presented here, exhibiting significant carbohydrate signals with well-resolved anomeric carbon peaks, and near negligible concentrations of ketones (Thorn and others, 2003).

Although the existence of biomolecules in the Bemidji DOC is plausible, there is no more evidence for their occurrence in the contaminant wells than in the background DOC. The critiques of O'Reilly (2018), O'Reilly and others (2019), and Mohler and others (2020) did not take into account sulfur and nitrogen compounds, which are critical to an understanding of the DOC. Molecular formulas containing sulfur are a significant percentage of the NVOAs in the contaminant well HPOA and HPIA fractions, but none of these contain nitrogen as well (table 6), ruling out the occurrence of proteins or peptides, the major class of biomolecules that would contain sulfur, in the form of the sulfur-containing amino acids (methionine and cysteine). The increased number of molecular formulas in the contaminant wells that contain sulfur almost certainly then represent partial oxidation products of the sulfur-containing constituents of the crude oil. The number of molecular formulas that contain both nitrogen and oxygen is lower in the contaminant than in the background well HPOA and HPIA fractions, ruling out an increase in concentration of peptides, proteins, and nucleotides in the contaminated groundwater. For both background and contaminant well HPOA and HPIA fractions, among molecular formulas that contain nitrogen, formulas containing two nitrogens are most abundant, while N_2O_1 species are most abundant within the N_2O_n class. These distributions are inconsistent with the presence of significant concentrations of peptides, proteins, or nucleotides. (In this regard, positive-mode [+] ESI analyses could potentially provide additional information.) The ^{13}C NMR spectra of the contaminant well NVOAs do not show direct evidence of a contribution from peptides, proteins, or nucleotides. Methylation analysis confirmed the assignment of the peaks at approximately 160 to 190 ppm as primarily carboxylic acids and not peptide amides.

As discussed in the "Nuclear Magnetic Resonance Spectra" section, of the carbohydrate material that sorbs to the XAD resins, there is a preference for XAD-4 (HPIA) over XAD-8 (HPOA and HPON). None of the ^{13}C NMR spectra of contaminant well HPIA fractions (1987 603,1987 515, 1986 530, and 1998 530) show greater concentrations of carbohydrate (peaks at 79 and 106 ppm) than the background 1987 310 HPIA fraction. Likewise, in the ^{13}C NMR spectra of the HPOA fractions along the well transect (fig. 15), the background 1987 310 HPOA exhibits resolved carbohydrate peaks at 79 and 106 ppm, whereas the peaks at ~ 79 ppm are of significantly less intensity and the anomeric carbons not at all resolved in the contaminant well fractions. In other words, carbohydrates are lower in concentration if present at all in the contaminant well HPOA fractions. Concentrations of carbohydrates are also insignificant if present at all in the ^{13}C NMR spectra of the well 603 and 530 HPON fractions (fig. 20). Furthermore, from the FTICR-MS data, assuming a range of O/C ratios from 0.8 to 1.0 for carbohydrates, molecular formulas that have O/C ratios in this range are limited to the O_8, O_9, and O_{10} species of the O_n compound classes for 1986 530 HPIA, O_9 and O_{10} for 1987 603 HPIA, and O_{10} for 1998 530 HPOA (table 8).

The proposal that the contaminant well DOC may consist, in part, of C_9 to C_{18} fatty acids is not supported by evidence. Fatty acids (molecular formulas containing two oxygens) are most likely to occur in the HPON fraction of the NVOAs. Compared to O_4 through O_9 species among O_n class compounds, O_2 species were not detected in significant quantities by (-) ESI in the 1998 530 HPON fraction (fig. 30). The ^{13}C NMR spectra of the well 530 and 603 HPON fractions indicate a mixture of aromatic, alkylaromatic, and aliphatic structures (fig. 19). However, as discussed above, in the case of 1998 530 HPON, the majority of compounds in the HPON DBE versus $C^{\#}$ plots appear to contain aromatic or saturated rings for all oxygen class compounds (figs. 60–65). Olefinic protons of unsaturated fatty acids have characteristic ^1H NMR chemical shifts at approximately 5.3 to 5.5 ppm. These chemical shifts were not detected in the liquid-state ^1H NMR spectra of the 1989 530 HPON and 1987 603 HPON fractions reported previously (Thorn and Aiken, 1998), ruling out the presence of unsaturated fatty acids in free form or as acylglycerides.

The microbial biosynthesis hypothesis was derived primarily on the basis of molecular weight observations (Mohler and others, 2020). Molecular formulas of DOC from wells downgradient of the oil body were shown to contain higher carbon numbers than background well 310 DOC, where the DOC was isolated in 2016 from groundwater by liquid-liquid extraction (methylene chloride) and molecular formulas determined by (-) ESI orbitrap analyses. The argument was that molecules with higher carbon numbers could only result from biosynthesis and not from metabolism of petroleum hydrocarbons. However, no evidence was provided to exclude the possibility that the molecular formulas from contaminant wells containing higher carbon numbers correspond to polar metabolites of higher molecular weight crude-oil constituents.

Summary

Elemental analysis, radiocarbon dating, nuclear magnetic resonance spectroscopy, and Fourier transform ion cyclotron resonance mass spectrometry (FTICR-MS) each distinguished between dissolved organic carbon from the background well (301) and contaminant wells (515, 530, 532, 533, and 603). The data suggest the nonvolatile organic acids (NVOAs) originate from biodegradation of several classes of C_{12} and greater (12 carbons and greater) crude oil constituents, including (1) sulfur-containing constituents, including possibly the resins and asphaltenes; (2) aromatic, alkylaromatic, and naphthenoaromatic constituents, including those with methyl-substituted aromatic carbons; and C_{12} to C_{22} aliphatic constituents.

Crude-oil constituents containing branched alkyl moieties or saturated rings, either in alkylaromatic or purely aliphatic structures, may be inferred as parent compounds from the presence of cyclic ketones and from the concentrations of sp^3 hybridized methine carbons at 41–48 parts per million in the carbon-13 nuclear magnetic resonance (^{13}C NMR) spectra of the contaminant well nonvolatile organic acids (NVOAs). Fourier transform ion cyclotron resonance mass spectrometry (FTICR-MS) analyses reveal differences in distributions of compound classes between the spray zone well 603 and the downgradient well 530 dissolved organic carbon that may reflect the different proportions of aerobic versus anaerobic biodegradation at the two locations and the possibility of photooxidation of oil at the soil surface of the spray zone. Finally, the composition of the dissolved organic carbon at these two contaminant wells appears to have reached a steady state between the 1986–1989 and 1998 sampling dates.

References Cited

Aiken, G.R., McKnight, D.M., Thorn, K.A., and Thurman, E.M., 1992, Isolation of hydrophilic organic acids from water using nonionic macroporous resins: Organic Geochemistry, v. 18, no. 4, p. 567–573. [Also available at https://doi.org/10.1016/0146-6380(92)90119-I.]

Aiken, G.R., Thorn, K.A., and Brooks, M.H., 1987, Nonvolatile organic acids in ground water contaminated with crude oil, *in* Franks, B.J., ed., U.S. Geological Survey program on toxic waste—Ground-water contamination: U.S. Geological Survey Open-File Report 87–109, p. C31–C32. [Also available at https://pubs.usgs.gov/of/1987/0109/report.pdf.]

Amos, R.T., Bekins, B.A., Cozzarelli, I.M., Voytek, M.A., Kirshtein, J.D., Jones, E.J.P., and Blowes, D.W., 2012, Evidence for iron-mediated anaerobic methane oxidation in a crude oil-contaminated aquifer: Geobiology, v. 10, no. 6, p. 506–517. [Also available at https://doi.org/10.1111/j.1472-4669.2012.00341.x.]

Baedecker, M.J., Cozzarelli, I.M., Eganhouse, R.P., Siegel, D.I., and Bennett, P.C., 1993, Crude oil in a shallow sand and gravel aquifer—III, Biogeochemical reactions and mass balance modeling in anoxic groundwater: Applied Geochemistry, v. 8, no. 6, p. 569–586. [Also available at https://doi.org/10.1016/0883-2927(93)90014-8.]

Ball, H.A., Johnson, H.A., Reinhard, M., and Spormann, M., 1996, Initial reactions in anaerobic ethylbenzene oxidation by a denitrifying bacterium, strain EB1: Journal of Bacteriology, v. 178, no. 19, p. 5755–5761 [Also available at https://doi.org/10.1128/jb.178.19.5755-5761.1996.]

Barrow, M.P., Peru, K.M., Fahlman, B., Hewitt, L.M., Frank, R.A., and Headley, J.V., 2015, Beyond naphthenic acids—Environmental screening of water from natural sources and the Athabasca oil sands industry using atmospheric pressure photoionization Fourier transform ion cyclotron resonance mass spectrometry: Journal of the American Society for Mass Spectrometry, v. 26, no. 9, p. 1508–1521. [Also available at https://doi.org/10.1007/s13361-015-1188-9.]

Barrow, M.P., Peru, K.M., and Headley, J.V., 2014, An added dimension—GC atmospheric pressure chemical ionization FTICR MS and the Athabasca oil sands: Analytical Chemistry, v. 86, no. 16, p. 8281–8288. [Also available at https://doi.org/10.1021/ac501710y.]

Bekins, B.A., 2019, Natural attenuation in source zone and groundwater plume—Bemidji crude oil spill: Enviro Wiki, accessed December 31, 2021, at https://www.enviro.wiki/index.php?title=Natural_Attenuation_in_Source_Zone_and_Groundwater_Plume_-_Bemidji_Crude_Oil_Spill&oldid=13002.

Bekins, B.A., Brennan, J.C., Tillitt, D.E., Cozzarelli, I.M., Illig, J.M., and Martinović-Weigelt, D., 2020, Biological effects of hydrocarbon degradation intermediates—Is the total petroleum hydrocarbon analytical method adequate for risk assessment?: Environmental Science & Technology, v. 54, no. 18, p. 11396–11404. [Also available at https://doi.org/10.1021/acs.est.0c02220.]

Bekins, B.A., Cozzarelli, I.M., Erickson, M.L., Steenson, R.A., and Thorn, K.A., 2016, Crude oil metabolites in groundwater at two spill sites: Ground Water, v. 54, no. 5, p. 681–691. [Also available at https://doi.org/10.1111/gwat.12419.]

Bekins, B.A., Hostettler, F.D., Herkelrath, W.N., Delin, G.N., Warren, E., and Essaid, H.I., 2005, Progression of methanogenic degradation of crude oil in the subsurface: Environmental Geoscience, v. 12, no. 2, p. 139–152. [Also available at https://doi.org/10.1306/eg.11160404036.]

Bekins, B.A., Godsy, E.M., and Warren, E., 1999, Distribution of microbial physiologic types in an aquifer contaminated by crude oil: Microbial Ecology, v. 37, no. 4, p. 263–275. [Also available at https://doi.org/10.1007/s002489900149.]

Biegert, T., Fuchs, G., and Heider, J., 1996, Evidence that anaerobic oxidation of toluene in the denitrifying bacterium *Thauera aromatica* is initiated by formation of benzylsuccinate from toluene and fumarate: European Journal of Biochemistry, v. 238, no. 3, p. 661–668. [Also available at https://doi.org/10.1111/j.1432-1033.1996.0661w.x.]

Bossert, I., and Bartha, R., 1984, The fate of petroleum in soil ecosystems, *in* Atlas, R.M., ed., Petroleum microbiology: New York, Macmillan Publishing Company, p. 435–473.

Breitmaier, E., and Voelter, W., 1987, Carbon-13 NMR spectroscopy—High-resolution methods and applications in organic chemistry and biochemistry 3rd ed.: New York, VCH Publishers, 515 p.

Cerniglia, C.E., 1984, Microbial transformation of aromatic hydrocarbons, *in* Atlas, R.M., ed., Petroleum Microbiology: New York, Macmillan, p. 99–128.

Charrié-Duhaut, A., Lemoine, S., Adam, P., Connan, J., and Albrecht, P., 2000, Abiotic oxidation of petroleum bitumens under natural conditions: Organic Geochemistry, v. 31, no. 10, p. 977–1003. [Also available at https://doi.org/10.1016/S0146-6380(00)00109-1.]

Connan, J., 1984, Biodegradation of crude oils in reservoirs, *in* Brooks, J., and Welte, D., eds., Advances in petroleum geochemistry: London, Academic Press, p. 299–335. [Also available at https://doi.org/10.1016/B978-0-12-032001-1.50011-0.]

Cozzarelli, I.M., Baedecker, M.J., Eganhouse, R.P., and Goerlitz, D.F., 1994, The geochemical evolution of low molecular-weight organic acids derived from the degradation of petroleum contaminants in groundwater: Geochimica et Cosmochimica Acta, v. 58, no. 2, p. 863–877. [Also available at https://doi.org/10.1016/0016-7037(94)90511-8.]

Cozzarelli, I.M., Eganhouse, R.P., and Baedecker, M.J., 1990, Transformation of monoaromatic hydrocarbons to organic acids in anoxic groundwater environment: Environmental Geology and Water Sciences, v. 16, no. 2, p. 135–141. [Also available at https://doi.org/10.1007/BF01890379.]

Cozzarelli, I.M., Schreiber, M.E., Erickson, M.L., and Ziegler, B.A., 2016, Arsenic cycling in hydrocarbon plumes—Secondary effects of natural attenuation: Ground Water, v. 54, no. 1, p. 35–45. [Also available at https://doi.org/10.1111/gwat.12316.]

Das, N., and Chandran, P., 2011, Microbial degradation of petroleum hydrocarbon contaminants—An overview: Biotechnology Research International, v. 2011, p. 1–13. [Also available at https://doi.org/10.4061/2011/941810.]

Delin, G.N., and Herkelrath, W.N., 2014, Effects of a dual-pump crude-oil recovery system, Bemidji, Minnesota, USA: Ground Water Monitoring and Remediation, v. 34, no. 1, p. 57–67. [Also available at https://doi.org/10.1111/gwmr.12040.]

Eganhouse, R., Baedecker, M.J., Cozzarelli, I., Aiken, G.R., Thorn, K.A., and Dorsey, T.F., 1993, Crude oil in a shallow sand and gravel aquifer—II, Organic geochemistry: Applied Geochemistry, v. 8, no. 6, p. 551–567. [Also available at https://doi.org/10.1016/0883-2927(93)90013-7.]

Eggert, H., and Djerassi, C., 1973, Carbon-13 nuclear magnetic resonance spectra of keto steroids: The Journal of Organic Chemistry, v. 38, no. 21, p. 3788–3792. [Also available at https://doi.org/10.1021/jo00961a031.]

Essaid, H.I., Bekins, B.A., Herkelrath, W.N., and Delin, G.N., 2011, Crude oil at the Bemidji site—25 years of monitoring, modeling, and understanding: Ground Water, v. 49, no. 5, p. 706–726. [Also available at https://doi.org/10.1111/j.1745-6584.2009.00654.x.]

Essaid, H.I., Cozzarelli, I.M., Eganhouse, R.P., Herkelrath, W.N., Bekins, B.A., and Delin, G.N., 2003, Inverse modeling of BTEX dissolution and biodegradation at the Bemidji, MN crude-oil spill site: Journal of Contaminant Hydrology, v. 67, no. 1-4, p. 269–299. [Also available at https://doi.org/10.1016/S0169-7722(03)00034-2.]

Fedorak, P.M., 1990, Microbial metabolism of organosulfur compounds, chap. 6 *of* Orr, W.L., and White, C.M., eds., Geochemistry of sulfur in fossil fuels— Washington, D.C.: American Chemical Society, ACS Publications, p. 93–112. [Also available at https://doi.org/10.1021/bk-1990-0429.ch006.]

Gieg, L.M., and Suflita, J.M., 2005, Metabolic indicators of anaerobic hydrocarbon biodegradation in petroleum-laden environments, *in* Ollivier, B., and Magot, M., eds., Petroleum Microbiology: Washington, D.C., ASM Press, p. 337–356. [Also available at https://doi.org/10.1128/9781555817589.ch17.]

Headley, J.V., Barrow, M.P., Peru, K.M., Fahlman, B., Frank, R.A., Bickerton, G., McMaster, M.E., Parrott, J., and Hewitt, L.M., 2011, Preliminary fingerprinting of Athabasca oil sands polar organics in environmental samples using electrospray ionization Fourier transform ion cyclotron resonance mass spectrometry: Rapid Communications in Mass Spectrometry, v. 25, no. 13, p. 1899–1909.

Headley, J.V., Peru, K.M., and Barrow, M.P., 2016, Advances in mass spectrometric characterization of naphthenic acids fraction compounds in oil sands environmental samples and crude oil—A review: Mass Spectrometry Reviews, v. 35, no. 2, p. 311–328. [Also available at https://doi.org/10.1002/mas.21472.]

Hernández-López, E.L., Ayala, M., and Vazquez-Duhalt, R., 2015, Microbial and enzymatic biotransformations of asphaltenes: Petroleum Science and Technology, v. 33, no. 9, p. 1017–1029. [Also available at https://doi.org/10.1080/10916466.2015.1014960.]

Hostettler, F.D., and Kvenvolden, K.A., 2002, Alkylcyclohexanes in environmental geochemistry: Environmental Forensics, v. 3, no. 3–4, p. 293–301. [Also available at https://doi.org/10.1080/713848390.]

Hur, M., Oh, H.B., and Kim, S., 2009, Optimized automatic noise level calculations for broadband FT-ICR mass spectra of petroleum give more reliable and faster peak picking results: Bulletin of the Korean Chemical Society, v. 30, no. 11, p. 2665–2668. [Also available at https://doi.org/10.5012/bkcs.2009.30.11.2665.]

Hur, M., Yeo, I., Park, E., Kim, Y.H., Yoo, J., Kim, E., No, M., Koh, J., and Kim, S., 2010, Combination of statistical methods and Fourier transform ion cyclotron resonance mass spectrometry for more comprehensive, molecular-level interpretations of petroleum samples: Analytical Chemistry, v. 82, no. 1, p. 211–218. [Also available at https://doi.org/10.1021/ac901748c.]

Islam, A., Ahmed, A., Hur, M., Thorn, K., and Kim, S., 2016, Molecular-level evidence provided by ultrahigh resolution mass spectrometry for oil-derived doc in groundwater at Bemidji, Minnesota: Journal of Hazardous Materials, v. 320, p. 123–132. [Also available at https://doi.org/10.1016/j.jhazmat.2016.08.018.]

Islam, A., Cho, Y., Yim, U.H., Shim, W.J., Kim, Y.H., and Kim, S., 2013, The comparison of naturally weathered oil and artificially photo-degraded oil at the molecular level by a combination of SARA fractionation and FT-ICR MS: Journal of Hazardous Materials, v. 263, no. 2, p. 404–411. [Also available at https://doi.org/10.1016/j.jhazmat.2013.09.030.]

Islam, A., Kim, D., Yim, U.H., Shim, W.J., and Kim, S., 2015, Structure-dependent degradation of polar compounds in weathered oils observed by atmospheric pressure photoionization hydrogen/deuterium exchange ultrahigh resolution mass spectrometry: Journal of Hazardous Materials, v. 296, no. 1, p. 93–100. [Also available at https://doi.org/10.1016/j.jhazmat.2015.04.042.]

Kropp, K.G., Andersson, J.T., and Fedorak, P.M., 1997, Biotransformations of three dimethyldibenzothiophenes by pure and mixed bacterial cultures: Environmental Science & Technology, v. 31, no. 5, p. 1547–1554. [Also available at https://doi.org/10.1021/es960869a.]

McGuire, J.T., Cozzarelli, I.M., Bekins, B.A., Link, H., and Martinović-Weigelt, D., 2018, Toxicity assessment of groundwater contaminated by petroleum hydrocarbons at a well-characterized, aged, crude oil release site: Environmental Science & Technology, v. 52, no. 21, p. 12172–12178. [Also available at https://doi.org/10.1021/acs.est.8b03657.]

Mohler, R.E., Ahn, S., O'Reilly, K., Zemo, D.A., Espino Devine, C., Magaw, R., and Sihota, N., 2020, Towards comprehensive analysis of oxygen containing organic compounds in groundwater at a crude oil spill site using GC×GC-TOFMS and Orbitrap ESI-MS: Chemosphere, v. 244, p. 125504. [Also available at https://doi.org/10.1016/j.chemosphere.2019.125504.]

Morris, G.A., and Freeman, R., 1979, Enhancement of nuclear magnetic resonance signals by polarization transfer: Journal of the American Chemical Society, v. 101, no. 3, p. 760–762. [Also available at https://doi.org/10.1021/ja00497a058.]

Ng, G.H.C., Bekins, B.A., Cozzarelli, I.M., Baedecker, M.J., Bennett, P.C., and Amos, R.T., 2014, A mass balance approach to investigating geochemical controls on secondary water quality impacts at a crude oil spill site near Bemidji, MN: Journal of Contaminant Hydrology, v. 164, p. 1–15. [Also available at https://doi.org/10.1016/j.jconhyd.2014.04.006.]

O'Reilly, K.T., 2018, Comment on "examining natural attenuation and acute toxicity of petroleum-derived dissolved organic matter with optical spectroscopy": Environmental Science & Technology, v. 52, no. 20, p. 11960–11961. [Also available at https://doi.org/10.1021/acs.est.8b03035.]

O'Reilly, K.T., Mohler, R.E., Zemo, D.A., Ahn, S., Magaw, R.I., and Espino Devine, C., 2019, Oxygen-containing compounds identified in groundwater from fuel release sites using GCxGC-TOF-MS: Ground Water Monitoring and Remediation, v. 39, no. 4, p. 32–40. [Also available at https://doi.org/10.1111/gwmr.12350.]

O'Reilly, K.T., Mohler, R.E., Zemo, D.A., Ahn, S., Tiwary, A.K., Magaw, R.I., Espino Devine, C., and Synowiec, K.A., 2015, Identification of ester metabolites from petroleum hydrocarbon biodegradation in groundwater using GC×GC-TOFMS: Environmental Toxicology and Chemistry, v. 34, no. 9, p. 1959–1961.

Patt, S.L., 1982, Alternating compound one eighties used to suppress transients in the coil: Journal of Magnetic Resonance (San Diego, Calif.), v. 49, p. 161–163.

Perry, J.J., 1984, Microbial metabolism of cyclic alkanes, *in* Atlas, R.M., ed., Petroleum Microbiology: New York, Macmillan, p. 61–97.

Peters, K.E., and Moldowan, J.M., 1993, The biomarker guide—Interpreting molecular fossils in petroleum and ancient sediments: Englewood Cliffs, N.J., Prentice-Hall Inc., 363 p.

Podgorski, D.C., Zito, P., Kellerman, A.M., Bekins, B.A., Cozzarelli, I.M., Smith, D.F., Cao, X., Schmidt-Rohr, K., Wagner, S., Stubbins, A., and Spencer, R.G.M., 2021, Hydrocarbons to carboxyl-rich alicyclic molecules—A continuum model to describe biodegradation of petroleum-derived dissolved organic matter in contaminated groundwater plumes: Journal of Hazardous Materials, v. 402, p. 123998. [Also available at https://doi.org/10.1016/j.jhazmat.2020.123998.]

Podgorski, D.C., Zito, P., McGuire, J.T., Martinovic-Weigelt, D., Cozzarelli, I.M., Bekins, B.A., and Spencer, R.G.M., 2018a, Examining natural attenuation and acute toxicity of petroleum-derived dissolved organic matter with optical spectroscopy: Environmental Science & Technology, v. 52, no. 11, p. 6157–6166. [Also available at https://doi.org/10.1021/acs.est.8b00016.]

Podgorski, D.C., Zito, P., McGuire, J.T., Martinovic-Weigelt, D., Cozzarelli, I.M., Bekins, B.A., and Spencer, R.G.M., 2018b, Rebuttal to comment on "examining natural attenuation and acute toxicity of petroleum-derived dissolved organic matter with optical spectroscopy": Environmental Science & Technology, v. 52, no. 20, p. 11962–11963. [Also available at https://doi.org/10.1021/acs.est.8b04976.]

Prince, R.C., and Walters, C.C., 2016, Biodegradation of oil hydrocarbons and its implications for source identification, chap. 19 *of* Stout, S.A., and Wang, Z., eds., Standard handbook oil spill environmental forensics (2d ed.): Boston, Academic Press, p. 869–916. [Also available at https://doi.org/10.1016/B978-0-12-803832-1.00019-2.]

Rabus, R., and Widdel, F., 1995, Anaerobic degradation of ethylbenzene and other aromatic hydrocarbons by new denitrifying bacteria: Archives of Microbiology, v. 163, no. 2, p. 96–103. [Also available at https://doi.org/10.1007/BF00381782.]

Robson, W.J., Sutton, P.A., McCormack, P., Chilcott, N.P., and Rowland, S.J., 2017, Class type separation of the polar and apolar components of petroleum: Analytical Chemistry, v. 89, no. 5, p. 2919–2927. [Also available at https://doi.org/10.1021/acs.analchem.6b04202.]

Rose, K.D., and Francisco, M.A., 1987, Characterization of acidic heteroatoms in heavy petroleum fractions by phase-transfer methylation and NMR spectroscopy: Energy & Fuels, v. 1, no. 3, p. 233–239. [Also available at https://doi.org/10.1021/ef00003a001.]

Ruiz, A.L.T.G., Magalhães, A.F., Faria, A.D., Magalhães, E.G., and Amaral, M.C.E., 2006, New hopane triterpene from *Eleocharis sellowiana* (Cyperaceae): Journal of the Brazilian Chemical Society, v. 17, no. 4, p. 803–806. [Also available at https://doi.org/10.1590/S0103-50532006000400025.]

Shahebrahimi, Y., Fazlali, A., Motamedi, H., and Kord, S., 2018, Experimental and modeling study on precipitated asphaltene biodegradation process using isolated indigenous bacteria: Industrial & Engineering Chemistry Research, v. 57, no. 50, p. 17064–17075. [Also available at https://doi.org/10.1021/acs.iecr.8b04661.]

Sihota, N.J., Singurindy, O., and Mayer, K.U., 2011, CO_2-efflux measurements for evaluating source zone natural attenuation rates in a petroleum hydrocarbon contaminated aquifer: Environmental Science & Technology, v. 45, no. 2, p. 482–488. [Also available at https://doi.org/10.1021/es1032585.]

Singer, M.E., and Finnerty, W.R., 1984, Microbial metabolism of straight chain and branched alkanes, *in* Atlas, R.M., ed., Petroleum Microbiology: New York, Macmillan, p. 1–59.

Thorn, K.A., 1987, The use of carbon-13 nuclear magnetic resonance spectroscopy in the analysis of complex samples of environmental interest, *in* Franks, B.J., ed., U.S. Geological Survey program on toxic waste—Ground-water contamination: U.S. Geological Survey Open-File Report 87–109, p. E13–E18. [Also available at https://pubs.usgs.gov/of/1987/0109/report.pdf.]

Thorn, K.A., 1989, Nuclear-magnetic-resonance spectrometry investigations of fulvic and humic acids from the Suwannee River, chap. N *of* Averett, R.C., Leenheer, J.A., McKnight, D.M., and Thorn, K.A., eds., Humic substances in the Suwannee river, Georgia—Interactions, properties, and proposed structures: U.S. Geological Survey Open File Report 87–557, p. 251–309. [Also available at https://pubs.usgs.gov/of/1987/0557/report.pdf.]

Thorn, K.A., and Aiken, G.R., 1998, Biodegradation of crude oil into nonvolatile organic acids in a contaminated aquifer near Bemidji, Minnesota: Organic Geochemistry, v. 29, no. 4, p. 909–931. [Also available at https://doi.org/10.1016/S0146-6380(98)00167-3.]

Thorn, K.A., Arterburn, J.B., and Mikita, M.A., 1992, Nitrogen-15 and carbon-13 NMR investigation of hydroxylamine-derivatized humic substances: Environmental Science & Technology, v. 26, no. 1, p. 107–116. [Also available at https://doi.org/10.1021/es00025a011.]

Thorn, K.A., and Cox, L.G., 2009, N-15 NMR spectra of naturally abundant nitrogen in soil and aquatic natural organic matter samples of the International Humic Substances Society: Organic Geochemistry, v. 40, no. 4, p. 484–499. [Also available at https://doi.org/10.1016/j.orggeochem.2009.01.007.]

Thorn, K.A., and Cox, L.G., 2015, Probing the carbonyl functionality of a petroleum resin and asphaltene through oximation and Schiff Base Formation in conjunction with N-15 NMR: PLoS One, v. 10, no. 11, p. e0142452. [Also available at https://doi.org/10.1371/journal.pone.0142452.]

Thorn, K.A., Folan, D.W., and MacCarthy, P., 1989, Characterization of the International Humic Substances Society standard and reference fulvic and humic acids by solution state carbon-13 (^{13}C) and hydrogen-1(^{1}H) nuclear magnetic resonance spectrometry: U.S. Geological Survey Water Resources Investigations Report 89–4196. [Also available at https://pubs.usgs.gov/wri/1989/4196/report.pdf.]

Thorn, K.A., Rostad, C.E., and Noyes, T.I., 2003, Isolation and characterization of colloids, chap. 7 *of* Schroeder, R.A., ed., Water-quality changes and organic-carbon characterization during recharge with recycled water at a research basin in Montebello Forebay, Los Angeles County, California, 1991–1996: U.S. Geological Survey Water-Resources Investigations Report 03–4146, p. 61–77. [Also available at https://pubs.usgs.gov/wri/wrir034146/wrir034146.pdf.]

Thorn, K.A., Steelink, C., and Wershaw, R.L., 1987, Methylation patterns of aquatic humic substances determined by ^{13}C NMR spectroscopy: Organic Geochemistry, v. 11, no. 3, p. 123–137. [Also available at https://doi.org/10.1016/0146-6380(87)90016-7.]

Thorn, K.A., Younger, S.J., and Cox, L.G., 2010, Order of functionality loss during photodegradation of aquatic humic substances: Journal of Environmental Quality, v. 39, no. 4, p. 1416–1428. [Also available at https://doi.org/10.2134/jeq2009.0408.]

Thurman, E.M., Yu, Y., Ferrer, I., Thorn, K.A., and Rosario-Ortiz, F.L., 2020, Molecular identification of water-extractable organic carbon from thermally heated soils—C-13 NMR and accurate mass analyses find benzene and pyridine carboxylic acids: Environmental Science & Technology, v. 54, no. 5, p. 2994–3001. [Also available at https://doi.org/10.1021/acs.est.9b05230.]

Townsend, G.T., Prince, R.C., and Suflita, J.M., 2004, Anaerobic biodegradation of alicyclic constituents of gasoline and natural gas condensate by bacteria from an anoxic aquifer: FEMS Microbiology Ecology, v. 49, no. 1, p. 129–135. [Also available at https://doi.org/10.1016/j.femsec.2003.08.015.]

U.S. Geological Survey, 2021, National crude oil spill fate and natural attenuation research site near Bemidji, Minnesota, USA, U.S. Geological Survey website, accessed December 20, 2021, at https://mn.water.usgs.gov/projects/bemidji/index.html]

Vaughan, P.P., Wilson, T., Kamerman, R., Hagy, M.E., McKenna, A., Chen, H., and Jeffrey, W.H., 2016, Photochemical changes in water accommodated fractions of MC252 and surrogate oil created during solar exposure as determined by FT-ICR MS: Marine Pollution Bulletin, v. 104, no. 1–2, p. 262–268. [Also available at https://doi.org/10.1016/j.marpolbul.2016.01.012.]

Waldo, G.S., Carlson, R.M.K., Moldowan, J.M., Peters, K.E., and Penner-hahn, J.E., 1991, Sulfur speciation in heavy petroleums—Information from X-ray absorption near-edge structure: Geochimica et Cosmochimica Acta, v. 55, no. 3, p. 801–814. [Also available at https://doi.org/10.1016/0016-7037(91)90343-4.]

Williams, P.J.B., 2000, Heterotrophic bacteria and the dynamics of dissolved organic material, *in* Kirchman, D.L., ed., Microbial ecology of the oceans: New York, Wiley, p. 153–200.

Zhang, X., and Young, L.Y., 1997, Carboxylation as an initial reaction in the anaerobic metabolism of naphthalene and phenanthrene by sulfidogenic consortia: Applied and Environmental Microbiology, v. 63, no. 12, p. 4759–4764. [Also available at https://doi.org/10.1128/aem.63.12.4759-4764.1997.]

ISSN 2331-1258 (online)
https://doi.org/10.3133/ofr20221042